

Yusuf Mehta
Department of Civil and Environmental Engineering
Rowan University

September 2007

**Wisconsin Highway Research Program
0092- 02-13**

**PHASE 1: Evaluation of Interlayer Bonding In
HMA Pavements**

**PHASE 2: Effect of Stiffness Ratio on Slippage
Cracking Due to Interlayer Bonding Failure in
Hot Mix Asphalt Pavements**

Final Report

by

Yusuf A. Mehta, Ph.D., P.E

Nusrat Siraj

of the

Department of Civil and Environmental Engineering

Rowan University, Glassboro NJ 08028

Submitted to the

**Wisconsin Department of
Transportation**

June 2007

DISCLAIMER

This research was funded through the Wisconsin Highway Research Program by the Wisconsin Department of Transportation and the Federal Highway Administration under Project # (0092- 03-13). The contents of this report reflect the views of the authors who are responsible for the facts and the accuracy of the data presented herein. The contents do not necessarily reflect the official views of the Wisconsin Department of Transportation or the Federal Highway Administration at the time of publication.

This document is disseminated under the sponsorship of the Department of Transportation in the interest of information exchange. The United States Government assumes no liability for its contents or use thereof. This report does not constitute a standard, specification or regulation.

The United State Government does not endorse products or manufacturers. Trade and manufacturers' names appear in this report only because they are considered essential to the object of the document.

Technical Report Documentation Page

1. Report No. WHRP 07-07	2. Government Accession No	3. Recipient's Catalog No	
4. Title and Subtitle Evaluation of Interlayer Bonding in HMA Pavements		5. Report Date September 2007	6. Performing Organization Code Univ. of Wisconsin - Madison
7. Authors Yusuf Mehta		8. Performing Organization Report No.	
9. Performing Organization Name and Address Department of Civil and Environmental Engineering Rowan University		10. Work Unit No. (TR AIS)	11. Contract or Grant No. WisDOT SPR# 0092-02-13
12. Sponsoring Agency Name and Address Wisconsin Department of Transportation Division of Business Services Research Coordination Section 4802 Sheboygan Ave. Rm 104 Madison, WI 53707		13. Type of Report and Period Covered Final Report, 2002-2004	14. Sponsoring Agency Code
15. Supplementary Notes			
<p>16. Abstract</p> <p>Some states, such as Wisconsin DOT have experienced pavement failures that were attributed to poor bonding at the interlayer. Three roads of WisDOT were analyzed in this study, which experienced varied degrees of slippage distress. The effect of slip can be minimized by making the surface layer sufficiently thick or stiff. It was observed that the stiffness ratio between the top two layers were higher for no distress sections than that of high distress sections. The additional thickness needed to increase structural capacity of a pavement with lower stiffness ratio to a level that will minimize slippage cracking was also investigated. The structural capacity of pavement with lower stiffness ratio ($E_1/E_2 = 2$) can be changed to the same structural capacity as that of a pavement with high E_1/E_2 (say, $E_1/E_2 = 10$) by providing additional thickness of 2 in and 4 in on existing top layer of 2 in and 3 in thickness, respectively. This study provides the state agency with tools during pavement design to minimize slippage cracking due to interlayer bonding failure.</p>			
17. Key Words Asphalt, backcalculation, falling weight deflectometer, interlayer bonding, slippage cracking, stiffness ratio		18. Distribution Statement No restriction. This document is available to the public through the National Technical Information Service 5285 Port Royal Road Springfield VA 22161	
19. Security Classif.(of this report) Unclassified	19. Security Classif. (of this page) Unclassified	20. No. of Pages	21. Price

Executive Summary

Project Summary

In recent years, slippage failure or interlayer tack coat distresses have been observed in some of the projects of the Wisconsin Department of Transportation (WisDOT), both during and after construction. These slippages are erratic making them difficult to understand, and hence it is difficult to take appropriate measures to prevent them. Three roads of WisDOT, named I-94 EB, USH 18, and HWY 81 were analyzed in this study. The purpose of this research is to provide guidelines during pavement design in terms of the stiffness ratio between the top two layers of a pavement system to minimize slippage cracking due to interlayer bonding failure.

The study showed that the stiffness ratio between the top two layers of no distress sections were higher than those in the high distress sections. The structural capacity of the pavement can be changed from a lower stiffness ratio to the same structural capacity as that of a higher stiffness ratio by providing additional thickness.

Background

Slippage cracking is the typical indication of interlayer bonding failure of a pavement system. The first phase of the research was the evaluation of the interlayer bonding failure and is attached as an appendix to this report. This is a second phase of the research, which is based on minimizing the slippage cracking which results from interlayer bonding failure.

The slippage between the layers is the result of a weak interlayer bond. Part of the asphalt surface moves laterally away from the rest of the surface due to induced lateral and shear stresses caused by traffic loads (Huang, 1993). Few studies (Shahin et al.;1987; Uzan et al., 1978) have been done on the failure mechanism in interlayer bonding failure. Slippage cracking consists of crescent-shaped cracks that develop at the pavement surface and are the direct result of a slippage between layers (Shahin et al., 1987; Uzan et al., 1978). The crescent cracks, while certainly a problem themselves, are not the only problem resulting from slippage. Due to a poor interlayer bond, the upper layer slips and the pavement system as a whole is weakened. This is because the broken bond reduces the stiffness of the system as a whole and loads may no longer be supported and distributed by the system as designed (Shahin et al., 1987). Slippage cracks are caused by the insufficient pavement stiffness and thickness or a weak bond between the surface course and the layer below. The complex interaction between these factors makes it difficult to control slippage cracking. This study utilizes backcalculated stiffness and field-observed distresses to understand the factors which are critical to slippage cracking and develop guidelines during the pavement design for minimizing the slippage cracking that results from the interlayer bonding failure.

The Department of Civil and Environmental Engineering at Rowan University conducted this research project through the Wisconsin Highway Research Program. The

research team for phase 1 includes Dr. Yusuf Mehta (Associate Professor), Stephen M. Gomba (Graduate student), and Joseph Cugino (Undergraduate student). The research team for phase 2 includes Dr. Yusuf Mehta (Associate Professor) and Nusrat Siraj (Graduate student).

Process

As mentioned before, three roads of WisDOT were analyzed in this study and they are located in three different counties of Wisconsin. I-94 EB, USH 18, and HWY 81 are located in Jefferson, Iowa, and Lafayette counties, respectively. The FWD data and the observed intensity of distress data of the three roads were provided by WisDOT. The information about the thickness of the two roads (I-94 EB and HWY 81) was provided by WisDOT. The analysis of USH 18 was done by different thickness assumptions, which is explained in the data section of this report. The second phase of the research was conducted in 24 months (12 months were lost due to delay of getting the data). The first phase of the work was conducted in 24 months.

FWD data can be used to estimate the stiffness of the pavement layer for both no distress and high distress sections. This estimation of the stiffness of the layers can be performed through a method called backcalculation. Based on the measured surface deflections, the backcalculation programs determine the pavement layer stiffness. For the same FWD load, the deflections of the high distress sections (fully slipped, F.S.) are higher than that of the no distress sections (fully bonded, F.B.), which is shown schematically in Figure 1. The deflection sensors along with the distance from the center are shown in Figure 1.

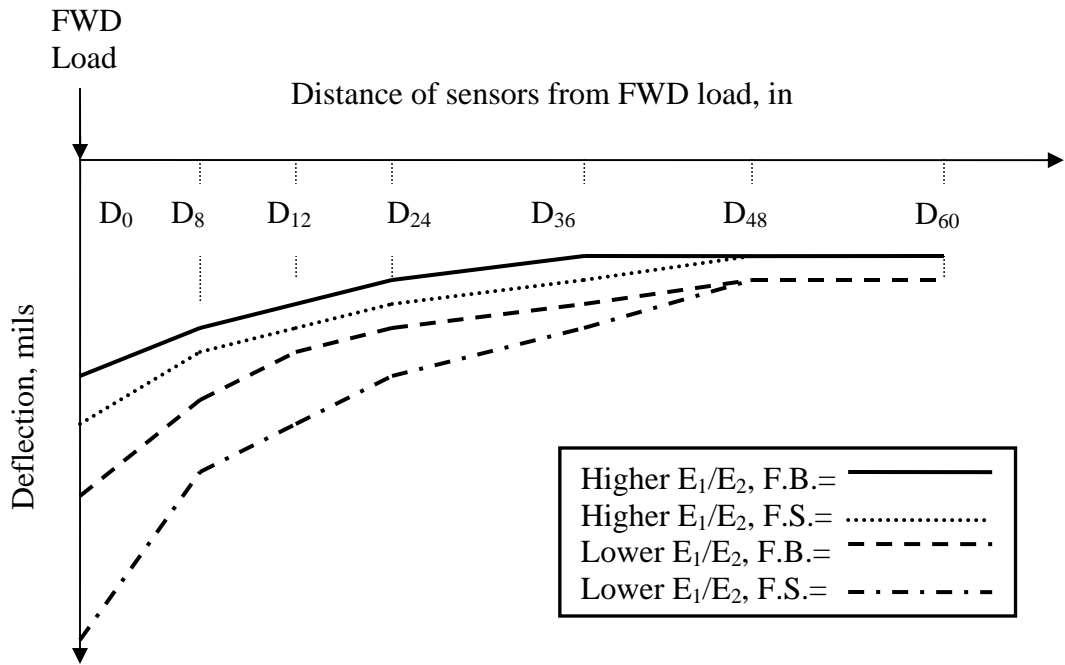


Figure 1: Schematic diagram for the measured deflection due to the FWD load for the full bond (F.B.) and the full slip (F.S.) interface conditions.

The phenomenon of slip is manifested in FWD data. Theoretically, the deflection basin from FWD of a fully bonded pavement structure will be a lot lower than the deflection basin of a fully slipped section. A fully bonded pavement structure will transfer the load better through the pavement system and hence utilize the structural capacity of all layers effectively. On the other hand, a poorly bonded pavement system will be a relatively more flexible system due to poor load transfer.

As explained before, the higher stiffness ratio minimizes the impact of slip. The difference in the deflection basin of the fully slipped and the fully bonded section will be greater for the pavement structure with a low stiffness ratio, as shown in Figure 1. The researchers have used this concept in this study to provide an appropriate stiffness ratio needed to minimize the effect of slip.

Findings

The summary of the findings based on the analysis conducted is presented below:

- 1) For I-94 EB, the distresses observed by WisDOT correlated with the tensile strain at the bottom of the asphalt concrete, which were indicative of slippage failure.

But for USH 18, distresses observed by WisDOT did not correlate with the tensile strain at the bottom of the asphalt concrete. This may be because the distress was observed in shoulders but the FWD might be taken along the main lane.

- 2) The distresses observed by WisDOT for both I-94 EB and USH 18 did not correlate with the parameters such as AREA and the surface flexural rigidity because these parameters are influenced by the stiffness and the thickness of the entire pavement system.
- 3) The stiffness ratio between the top two layers for no distress sections were between 5 and 65 which were higher than that of the high distress sections between 1 and 7; this was observed for all the sections where the stiffness of the second layer was greater than 20 ksi.
- 4) The percentage differences of the stiffness between the full bond and the full slip may not be an accurate indicator of the effect of slippage.
- 5) The normalized percentage differences of stiffness ($P.D./E_1$) between the full bond and the full slip appeared to correlate quite well with the observed distresses.
- 6) A very strong inverse correlation was observed between $P.D./E_1$ vs. E_1/E_2 with the root mean square value of the curve ($P.D./E_1$ vs. E_1/E_2) of 0.94.
- 7) The stiffness ratio appeared to inversely correlate with observed distresses. Higher E_1/E_2 ($E_1/E_2 > 10$) consistently showed a better interlayer bonding performance.
- 8) When the stiffness ratio was greater than 10 the differences in the slopes of the curve ($P.D./E_1$ vs. E_1/E_2) were almost zero. Since $P.D./E_1$ is directly related to the effect of slip, when E_1/E_2 were greater than 10, the pavement was not as adversely impacted due to poor interlayer bonding.
- 9) By providing additional thickness of 2 in (on the existing 2 in layer) and 4 in (on the existing 3 in top layer) on the pavement with low E_1/E_2 ($E_1/E_2 < 10$) can be changed to the same structural capacity as that of a pavement with high E_1/E_2 (say $E_1/E_2 = 10$).

Conclusions and recommendation

If the stiffness ratio between the top HMA layer and the second layer is greater than 10 during the design and if the second layer stiffness is greater than 20 ksi, the pavement will be less affected by slippage than that when the stiffness ratio is less than 10.

Based on limited cases, this study demonstrated that the structural capacity of the slipped pavement with $E_1/E_2 = 2$ can be increased to the stiffness ratio of $E_1/E_2 = 10$ by increasing the thickness of the surface layer. The additional top layer thicknesses are 2 in for an existing 2 in top layer thickness and 4 in for an existing 3 in top layer thickness.

Significance of the study

The objective of this study was to determine the stiffness ratio (E_1/E_2) between the top two layers during design, which is necessary to minimize slippage cracking due to

interlayer bonding failure. In this analysis it was observed that higher E_1/E_2 ($E_1/E_2 > 10$ and $E_2 > 20$ ksi) consistently showed better interlayer bonding performance. The significance of this study for the state agency is described as a flow chart, as shown in Figure 2.

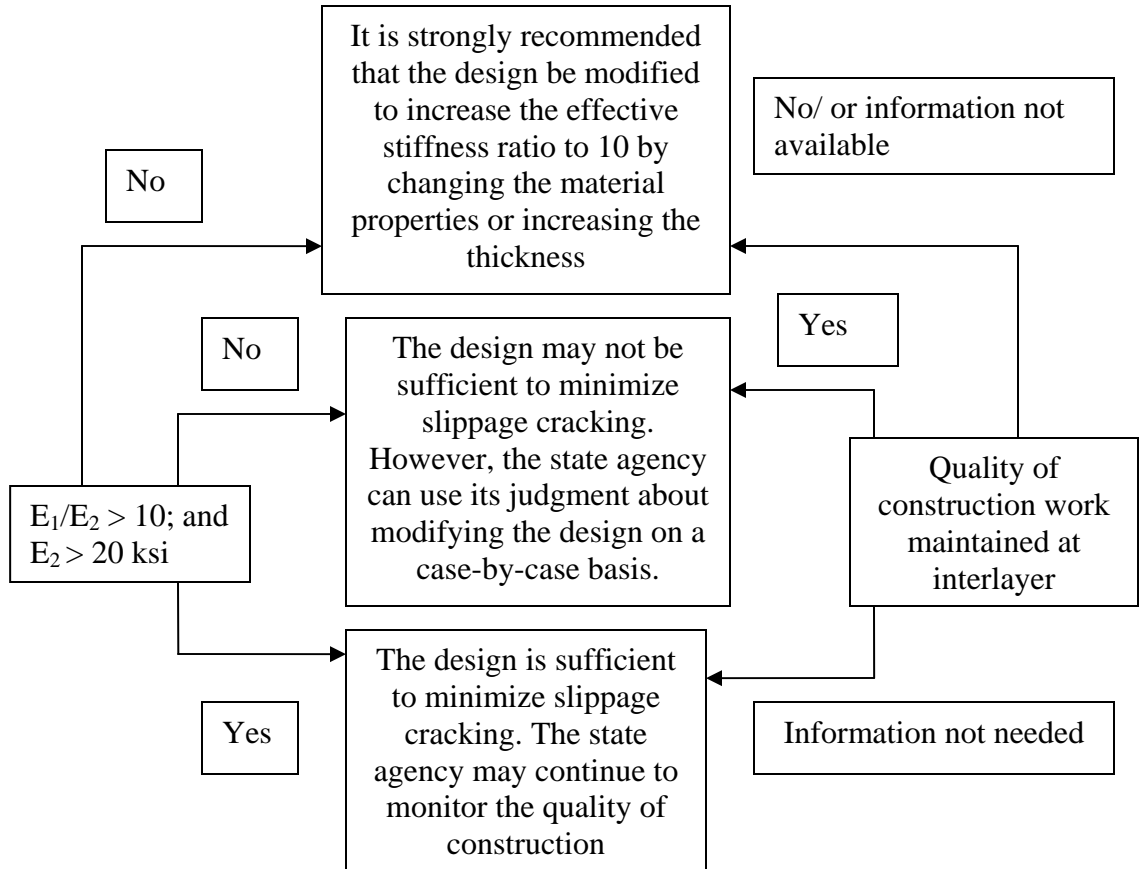


Figure 2: Recommendation to the state agency for minimizing slippage failure.

During pavement design, the designer may calculate a certain stiffness ratio necessary for the pavement to last the design life for the given traffic, the subgrade, and the environmental conditions. However, if the designer requires a stiffness ratio less than 10, there may be a possibility of slippage failure if proper construction practices are not followed. To minimize this probability it might be advisable to invest earlier during construction by providing a minimum E_1/E_2 of 10. Low stiffness ratio ($E_1/E_2 < 10$) may give an economical design but there may be a greater probability of slippage at low stiffness ratios; if the contractors do a bad job or the quality of the work is not maintained. It will be expensive to reconstruct the slipped pavement once the slippage has happened.

The initial cost may be high to achieve a stiffness ratio between the top two layers greater than 10 ($E_1/E_2 > 10$ and $E_2 > 20$ ksi), but the pavement may be less likely to be affected by slippage, decreasing the cost of maintenance or reconstruction. This analysis may help the designers to design a slippage resistant pavement economically.

In addition, in this analysis the observed ability of the pavement to resist slippage was almost similar from the stiffness ratio of 10 to 65. Thus from an economic point of view, it can be concluded that the pavement may be safe from slippage failure for the stiffness ratio, E_1/E_2 at least 10; for $E_2 > 20$ ksi. The recommendations are valid if the base layer is not cement concrete.

Recommendations for Further Action

This study is based on three roads of WisDOT. Even though, these results were based on field performance, the findings need to be independently validated. The research team suggests the following:

- (a) To determine the stiffness of all layers of new construction pavements using backcalculation, following the checks suggested in this study.
- (b) Monitor the slippage cracking performance of those pavement sections.
- (c) Determine whether, as observed in this study, the slippage cracking performance correlates with the stiffness ratio. The results of the above will independently validate the study.

As a step towards implementing a stiffness ratio greater than 10, a good place to start would be to use the Witczak Model to calculate the dynamic modulus of asphalt layers and obtain resilient modulus of lower layers from CBR test. One of the most comprehensive mixture dynamic modulus models developed by Witczak et al 2002 $|E^*|$. It is proposed in the AASHTO M-E Design Guide and the calculations were based on the volumetric properties of a given mixture (Ping and Xiao, 2007). Laboratory data is always preferred to using the Witczak Model. If lab data exist in the database, that could be used.

Scope of the Project

In this section, the PI will explain the reasons for the change in the scope of the project.

The objectives of the study as mentioned in the proposal were:

1. To evaluate the cause of the slippage failure problems on Wisconsin highways.
2. To evaluate the benefits of various techniques to maintain interlayer bonding in HMA, especially the benefit of different types of tack coats and their application rate.

The first task towards achieving the objective, as outlined in the proposal, was: “To identify projects in Wisconsin which have shown interlayer slippage problems during and after construction and also projects that have not shown any problems. Collect construction and quality control data (these include type of tack coat used, rate of application and curing period), any known construction problems, structural design and

laboratory data, typical placement and ambient temperature data, and collect FWD data measurements on these projects.

An assistant from ERES Consultants, Inc will be conducting an inspection of these projects in Wisconsin highways and collecting the data under the supervision of Dr. Leslie Myers.

P.S. These FWD measurements will be part of the Pavement Condition Survey collected by the Wisconsin DOT.”

This task required close communication between WisDOT and our collaborator ERES Consultant in the state of Wisconsin. The PI contacted the Point of Contact, Thomas Brokaw, every month to determine how the data could be obtained and what could be done to facilitate getting the data. While the PI was communicating with Thomas Brokaw, we started on the second task as outlined below and conducted the survey as outlined in Phase I Executive Summary of the report..

Task II. Literature Review

- a. Identify sections all over the country with known structural composition and performance history, especially those using tack coats and also including cases in which different types of techniques of interlayer bonding between HMA were used.
- b. Various properties of different types of tack coat, the rate of application, and construction practices like the curing period on the performance will be documented for the pavement sections identified above.
- c. Other techniques used to maintain interlayer slippage and steps taken to offset the effect of the poor interlayer bond, like increasing the thickness of the surface layer will be documented.
- d. To identify various methods of determining critical mechanical responses and properties that can describe the interface behavior.
- e. Prepare an interim report to document the findings of Tasks I and II.”

We conducted an extensive literature review which is presented in Phase I of the report and also conducted a survey of the state of practice. The PI called Greg Waidley and Thomas Brokaw submitted timely quarterly reports to solicit feedback from the Technical Oversight Committee (TOC) as we moved along with the tasks.

The beginning of Task III, as outlined in the proposal would be dependent on getting data from Task I, especially, construction, tack coat, and FWD data from the slipped and the un-slipped section. Therefore we could not begin Task III.

“Task III. Evaluation of Tack Products and Application Rates and Other Techniques

- a. The material properties of different types of tack coat, the rate of application, and construction practices like the curing period on the performance will be analyzed to determine the parameters that correlate to shear strength.
- b. Since, the critical mechanical responses like shear stresses at the interface attribute to the interlayer slippage on the pavement with different structures, an FWD analysis will be conducted to determine the effective layer moduli and subsequently calculate the shear stresses using BISAR.
- d. Identify correlations between the parameters that reflect on the shear strength (step IIIa) and the shear stress at interface (step IIIb) with pavement performance.
- e. Evaluate the feasibility of other methods in addition to using tack coat to maintain interlayer bonding between HMA on Wisconsin highways.”

In spite of all the good intentions and effort of WisDOT no data was received for more than one and a half years. Around the same time, the Federal Aviation Administration had observed a similar problem of slippage. While I was waiting and had already hired a graduate student, Stephen Gomba, on this project, I decided to analyze the Federal Aviation Administration Data. The results of the entire study are presented in Phase I. This data was also published in the International Journal of Pavements.

Three years had passed and we had just finished Phase I; we really needed the data to continue on this project. Dr. Husain Bahia graciously assigned his then student Andrew Hanz to provide the data. Mr. Andrew Hanz provided limited data on three sections. I did ask him repeatedly about structural and materials data. He said that he had checked everything he could and that is all he had. He provided the following:

- a. FWD data for three sections
- b. Limited materials, structural, and construction data.

Based on the limited data, the PI had to modify the scope of the project as mentioned below:

“Provide guidelines during pavement design in terms of stiffness ratio between the top two layers to minimize slippage cracking due to interlayer bonding failure”

It was not possible to evaluate materials and construction practices without any relevant data. Thus, the scope of the project changed to reflect the realities that were facing the PI. As mentioned earlier, the PI was always seeking feedback after every quarterly report. However, due to the busy schedules of the state agency personnel there is no mechanism in-place to provide regular feedback on research projects.

The PI was aware that backcalculated moduli values depend on the thickness, but had little choice. We went to the specifications to obtain reasonable range of thickness and moduli values of ALL layers from the structural coefficients. The PI was working hard to provide something of value to WisDOT with very little data in hand. The PI started

the analysis in June 2006 and the first report with the new analysis was submitted in September 2006. The PI continued the effort to solicit feedback from WisDOT and called Andrew Hanz regularly.

In summary, the PI would like to conclude that the state agency may have tried the best they could to provide the data and the PI tried his best to keep constant communication with WisDOT but due to circumstances beyond the PI's control the scope of the project was changed.

Table of Contents

1.0. Introduction.....	1
1.1. Problem Statement.....	1
1.2. Study Objectives.....	1
1.3. Background.....	1
1.4. Research Approach.....	2
2.0. Data.....	4
2.1. Data.....	4
2.2. Data of I-94 EB.....	6
2.3. Data of USH 18.....	6
2.3.1. Assumptions related to thickness and pavement structure of USH 18...7	7
3.0. Analysis Based on Tensile Strain and Stiffness Parameters.....	9
3.1. Tensile strain at bottom of the HMA layer for distress analysis.....	9
3.2. AREA and surface flexural rigidity for distress analysis.....	11
3.2.1. AREA.....	11
3.2.2. Surface flexural rigidity.....	13
3.3. Conclusions.....	14
4.0. Backcalculation of Pavement Layer Stiffness.....	15
4.1. Backcalculation of pavement layer stiffness.....	15
4.2. Stiffness of pavement layers.....	15
4.2.1. I-94 EB.....	15
4.2.2. USH 18.....	19
4.2.2.1. Stiffness of pavement layers for first set of assumption.....	19
4.2.2.2. Stiffness of pavement layers for second, third, and fourth sets of assumptions.....	22
4.2.2.3. Summary of the analysis of USH 18.....	25
4.3. Evaluation of the accuracy of backcalculated stiffness.....	26
4.3.1. Subgrade stiffness.....	26
4.3.2. Swapping.....	28
4.3.3. Root mean square error.....	28
4.3.4. Variation of stiffness along the road for a given section.....	32
4.4. Summary of the findings.....	33
5.0. Combined Analysis of I-94 EB and USH 18.....	34
5.1. Analysis based on percentage differences of stiffness with stiffness ratio.....	34
5.2. Estimation of strain difference in KENLAYER.....	35
5.3. Normalized percentage differences of stiffness with stiffness ratio.....	35
5.4. Summary of findings.....	38
6.0. Case Study.....	39
6.1. Data of HWY 81.....	39

6.2. No distress sections(LWP).....	39
6.3. Slippage section (REOP) and no distress section (LWP)	41
6.4. Summary of the findings.....	43
7.0. Degree Of Slip	46
7.1. Estimation of degree of slip.....	46
7.2. Achieving stiffness ratio by increasing thickness.....	47
8.0. Summary of the Findings and Recommendations.....	50
8.1. Summary of the findings.....	50
8.2. Recommendation	50
9.0. References	51

List of Figures

Figure	Page
Figure 1. Schematic Diagram of the Measured Deflection due to the FWD Load for the Full Bond (F.B.) and the Full Slip (F.S.) Interface Conditions	iii
Figure 2. Recommendation to the State Agency for Minimizing Slippage Failure.....	v
Figure 1.1. Failure Mechanism	2
Figure 3.1. Tensile Strain at bottom of HMA Layer vs. Sections (I-94 EB).....	10
Figure 3.2. Tensile Strain at bottom of HMA Layer vs. Sections (USH 18).....	10
Figure 3.3. AREA vs. Sections (I-94 EB).....	12
Figure 3.4. AREA vs. Sections (USH 18)	12
Figure 3.5. Surface Flexural Rigidity vs. Sections (I-94 EB).....	13
Figure 3.6. Surface Flexural Rigidity vs. Sections (USH 18).....	14
Figure 4.1. Stiffness vs. Distance (N.D., I-94 EB, F.B., actual).....	16
Figure 4.2. Stiffness vs. Distance (N.D., I-94 EB, F.S., assumption).....	17
Figure 4.3. Stiffness vs. Distance (H.D., I-94 EB, F.S., actual)	18
Figure 4.4. Stiffness vs. Distance (H.D., I-94 EB, F.B., assumption)	18
Figure 4.5. Stiffness Ratio (E_1/E_2) for No Distress vs. High Distress Sections (I-94 EB)	19
Figure 4.6. Stiffness vs. Distance (N.D., USH 18, F.B., actual).....	20
Figure 4.7. Stiffness vs. Distance (N.D., USH 18, F.S., assumption).....	20
Figure 4.8. Stiffness vs. Distance (H.D., USH 18, F.S., actual)	21
Figure 4.9. Stiffness vs. Distance (H.D., USH 18, F.B., assumption).....	21
Figure 4.10. Stiffness Ratio (E_1/E_2) for No Distress vs. High Distress Sections (USH 18).....	25
Figure 4.11. Backcalculated Subgrade Stiffness vs. Measured Deflections at d_{60}	26
Figure 4.12. Backcalculated Subgrade Stiffness vs. Subgrade Stiffness Provided by WisDOT.....	27
Figure 4.13. Deflections vs. the distance of sensors and the percentage differences of the deflections between the measured and the calculated values vs. the distance of sensors (RMSE 1.59, F.B.).....	29
Figure 4.14. Deflections vs. Distance of Sensors and Percentage Differences of Deflections Between Measured and Calculated values vs. Distance of Sensors (RMSE 0.88, F.B.).....	30
Figure 4.15. Deflections vs. the distance of sensors and the percentage differences of deflections between the measured and the calculated values vs. the distance of sensors (RMSE= 0.61, F.B.).....	30
Figure 4.16. Deflections vs. the distance of sensors and the percentage differences of the deflections between the measured and the calculated values vs. the distance of sensors (RMSE= 1.36, F.S.)	31
Figure 4.17. Deflections vs. the distance of sensors and the percentage differences of the deflections between the measured and the calculated values vs. the distance of sensors (RMSE= 1.12, F.S.)	31
Figure 4.18. Deflections vs. the distance of sensors and the percentage differences of	

deflections between the measured and the calculated values vs. the distance of sensors (RMSE= 0.80, F.S.)	32
Figure 5.1. Percentage differences of stiffness between the full bond and the full slip vs. the stiffness ratio (E_1/E_2).....	34
Figure 5.2. Normalized percentage differences of stiffness between the full bond and the full slip ($P.D./E_1$) vs. the stiffness ratio (E_1/E_2) for no distress sections.....	36
Figure 5.3. Normalized percentage differences of stiffness between full bond and full slip ($P.D./E_1$) vs. the stiffness ratio (E_1/E_2) for high distress sections.....	36
Figure 5.4. Normalized percentage differences of stiffness between the full bond and the full slip ($P.D./E_1$) vs. the stiffness ratio (E_1/E_2)	37
Figure 5.5. Differences in Slope of Curve ($P.D./E_1$ vs. E_1/E_2) vs. Stiffness Ratio (E_1/E_2)..	38
Figure 6.1. Stiffness vs. Distance (N.D., HWY 81, F.B., actual)	40
Figure 6.2. Stiffness vs. Distance (N.D., HWY 81, F.S., assumption)	40
Figure 6.3. Stiffness ratio (E_1/E_2) vs. Distance (N.D., HWY 81)	41
Figure 6.4. Stiffness of Subgrade vs. Distance (N.D., LWP, HWY 81).....	42
Figure 7.1. Deflections of Surface Layer (2”) vs. Distance from the FWD Load	48
Figure 7.2. Deflections of Surface Layer vs. Distance from the FWD Load	48
Figure 7.3. Deflections of Surface Layer (3”) vs. Distance from the FWD Load	49
Figure 7.4. Deflections of Surface Layer vs. Distance from the FWD Load	49

List of Tables

Table	Page
Table 2.1. Projects to be Evaluated in this Study	4
Table 2.2. Data of the Three Projects Given by WisDOT	5
Table 2.3. Observed Distress Data of I-94 EB.....	6
Table 2.4. Observed Distress Data of USH 18	6
Table 2.5. Thickness Data of HWY 81 and I-94 EB Given by WisDOT	7
Table 2.6. Thickness for USH 18.....	8
Table 4.1. Analysis of USH 18 for Assumptions 1, 2, and 3.....	23
Table 4.2. Analysis of USH 18 for Assumption 4	24
Table 4.3. Expected Layer Stiffness (Facilities Development Manual, Procedure 14-10-5, Wisconsin)	27
Table 4.4. Root Mean Square Error Values for Both I-94 EB and USH 18.....	29
Table 6.1. Thickness Data of HWY 81 Given by WisDOT	39
Table 6.2. Analysis of HWY 81 for No Distress section (LWP).....	44
Table 4.2. Analysis of HWY 81for Slippage Section (REOP).....	44

1.0. Introduction

1.1. Problem Statement

Slippage cracking is the typical indication of interlayer bonding failure of a pavement system. Slippage cracking consists of crescent-shaped cracks that develop at the pavement surface and are the direct result of slippage between layers (Shahin et al., 1987; Uzan, et al., 1978). In recent years, slippage failure or interlayer tack coat distresses have been observed on some projects of the Wisconsin Department of Transportation (WisDOT), both during and after construction. These slippages are erratic making them difficult to understand and hence making it difficult to take appropriate measures to prevent them.

The slippage between the layers is the result of a weak interlayer bond. Part of the asphalt surface moves laterally away from the rest of the surface due to induced lateral and shear stresses caused by traffic loads (Huang, 1993). The crescent cracks, while certainly a problem themselves, are not the only problem resulting from slippage. Due to a poor interlayer bond, the upper layer slips and the pavement system as a whole is weakened. This is because the broken bond reduces the stiffness of the system as a whole and loads may no longer be supported and distributed by the system as designed (Shahin et al., 1987). Slippage cracks are caused by insufficient pavement stiffness and thickness or a weak bond between the surface course and the layer below. The complex interaction between these factors makes it difficult to control the slippage cracking. This study utilizes backcalculated stiffness and field observed distresses to understand the factors which are critical to slippage cracking and develop guidelines during the pavement design for minimizing the slippage cracking that result from interlayer bonding failure.

1.2. Study Objectives

The objectives of this study are:

1. To determine whether the observed slippage cracking is due to failure at the interface.
2. To provide guidelines during pavement design in terms of the stiffness ratio between the top two layers of a pavement system to minimize slippage cracking due to interlayer bonding failure.
3. To determine additional thickness needed to increase the structural capacity of a pavement with a lower stiffness ratio to a level that will minimize slippage cracking.

1.3. Background

In a pavement system, a tensile strain occurs at the bottom of the second layer where the layers are fully bonded, as shown in Figure 1.1(a). In this case the differences of strain between the bottom of the top layer and the top of the bottom layer is zero. As the interlayer bond is weakened, the pavement system begins to act as two separate systems for a fully slipped section, as shown in Figure 1.1(b). This being so, the bottom of the top layer develops tensile strain and the top of the lower layer develops compressive strain. These opposing strains at the interface further develop slippage, since the interlayer is distorted by the stresses

between the two layers (Shahin et al., 1987). The surface layer must be able to withstand traffic loads and resulting strains on its own for a fully slipped section. The upper layer should be sufficiently stiff or thick for two reasons: (1) to minimize the strains at the interlayer and (2) to enable the layer to resist applied strains if the layer slips and separates from the lower layer. Thus the pavement structure influences the effect of slip between layers. Structures with very stiff or very thick surface layers may experience low effect of slips (Gomba, et al., 2004). Pavement structures with higher surface stiffness compared to the layer below (higher stiffness ratio) will withstand much of the load itself than that of pavements with a lower stiffness ratio due to better load distribution. As a result of this, the effect of interlayer bonding failure is minimal for a higher stiffness ratio as compared to a lower stiffness ratio. This study focuses on providing an appropriate stiffness ratio between the top two layers to minimize the impact of slippage.

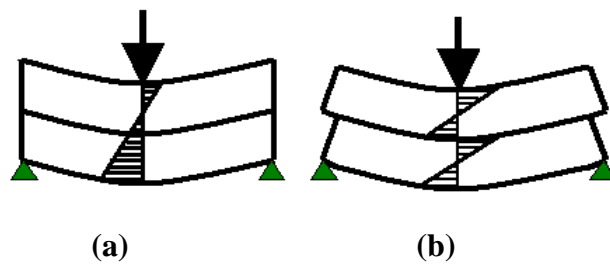


Figure 1.1: Failure Mechanism: (Gomba, et al., 2004).
(a) Fully Bonded Pavement Acting as One System
(b) Fully Slipped Pavement Acting as Two Systems

1.4. Research Approach

The following tasks were conducted to achieve objective 1:

- A. To correlate the observed distress to parameters such as the tensile strain at the bottom of the asphalt concrete, which are indicative of slippage failure.
- B. To correlate the observed distress to the stiffness of pavement structure using parameters, measured from FWD data, such as the area of the normalized deflection basin (AREA) and the surface flexural rigidity (ET^3).

The following tasks were conducted to achieve objective 2:

- C. To backcalculate the stiffness of different layers of the no distress section for the full bond condition. Then calculate the stiffness of the HMA layer for the full slip assumption, keeping the stiffness as a full bond condition of all other layers.
- D. To backcalculate the stiffnesses of different layers of the high distress section for the slip condition. Then calculate the stiffness of the HMA layer for the full bond assumption, keeping the stiffness as the full slip condition of all the other layers.
- E. To correlate the percentage differences of the stiffness between the full bond and the full slip of the no distress section to the stiffness ratios between the top HMA layer and the layer below the HMA layer.

- F. To verify the percentage differences of stiffness between the full bond and the full slip with differences of strain between the full bond and the full slip for specific stiffness ratio.
- G. To correlate the normalized percentage differences of stiffness between the full bond and the full slip (both no distress and high distress sections) to the stiffness ratios between the top HMA layer and the second layer below the HMA layer.

The following tasks were conducted to achieve objective 3:

- H. To calculate the surface deflection of the existing top layer for the FWD load for the high distress section with the actual lower stiffness ratio.
- I. To calculate the surface deflection of the existing top layer for the FWD load, assuming a higher stiffness ratio.
- J. To calculate the additional thickness by matching the deflection basin of the pavement from the FWD data with a lower stiffness ratio to that with a higher stiffness ratio.

The results of the tasks outlined above are presented below.

2.0. Data

2.1. Data

The data of the three roads were given by WisDOT. The data of the three projects are given in Table 2.1.

Table 2.1. Projects to be evaluated in this study

Project	Name of the project	County
1	I-94 EB	Jefferson
2	USH 18	Iowa
3	HWY 81	Lafayette

Projects 1 and 2 were analyzed to provide guidelines of WisDOT and project 3 was a case study. The detailed data of the three projects that were given by WisDOT are summarized in Table 2.2.

Table 2.2. Data of the three projects given by WisDOT

Project	FW D data	Thickne ss data	Section al drawing	Subgra de stiffness	Qc/ QA data	Asphalt mix design data	Performanc e graded binder data	Emulsified asphalt test data	Aggregate test data	Observed intensity of distress
I-94 EB	√	√	√	√	X	√	√	√	√	√
USH 18	√	X	X	√	X	√	X	√	√	√
HWY 81	√	Partially given	X	Partially given	√	X	X	X	X	Partially given

√ = Given, X = not given

2.2. Data of I- 94 EB

This section describes the data of I-94 EB, the data of one of the three roads given by WisDOT. The data of I-94 EB was analyzed first because it was more detailed as compared to the other two roads. I-94 EB is the portion of Madison-Waukesha Road (Crawfish River ECL), which is located in Jefferson County. The stations at which the Falling Weight Deflectometer (FWD) tests were conducted by WisDOT are given in Table 2.3. The different intensity of distresses on I-94 EB that were observed by WisDOT is also given in Table 2.3. The thicknesses of the different layers were taken from a sectional drawing, given by WisDOT. The thickness of the hot mix asphalt layer is 3”, the thickness of the concrete pavement is 9”, the thickness of the base is 6”, and the thickness of the subbase is 9”. These thicknesses were kept constant along the entire pavement, based on the plans provided by WisDOT.

Table 2.3. Observed Distress Data of I-94 EB

Section	Station (ft)	*Intensity of Distress
A	0 - 193	No distress (N.D.)
B	37138 - 37234	Low distress (L.D.)
C	38023 - 38244	Moderate distress (M.D.)
D	39072 - 39183	High distress (H.D.)
E	39468 - 39711	High distress (H.D.)
F	40850 - 41145	Low distress (L.D.)
G	41177 - 41203	No distress (N.D.)

*The distress as identified by WisDOT

2.3. Data of USH 18

This section describes the data of USH 18, the data of one of the three roads given by WisDOT. The stations at which the Falling Weight Deflectometer (FWD) tests were conducted by WisDOT are given in Table 2.4. The different intensity of the distresses on USH 18 that were observed by WisDOT is also given in Table 2.4.

Table 2.4. Observed Distress Data of USH 18

Section	Station(ft)	*Intensity of Distress
A	0 - 69	Moderate distress (M.D.)
B	13030 - 13078	Low distress (L.D.)
C	13735 - 13800	Low distress (L.D.)
D	17038 - 17248	Patched distress (P.D.)
E	18235 - 18296	High distress (H.D.)
F	25980 - 26192	No distress (N.D.)

*Distress as identified by WisDOT

2.3.1. Assumptions related to the thickness and the pavement structure of USH 18

The information of the thickness of the different layers of USH 18 and the pavement structure was not provided by WisDOT. Due to unavailability of data, the research team determined the thickness from the following:

- 1) The information about the thickness and the orientation of layers of I-94 EB and HWY 81 were given by WisDOT, is shown as Table 2.5. Assumptions of USH 18 were made on the basis of information of these two projects.
- 2) Standard specification of WisDOT was also taken into consideration.

Table 2.5. Thickness data of HWY 81 and I-94 EB given by WisDOT

HWY 81						I-94 EB	
Rehabilitated section		First typical reconstruction section		Second typical reconstruction section			
HMA	3.5"	HMA	5"	HMA	3.5"	HMA	3"
Pul. and relay asphalt pavement	4"	CABC	9"	CABC	19.5"	Concrete Layer	9"
CABC	10"	Sal. Asphalt pavement base course	3"			Base	6"
						Subbase	9"

From Table 2.5, it was observed that the sum of the thicknesses of the base and the subbase are 12 to 19.5 in. After considering the above, the sum of the thickness of the base and the subbase of USH 18 was assumed as 15 in. Moreover, in I-94 EB the concrete layer was present but not in HWY 81. To obtain a more accurate wide range analysis, different sets of thickness assumptions were made which are given in Table 2.6. The thickness of HMA was considered on the basis of section 460.3.2 of the standard specification of WisDOT, from online. The thickness of HMA was assumed as 2" for the first set of assumptions and 3" for the second, third, and the fourth sets of assumptions. In the fourth set of assumptions the base was taken as 6" and the subbase was taken as 9". The thickness of the subgrade was assumed as 212" for all sets of assumptions. The Poisson's ratios were taken as 0.35 for all layers, which is typical for all layers.

Table 2.6. Thickness for USH 18

USH 18							
First set of assumption		Second set of assumption		Third set of assumption		Fourth set of assumption	
HMA	2''	HMA	3''	HMA	3''	HMA	3''
Concrete layer	9''	Concrete layer	9''	Base and subbase	15''	Base	6''
Base and subbase	15''	Base and subbase	15''			Subbase	9''

The results of the tasks outlined in section 1.4, are presented in the following chapters.

3.0. Analysis Based on Tensile Strain and Stiffness Parameters

3.1. Tensile Strain at Bottom of the HMA Layer for Distress Analysis

The tensile strain at the bottom of the AC layer (ϵ_{AC}) for full depth pavements and aggregate base pavements can be determined from AUPP using the relationship developed by Thompson [1989, 1995]. The AUPP were found using the following equation:

$$AUPP = \frac{1}{2} (5d_0 - 2d_{12} - 2d_{24} - d_{36}) \quad [3.1]$$

where:

AUPP= Area under Pavement Profile in mils

d_0 = deflection at the center of the loading plate in mils

d_{12} = deflection at 12 in. from the center of the loading plate in mils

d_{24} = deflection at 24 in. from the center of the loading plate in mils

d_{36} = deflection at 36 in. from the center of the loading plate in mils

For aggregate base pavements, the relationship between the tensile strain at the bottom of the AC layer and the AUPP is as follows:

$$\text{Log}(\epsilon_{AC}) = 0.821 \log(AUPP) + 1.210 \quad [3.2]$$

where:

ϵ_{AC} = strain at the bottom of the asphalt layer, microstrain

Garg and Thompson (1998) found that AUPP is an important deflection basin parameter that can be used to predict the tensile strain at the bottom of the AC layer accurately ($R^2 = 0.9319$).

I 94 EB

According to the intensity of distress data, given by WisDOT, both sections D and E are high distress sections. The average tensile strain (with 95% confidence interval) at the bottom of the HMA layer of sections D and E are higher than other sections, as shown in Figure 3.1. The 95% confidence interval indicates that 95 percent of the values will be within the interval. On the other hand the average ϵ_{AC} are lower for sections A and G, which are no distress sections and sections B and F, which are low distress sections, as given by WisDOT.

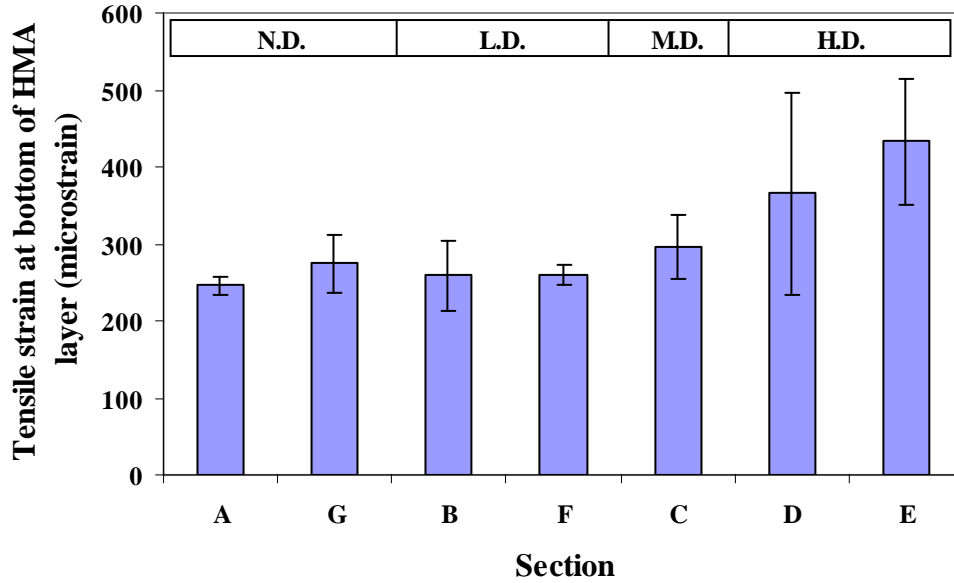


Figure 3.1. Tensile strain at bottom of HMA layer (ϵ_{AC}) vs. sections (I-94 EB)

USH 18

Although sections B, A, and E are L.D, M.D., and H.D. sections respectively, the average tensile strain (with 95% confidence interval) at the bottom of the HMA layer of section B, A, and E are similar, which is shown as Figure 3.2. Both sections B and C are L.D. sections but the average tensile strain at the bottom of the HMA layer are not similar.

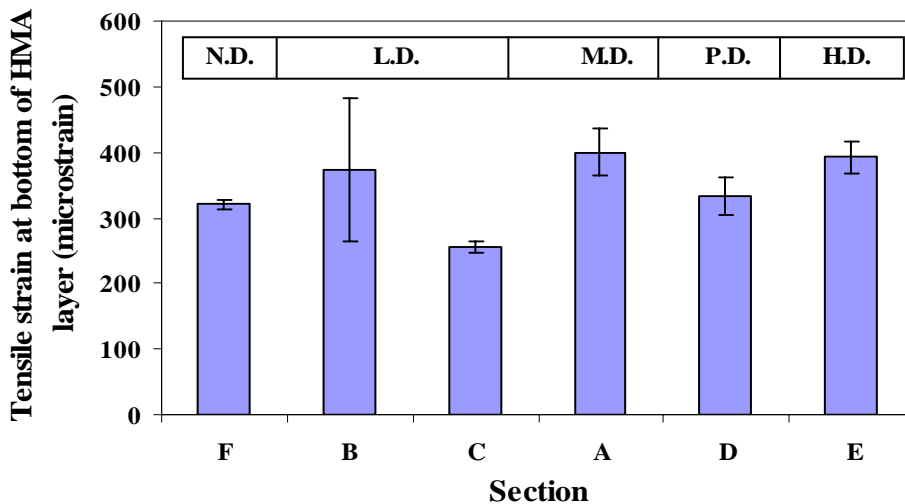


Figure 3.2. Tensile strain at the bottom of the HMA layer (ϵ_{AC}) vs. sections (USH 18)

High tensile strains occur at the bottom of the slipped layer. Pavement layers at either side of the interface move in different directions which causes slippage between the layers.

These high tensile strains further destroy the bond between the layers. As the average tensile strain of I-94 EB increases and the intensity of the distress increases, the distress might be due to slippage of the top HMA layer.

But in the case of USH 18, the average tensile strains are similar for different intensity of distresses. One possible reason may be that the slippage happened at the shoulder but FWD might be taken on the main line. From the data provided, it is not very clear where the distress is occurring.

3.2. AREA and Surface Flexural Rigidity for Distress Analysis

3.2.1. AREA

The actual pavement response to a load can be determined from field deflections generated and detected by nondestructive test (NDT) equipment. Changes in the pavement deflections predicted by the elastic layer theory and in the corresponding deflection basins were examined by (Shahin et al., 1987) as a possible means of detecting layer slippage. Layer slippage increases the predicted deflections and reduces the AREA deflection basin area at all points examined.

The AREA of the normalized deflection basin was also analyzed for the feasibility of using it in layer slippage detection. The AREA is determined using the following equation:

$$AREA = 6 + 12 \frac{d_{12}}{d_0} + 12 \frac{d_{24}}{d_0} + 6 \frac{d_{36}}{d_0} \quad [3.3]$$

where:

$AREA$ = area of the normalized deflection basin in mils

d_0 = deflection at the center of the loading plate in mils

d_{12} = deflection at 12 in. from the center of the loading plate in mils

d_{24} = deflection at 24 in. from the center of the loading plate in mils

d_{36} = deflection at 36 in. from the center of the loading plate in mils.

I-94 EB

According to the intensity of the distress data given by WisDOT, both sections A and G are no distress sections of I-94 EB, but the average AREA (with 95% confidence interval) of sections A and G are not similar, as shown in Figure 3.3. On the other hand, the average AREA of sections D and G are similar, as shown in Figure 3.3, although section D and G are high distress and no distress sections respectively.

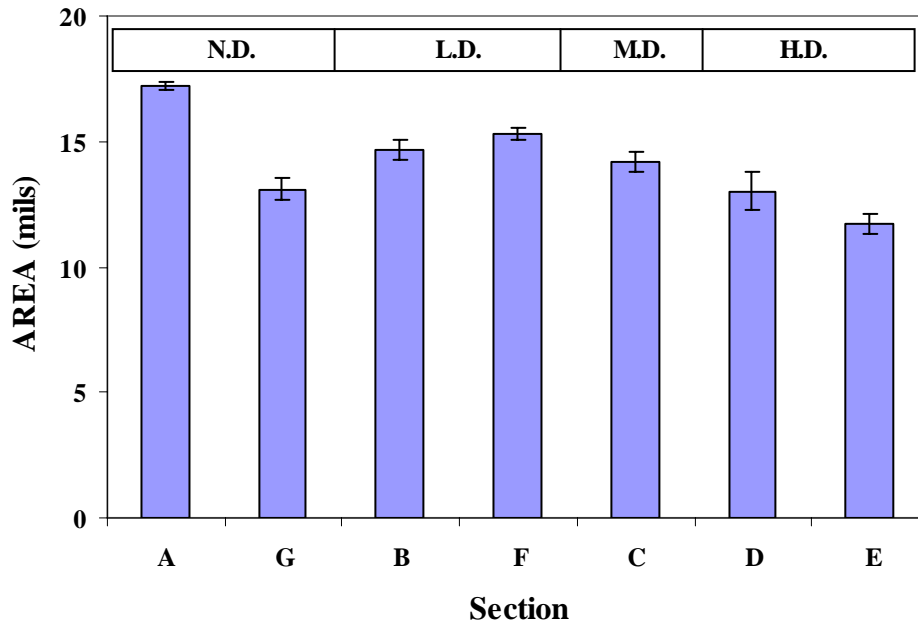


Figure 3.3. AREA vs. sections (I-94 EB)

USH 18

Both sections B and C are no distress sections of USH 18, but the average AREA (with 95% confidence interval) of sections B and C are not similar, as shown in Figure 3.4. On the other hand, the average AREA of sections A, D, and E are similar, as shown in Figure 3.4, although sections A, D, and E are the M. D, P. D, and H. D. sections respectively.

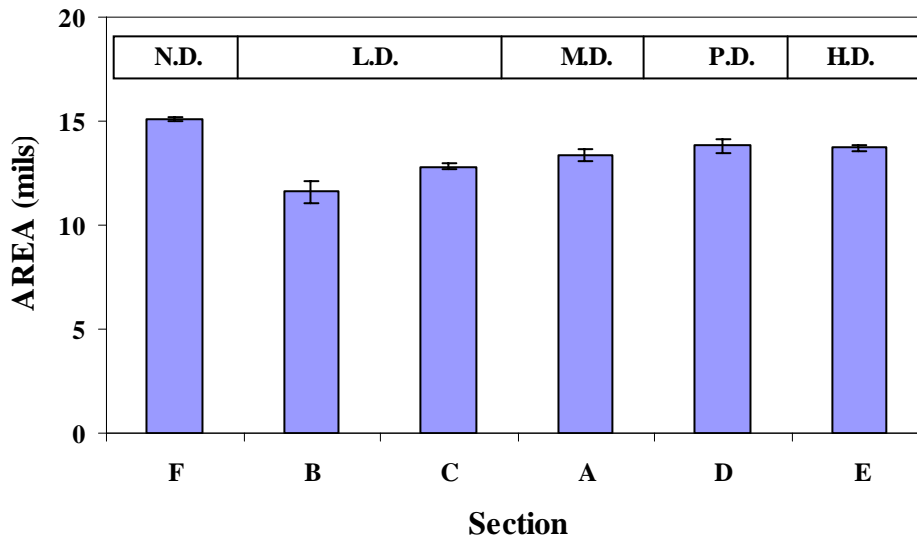


Figure 3.4. AREA vs. sections (USH 18)

As mentioned before, the layer slippage reduces the AREA deflection basin area. But the AREA of section G (L.D.) and D (H.D.) of I 94 EB are similar and section A (N.D.) and G

(N.D.) of I 94 EB are not similar. In the case of USH 18, the average AREA of low distress sections is lower than the M.D, P.D., and the H.D. sections. This is because the deflection basin AREA is influenced by the stiffness and the thickness of the entire pavement. Therefore, AREA does not correlate with slippage failure, which is primarily influenced by the layers between which the slippage is occurring.

3.2.2. Surface flexural rigidity (ET^3)

Surface flexural rigidity represents the overall stiffness of the pavement.

I-94 EB

In Figure 3.5, the average surface flexural rigidity of sections B and F (L.D.) of I-94 EB are higher than the average surface flexural rigidity of sections A and G, (N.D.). On the other hand, according to the given WisDOT data, sections D and E are high distress sections, but the average surface flexural rigidity of sections D and E are not similar, as shown in Figure 3.5.

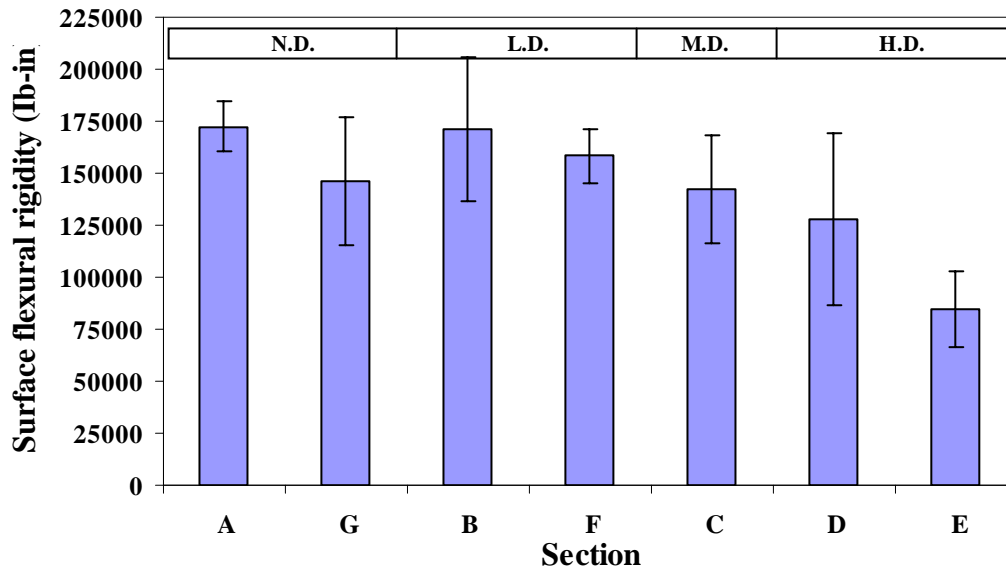


Figure 3.5. Surface flexural rigidity vs. sections (I-94 EB)

USH 18

Both sections B and C of USH 18 are low distress sections but the average surface flexural rigidity of sections B and C are not similar, which is shown as Figure 3.6. The average surface flexural rigidity of sections A and E are similar, although sections A and E are M.D. and H.D. sections respectively.

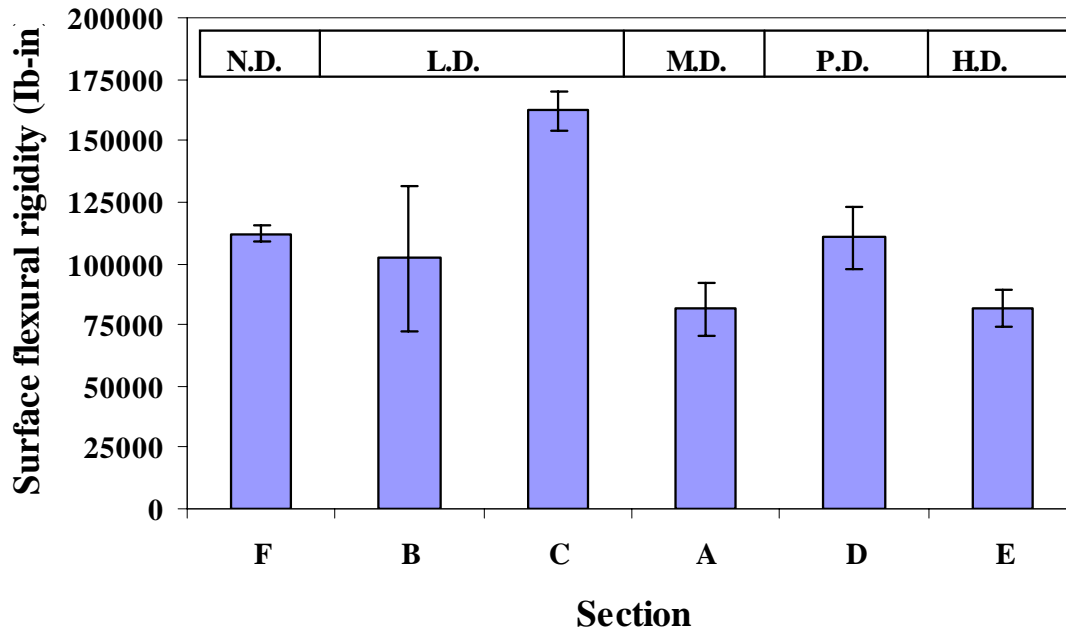


Figure 3.6. Surface flexural rigidity vs. sections (USH 18)

Surface flexural rigidity is the stiffness of the entire pavement system. The factors affecting the slippage are the stiffness of the top HMA, the stiffness of the layer below the HMA, and the bond between the layer and the thickness of the top HMA. If the distress is due to slippage of the top HMA layer, in that case the surface flexural rigidity may not be able to detect such type of distress. This may be the reason for the poor correlation between the calculated surface flexural rigidity with observed intensity of distress, given by WisDOT. Therefore, it is necessary to estimate the stiffness of the top HMA layer.

3.3. Conclusions

The following was found after analyzing the I-94 EB and USH 18 of WisDOT.

- 1) Distresses observed by WisDOT correlated with the tensile strain at the bottom of asphalt concrete for I-94 EB, which were indicative of slippage failure. But distresses observed by WisDOT did not correlate with the tensile strain at the bottom of the asphalt concrete for USH 18. This may be because the distress was observed in the shoulders but FWD might be taken along the main lane.
- 2) Distresses observed by WisDOT for both I-94 EB and USH 18 did not correlate with parameters such as AREA and the surface flexural rigidity because these parameters are influenced by the stiffness and the thickness of the entire pavement system.

4.0. Backcalculation of the Pavement Layer Stiffness

4.1. Backcalculation of the Pavement Layer Stiffness

Backcalculation is the “inverse” problem of determining material properties of pavement layers from its response to surface loading (Mehta and Roque, 2003). Through backcalculation the pavement layer stiffness was calculated. The common idea in backcalculation is to match the measured surface deflections with the estimated surface deflections, accomplished by adjusting the layer stiffness to change the shape of the estimated surface deflection basin. An important input parameter in backcalculation is the interface condition. During the backcalculation analysis no distress sections were considered as full bond interface conditions, whereas high distress sections were considered as full slip interface conditions. Several backcalculation programs are available such as BISDEF, CHEVDEF, EFROMD2, ELMOD, BAKFAA, MODULUS etc. In this study BAKFAA (FAA, 2000) is used for the calculation of stiffness of all layers of the pavement. As mentioned before, the objective of this study is to provide a recommendation during design to minimize slippage cracking. The next step towards this is to obtain the stiffness of the pavement layers for both the no distress and the high distress sections.

4.2. Stiffness of Pavement Layers

4.2.1. I-94 EB

In BAKFAA, the stiffness of the different layers were calculated for different sections. If the numbers of layers of the pavement are more, the computer program might give more accurate results. As the number of layers increase, the backcalculation program might fit the measured and the calculated deflection basin more accurately. However, this does not ensure that the backcalculated stiffness is accurate. On the contrary, as the number of layers increase the ability of the program to obtain accurate stiffness reduces because there are more parameters available to the program to fit the basin. This leads to many solutions making it difficult to determine the actual stiffness in the pavement, especially when independent data to verify these values are not available. One way to minimize the above-mentioned problem is to combine the lower layers. It was recognized that as the layers below the concrete layer are further away from the interface, their properties are not so critical for interlayer bonding and hence they were combined to hone-in on a more realistic backcalculated value. Hence, to obtain a unique solution of stiffness in BAKFAA, during analysis the layer of the base and the subbase were combined to one layer. The thickness of the subgrade was assumed as 212”.

No distress section

As mentioned before, section A is a no distress section, according to the intensity of the distress observed by WisDOT. The process is outlined in the following steps:

- 1) For the full bond condition the stiffness of HMA and all other layers is calculated.

2) For the full slip assumption the stiffness of the top HMA are calculated, keeping the stiffness of all the other layers constant (the stiffness values of the other layers are obtained from the above step).

The stiffness of all the layers of section A (N.D.) for the full bond condition is shown in Figure 4.1.

Initially the stiffness of all the layers were allowed to be calculated by the program in full slip assumption. However, this leads to the stiffness of the HMA for the full slip assumption which was a lot lower than the full bond condition. The concrete layer showed an exactly reverse trend (swapping was occurring). In some cases there was swapping between the concrete layer and the combined base and the subbase layer. These results appeared to show that the values were counterintuitive and hence incorrect. To avoid this problem, the lower layers were kept constant between the full bond condition and the full slip assumption. Even though, their stiffness values may not be similar, their assumptions were realistic in-lieu of the trends observed between the layers when they were allowed to be calculated by the program. The stiffness of all layers of section A (N.D.) for the full slip assumption is shown in Figure 4.2.

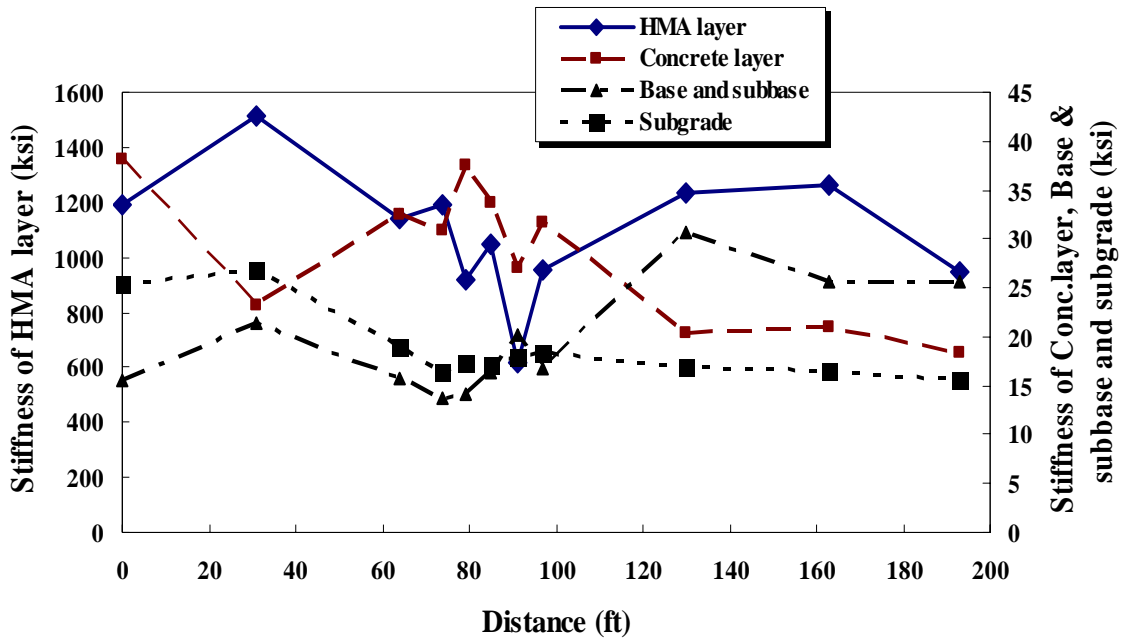


Figure 4.1. Stiffness vs. distance (N.D, I-94 EB, F.B., actual)

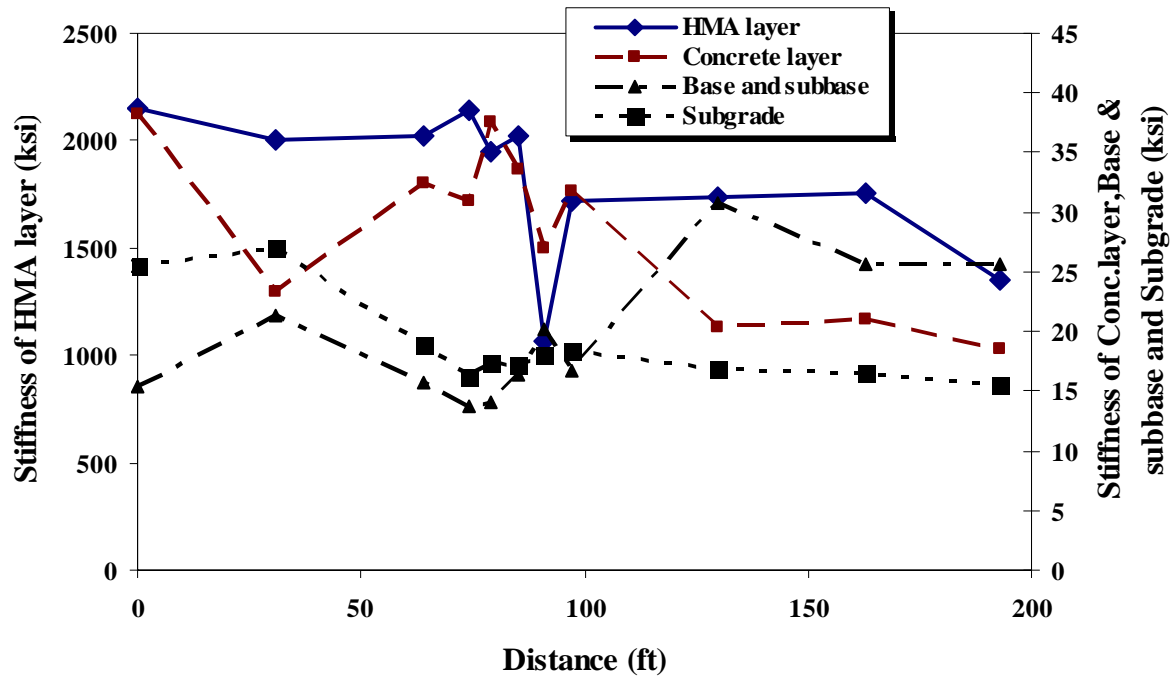


Figure 4.2. Stiffness vs. distance (N.D, I-94 EB, F.S., assumption)

High distress section E

The process is outlined in the following steps:

- 1) For the full slip condition the stiffness of the HMA and all other layers are calculated.
- 2) For full bond assumption the stiffness of the top HMA is calculated, keeping the stiffness of all the other layers constant (the stiffness values of the other layers are obtained from the above step).

The stiffness of all the layers of section E (H.D.) for the full slip condition and the full bond assumptions are shown in Figures 4.3 and 4.4, respectively.

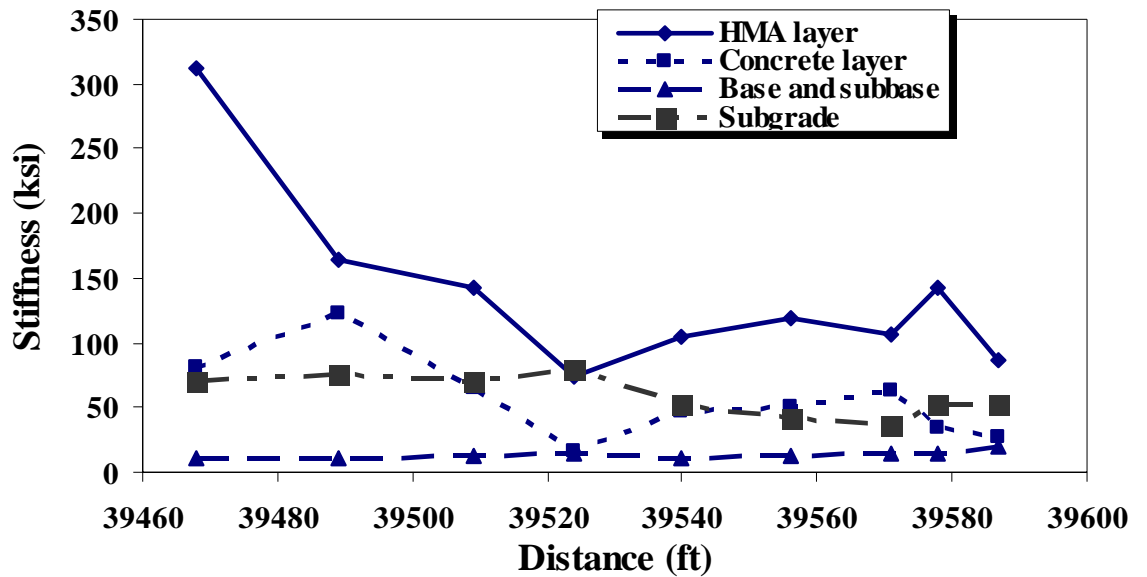


Figure 4.3. Stiffness vs. distance (H.D. I-94 EB, F.S., actual)

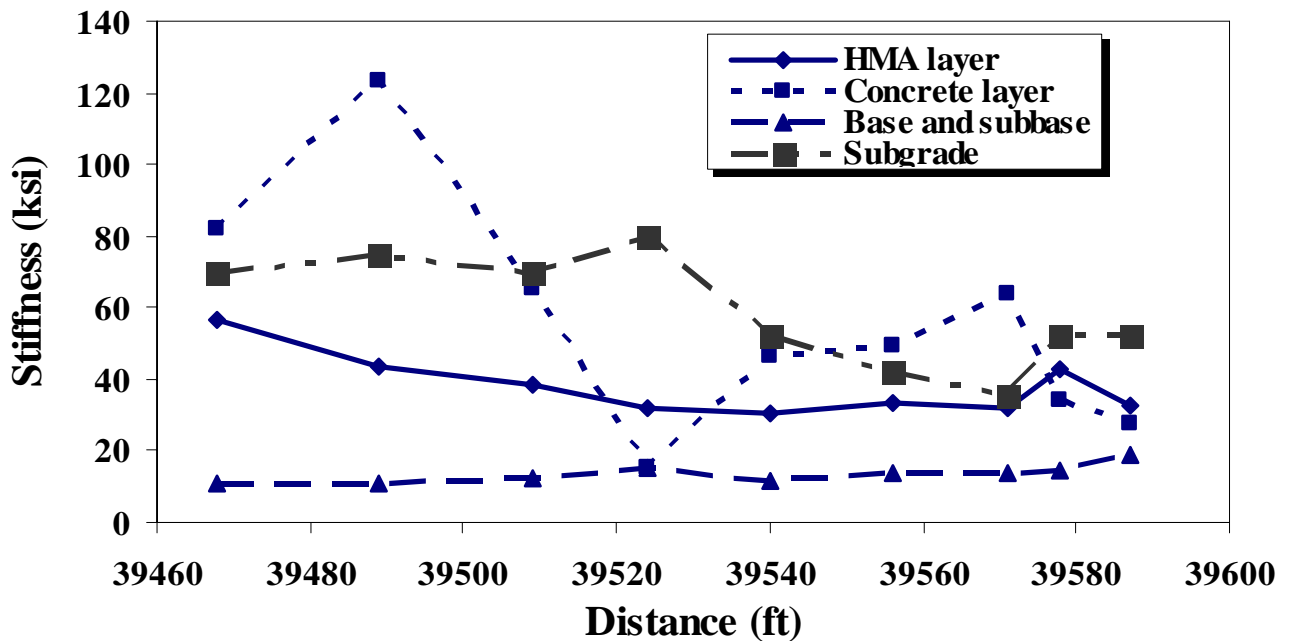


Figure 4.4. Stiffness vs. distance (H.D. I-94 EB, F.B., assumption)

In I-94 EB, it was observed that the stiffness ratio between the top two layers (23-65) for the no distress sections were higher than that of the high distress sections (1-5), which is shown as Figure 4.5.

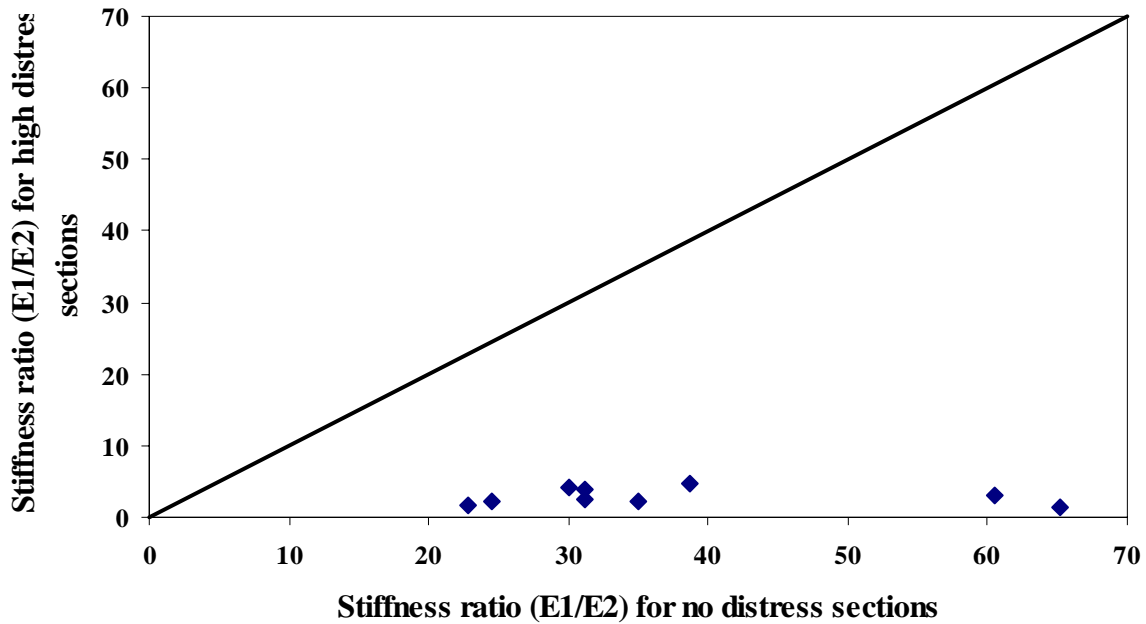


Figure 4.5. Stiffness ratio (E_1/E_2) for no distress vs. high distress sections (I-94 EB)

4.2.2. USH 18

4.2.2.1. Stiffness of the pavement layers for the first set of assumptions

No distress section F

The stiffness of all layers of USH 18 were calculated using the BAKFAA software program. The stiffness of all layers of section F (N.D.) for the full bond condition and the full slip assumption are shown in Figures 4.6 and 4.7, respectively. The “Actual” in the figure labels refer to the field condition of the road. For example, Figure 4.6 shows that the section was a no distress (N.D.) section and the analysis was done for the Full Bond (F.B.) condition which reflects the actual condition of the no distress observed in the field. On the other hand, Figure 4.7 shows that the analysis was done on a no distress section with a full-slip assumption which is contrary to what was observed in the field.

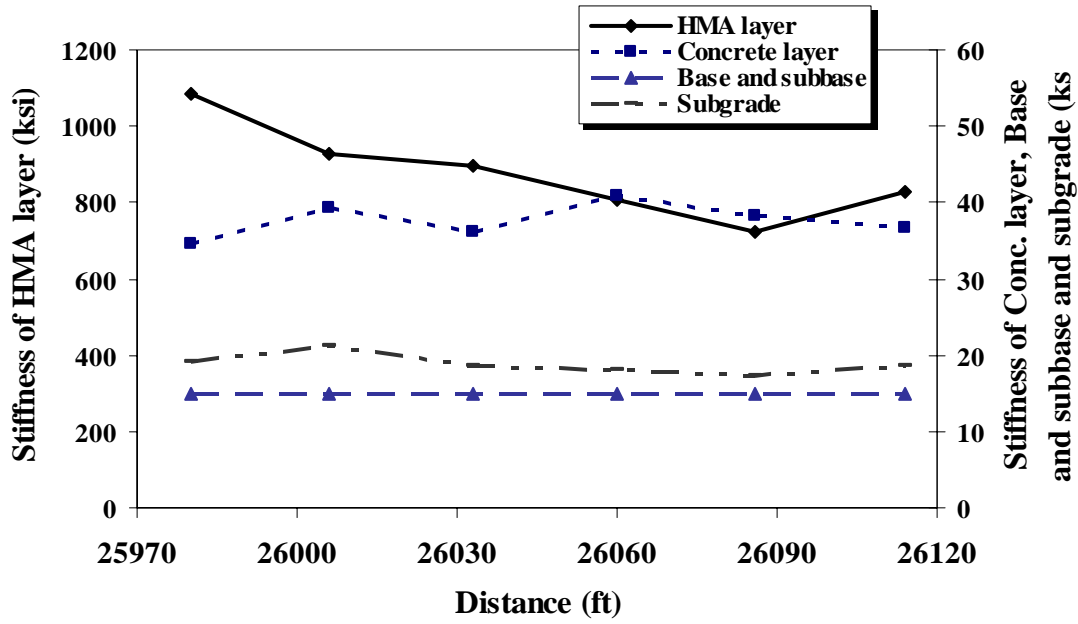


Figure 4.6. Stiffness vs. distance (N.D. USH 18, F.B., actual)

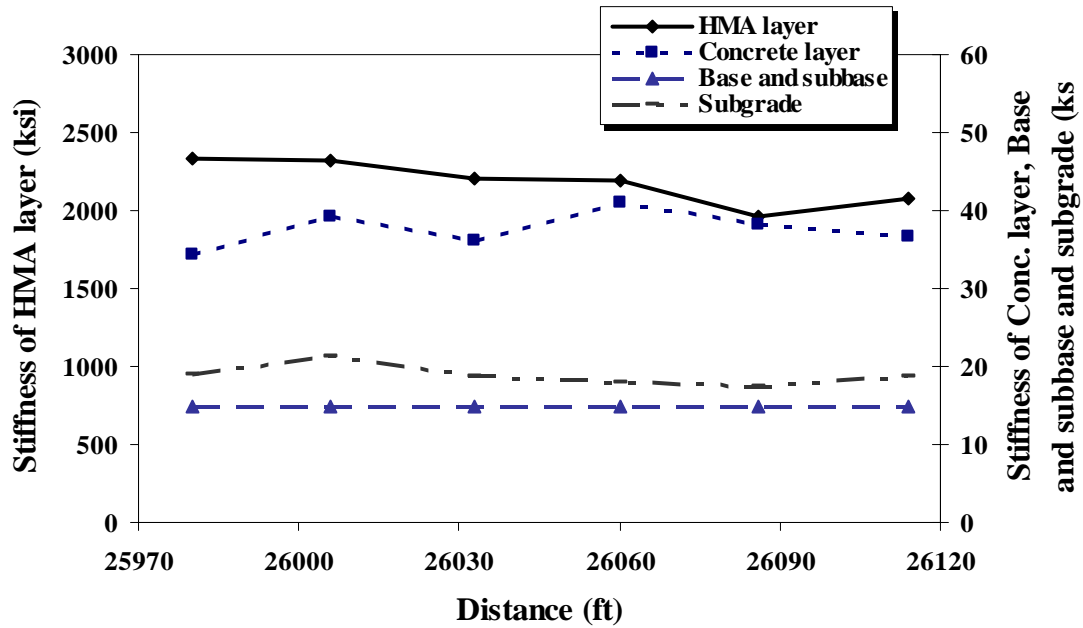


Figure 4.7. Stiffness vs. distance (N.D. USH 18, F.S., assumption)

High distress section E

The stiffness of all layers of the high distress section for the full slip condition and the full bond assumption are shown in Figures 4.8 and 4.9, respectively.

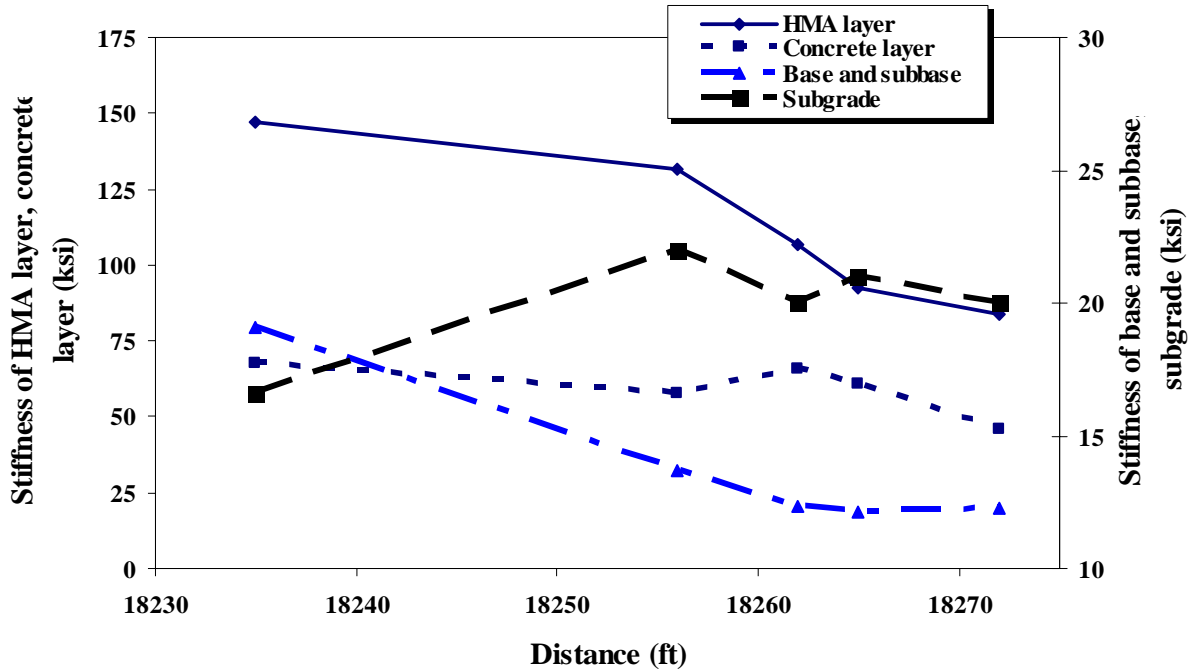


Figure 4.8. Stiffness vs. distance (H.D. USH 18, F.S., actual)

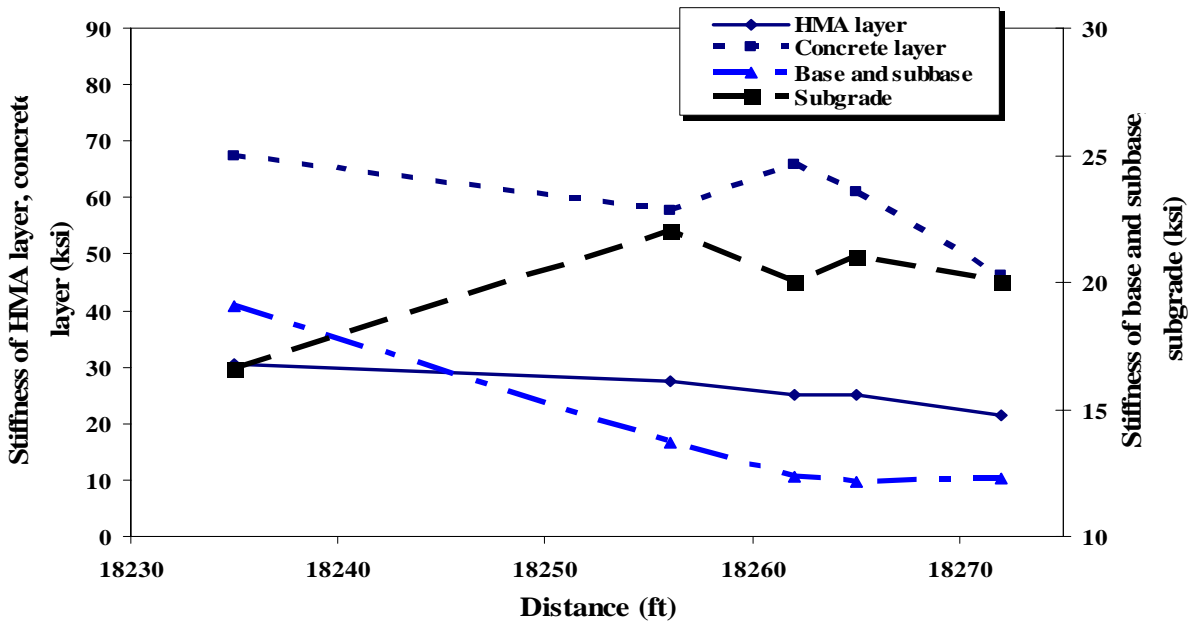


Figure 4.9. Stiffness vs. distance (H.D. USH 18, F.B., assumption)

4.2.2.2. Stiffness of the pavement layers for the second, third, and the fourth sets of assumptions

Instead of representing by figures, the results of the analysis for the second and the third sets of assumptions are summarized in Table 4.1. The results of the analysis for the first set of assumptions are also included in Table 4.1. The results of the analysis for the fourth set of assumptions are summarized in Table 4.2.

Table 4.1. Analysis of USH 18 for assumptions 1, 2, and 3.

		Station (ft)	Stiffness (ksi)					RMSE, mils		P.D./E ₁	E ₁ /E ₂
			HMA (F.B.)	HMA (F.S.)	Concrete layer	Base and Subbase	Subgrade	F.B.	F.S.		
Ass.1	N.D.	25980	1086	2335	34	15	19	0.30	0.73	0.11	31
		26006	926	2324	39	15	21	0.34	0.74	0.16	24
		26033	897	2202	36	15	19	0.34	0.78	0.16	25
		26060	808	2191	41	15	18	0.32	0.83	0.21	20
		26086	722	1966	38	15	17	0.43	0.99	0.24	19
		26114	827	2075	37	15	19	0.27	0.73	0.18	23
	H.D.	18235	30	147	67	19	17	0.88	0.91	0.54	2
		18256	27	132	58	14	22	0.51	0.35	0.60	2
		18262	25	107	66	12	20	0.56	0.45	0.72	2
		18265	25	93	61	12	21	0.72	0.63	0.79	2
18272		22	84	46	12	20	0.56	0.40	0.89	2	
Ass.2	N.D.	25980	356	804	32	15	19	0.31	0.74	0.35	11
		26006	269	806	40	15	19	0.44	0.89	0.74	7
		26033	311	749	33	15	19	0.35	0.80	0.45	9
		26060	270	744	39	15	18	0.35	0.86	0.65	7
		26086	185	604	40	15	18	0.43	0.94	1.23	5
		26114	293	723	34	15	19	0.28	0.76	0.50	9
	H.D.	18235	43	165	51	17	23	0.54	0.27	1.71	3
		18256	42	165	44	15	22	0.61	0.27	1.75	4
		18262	49	194	41	15	21	0.61	0.24	1.53	5
		18265	46	180	40	14	21	0.71	0.43	1.60	4
18272		36	132	34	13	20	0.61	0.26	2.03	4	
Ass.3	N.D.	25980	511	823		22	19	0.17	0.55	0.12	23
		26006	452	772		26	18	0.25	0.64	0.16	18
		26033	423	746		24	17	0.24	0.68	0.18	17
		26060	440	779		25	18	0.16	0.63	0.18	17
		26086	314	597		27	17	0.21	0.68	0.29	12
		26114	453	753		23	18	0.13	0.56	0.15	20
	H.D.	18235	35	84		41	24	1.20	1.01	1.68	2
		18256	31	57		40	23	1.59	1.36	1.49	1
		18262	31	73		37	22	1.48	1.28	1.83	2
		18265	32	74		34	22	1.46	1.27	1.79	2
18272		30	78		27	21	1.43	1.22	2.01	3	

Table 4.2. Analysis of USH 18 for assumption 4

		Station (ft)	Stiffness (ksi)					RMSE, mils		P.D./E ₁	E ₁ /E ₂
			HMA (F.B.)	HMA (F.S.)	Base	Subbase	Subgrade	F.B.	F.S.		
Ass.4	N.D.	25980	311	819	42	15	19	0.34	0.74	0.52	7
		26006	278	908	51	15	18	0.52	0.97	0.82	5
		26033	291	790	42	15	18	0.39	0.73	0.59	7
		26060	256	875	51	15	18	0.46	0.95	0.95	5
		26086	233	791	47	15	17	0.59	1.12	1.02	5
		26114	255	761	44	15	18	0.32	0.78	0.78	6
	H.D.	18235	63	283	50	18	22	0.41	0.11	1.24	6
		18256	65	275	43	15	22	0.48	0.11	1.17	6
		18262	67	289	42	15	20	0.50	0.09	1.16	7
		18265	58	246	41	15	21	0.61	0.25	1.30	6
		18272	52	175	30	15	21	0.72	0.36	1.36	6

4.2.2.3. Summary of the analyses of USH 18

The stiffness ratios between the top two layers of the no distress and the high distress sections for the different sets of assumptions are shown in Figure 4.10. The summary of the analyses of USH 18 for the different thickness assumptions are given below:

- 1) In USH 18 assumption 1, the stiffness ratios between the top two layers (19-31) for the no distress sections were higher than that of the high distress sections (1-3).
- 2) In USH 18 assumption 2, the stiffness ratios between the top two layers (5-11) for the no distress sections were higher than that of the high distress sections (3.26-4.69).
- 3) In USH 18 assumption 3, the stiffness ratios between the top two layers (12-23) for the no distress sections were higher than that of the high distress sections (1.42-2.83).
- 4) In USH 18 assumption 4, the stiffness ratios between the top two layers for the no distress sections were between 4.97 and 7.44 and for the high distress sections were between 5.65 and 6.83.

The different assumptions are related to different thickness assumptions that were made due to lack of structural data. Figure 4.10 appears to indicate that the stiffness ratio for the no distress section is significantly higher than that for the high distress section for the same pavement structure. This trend is true irrespective of the pavement structure. This comparison shows that the stiffness ratio can be correlated to distress.

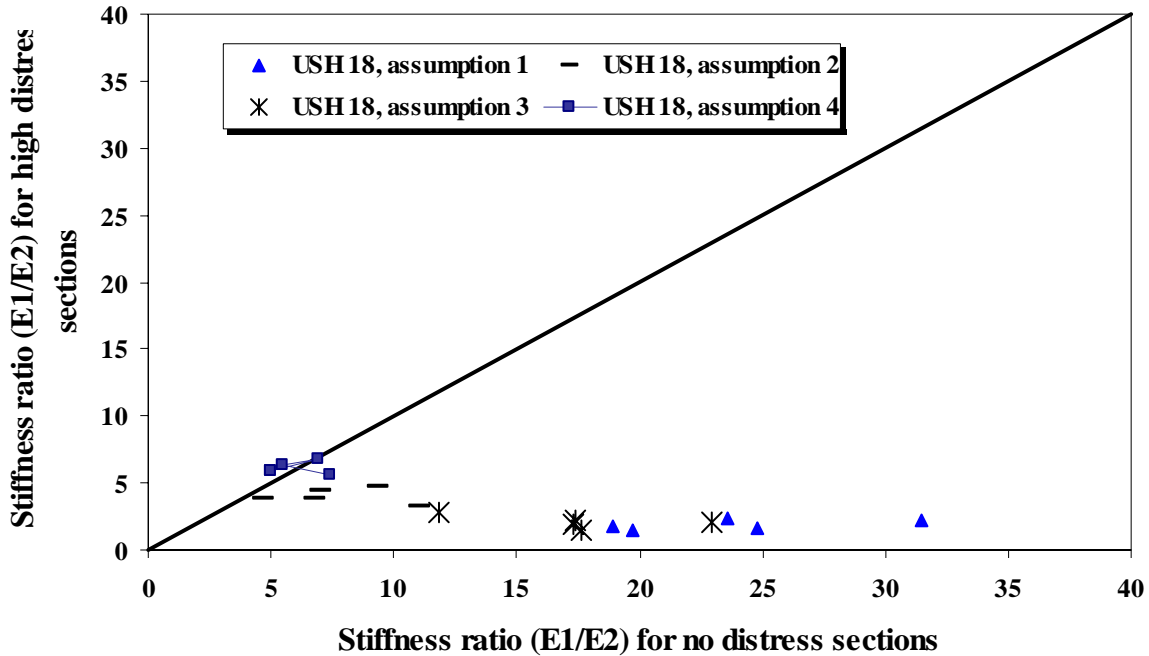


Figure 4.10. Stiffness ratio (E_1/E_2) for no distress vs. high distress sections (USH 18)

4.3. Evaluation of the Accuracy of Backcalculated Stiffness

The research team did not assume that stiffness values obtained from the BAKFAA program are accurate only because the fit between the measured and the calculated deflection is good (low RMSE). They took additional steps to ensure the accuracy of the stiffness data. Some of these are mentioned below.

4.3.1. Subgrade stiffness

The accuracy of the backcalculated stiffness is significantly affected by the seed value. To obtain reasonable seed values, at first the stiffness of the different layers were calculated by the program. In the FWD test, the deflections far away from the loading plate depend mainly on the stiffness of the subgrade. Then the analysis was done first by calculating the subgrade stiffness by manually changing it in the program to match the measured deflection at 60" (d_{60}). The inverse correlation between the backcalculated subgrade stiffness and the measured deflections at d_{60} for both I-94 EB and USH 18 were very good (the root mean square value of the curve was 0.98), which is shown as Figure 4.11. A good correlation indicates that the subgrade stiffness appropriately reflects the FWD deflection basin values.

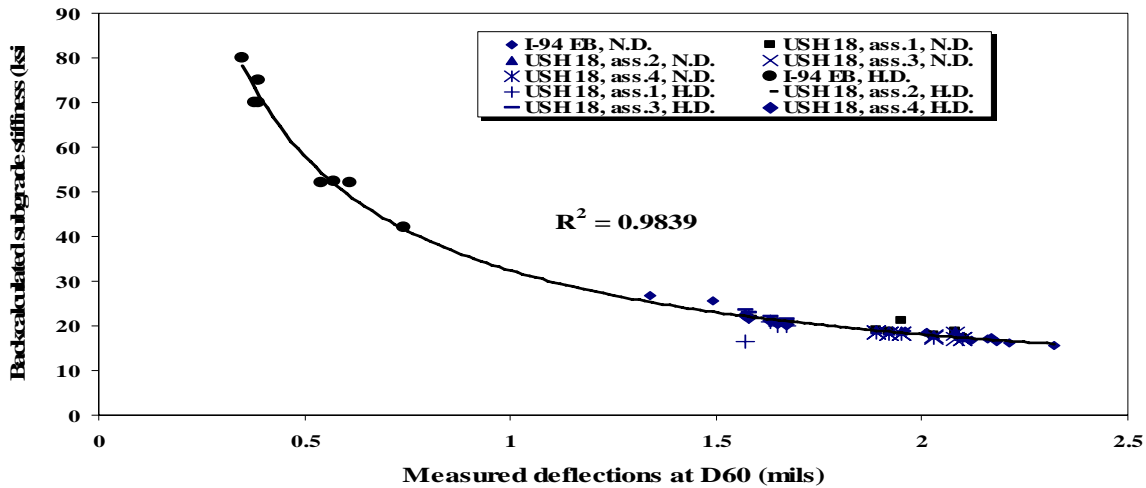


Figure 4.11. Backcalculated subgrade stiffness vs. the measured deflections at D₆₀

For both I-94 EB and USH 18, it was observed that the backcalculated subgrade stiffness was close (within 36%) to the values of the subgrade stiffness given by WisDOT, which is shown as Figure 4.12.

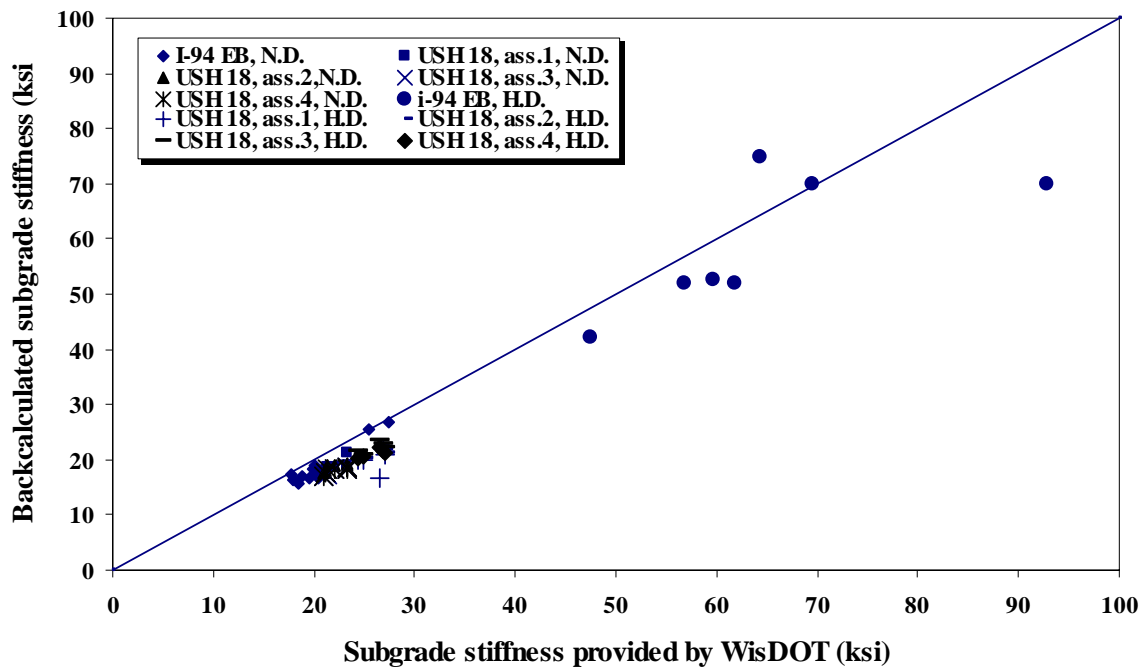


Figure 4.12. Backcalculated subgrade stiffness vs. the subgrade stiffness provided by WisDOT.

Therefore, from the above analysis and figures, it appears that the subgrade stiffness was reasonably accurate. In addition, almost all calculated stiffness (90%) of the base and the subbase were within the maximum and minimum range of the Facilities Development Manual of Wisconsin, which is shown as Table 4.3.

Table 4.3. Expected layer stiffness (Facilities Development Manual, Procedure 14-10-5, Wisconsin)

Layer	Minimum Expected E (ksi)	Maximum Expected E (ksi)
Base (crushed stone and Gravel)	21	30
Subbase (crushed stone and Gravel)	14	20
Base (concrete layer)	53	77
Subbase (concrete layer)	38	57
Base (pulverized HMA pavement)	21	85
Subbase (pulverized HMA pavement)	14	63

4.3.2. Swapping

Another important criterion for evaluating the accuracy of the backcalculated stiffness of different layers is to check for swapping. Along a pavement section, no relationship is observed between the stiffness of the different layers. As mentioned earlier, the backcalculation may not yield accurate or realistic stiffness values. One way to determine whether the values obtained are accurate or not is to conduct FWD testing along a section and analyze their variation of stiffness. In the field, the stiffness values are independent of each other and the unusual variation of the stiffness along a section may be an indication of incorrect value unless supported independently. Therefore, an analysis was conducted to determine whether a relationship exists between the stiffness values. If there is no relationship between the layers then the program did not swap the values between the layers. Swapping is a common mathematical artifact of testing measured and calculated deflection basins. But in this analysis swap was not observed between the stiffness of the concrete layer and that of the HMA layer for the full bond and the full slip condition. Swap was also not observed between the stiffness of the subgrade and that of the base and the subbase for section A (N.D.).

The research team feels confident about the base and the subbase values by ensuring that the values are within the range typically observed by WisDOT and addressing the issue of swapping which is commonly observed in backcalculation that often gives misleading backcalculated modulus values.

4.3.3. Root Mean Square Error (RMSE)

One of the most important parameters for evaluating the accuracy of the backcalculated stiffness is the degree of match between the measured and the calculated deflection. The degree of match is quantified by the root mean squared error. The Root Mean Squared Error (RMSE) is the square root of the mean square error, which can be represented as equation [4.1].

$$RMSE = \sqrt{\frac{\sum d_i^2}{n}} \quad [4.1]$$

where,

d_i = summation of the vertical differences of distance of points between measured and calculated curves

n = number of points.

The smaller the Mean Squared Error, the closer the fit is to the measured deflection data. Both I-94 EB and USH 18, the range of minimum to maximum root mean square error (RMSE) of the calculated deflection with the measured deflection from FWD was within 0.01 to 1.59 (F.B.) and .09 to 1.36 (F.S.), which is shown in Table 4.4.

Table 4.4. Root mean square error values for both I-94 EB and USH 18

Interface condition	Percentile	RMSE
F.B.	100	1.59
	90	0.88
	75	0.61
F.S.	100	1.36
	90	1.12
	75	0.80

For the full bond condition, the RMSE values for 75% of the total analysis were within 0.61 and for the full slip condition, the RMSE values for 75% of the total analysis were within 0.80, which is shown as Table 4.4. These are not the same as R-squared which has a range from -1 to +1.

The measured and the calculated deflections with the distance of sensors for the full bond condition are shown in Figures 4.13, 4.14, and 4.15 for the RMSE values 1.59, 0.88, and 0.61 respectively. The percentage differences of deflections between the measured and the calculated values are also shown in those figures.

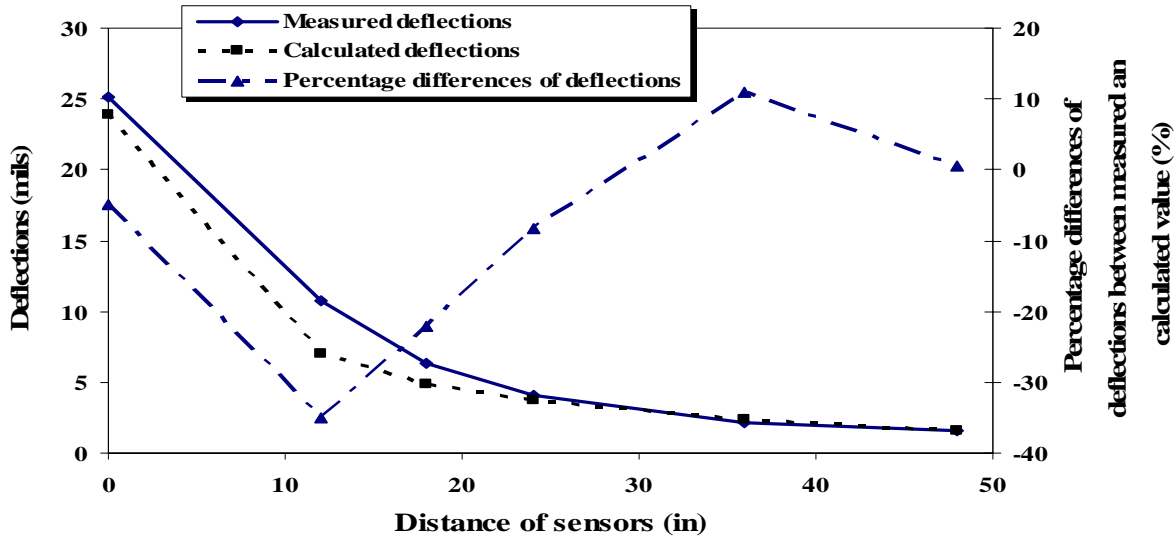


Figure 4.13. Deflections vs. the distance of sensors and the percentage differences of the deflections between the measured and the calculated values vs. the distance of sensors (RMSE 1.59, F.B.)

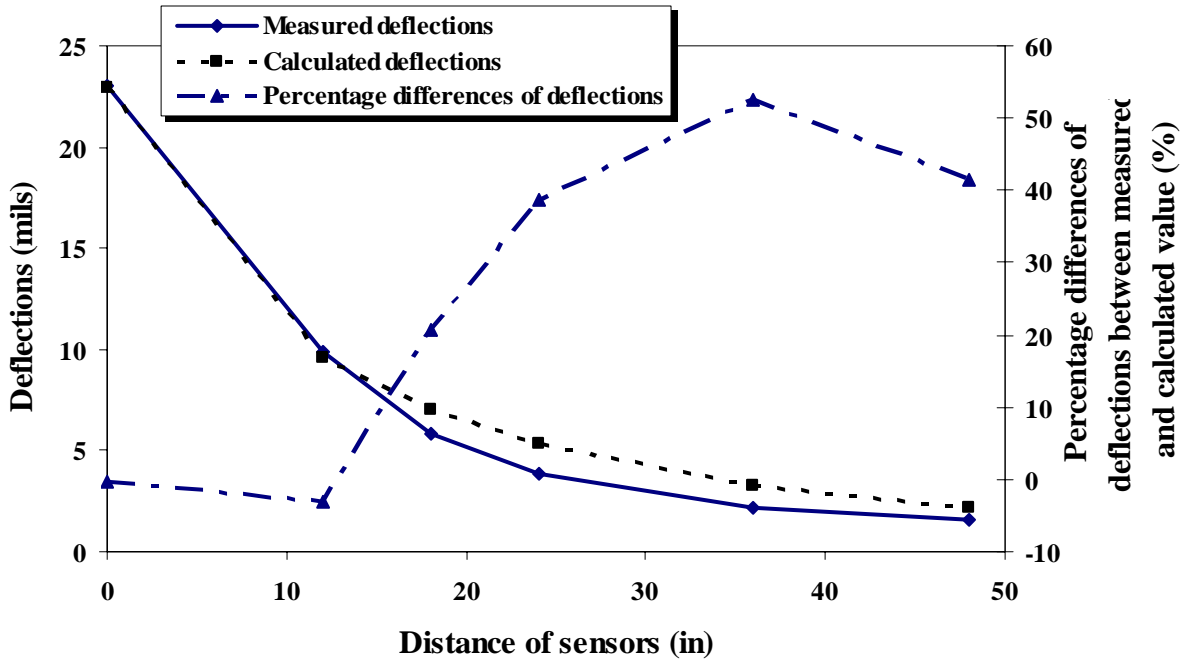


Figure 4.14. Deflections vs. the distance of sensors and the percentage differences of deflections between the measured and the calculated values vs. the distance of sensors (RMSE= 0.88, F.B.)

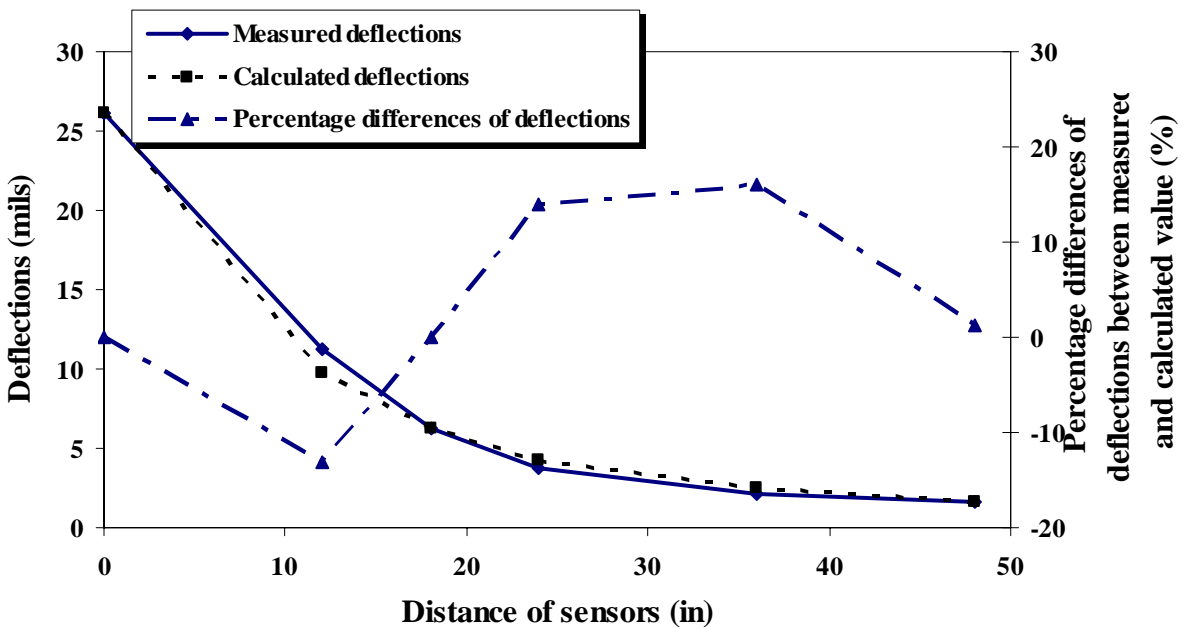


Figure 4.15. Deflections vs. the distance of sensors and the percentage differences of deflections between the measured and the calculated values vs. the distance of sensors (RMSE= 0.61, F.B.)

The measured and the calculated deflections with the distance of sensors for the full slip condition are shown in Figures 4.16, 4.17, and 4.18 for the RMSE values 1.36, 1.12, and

0.80 respectively. The percentage differences of deflections between the measured and the calculated values are also shown in those figures.

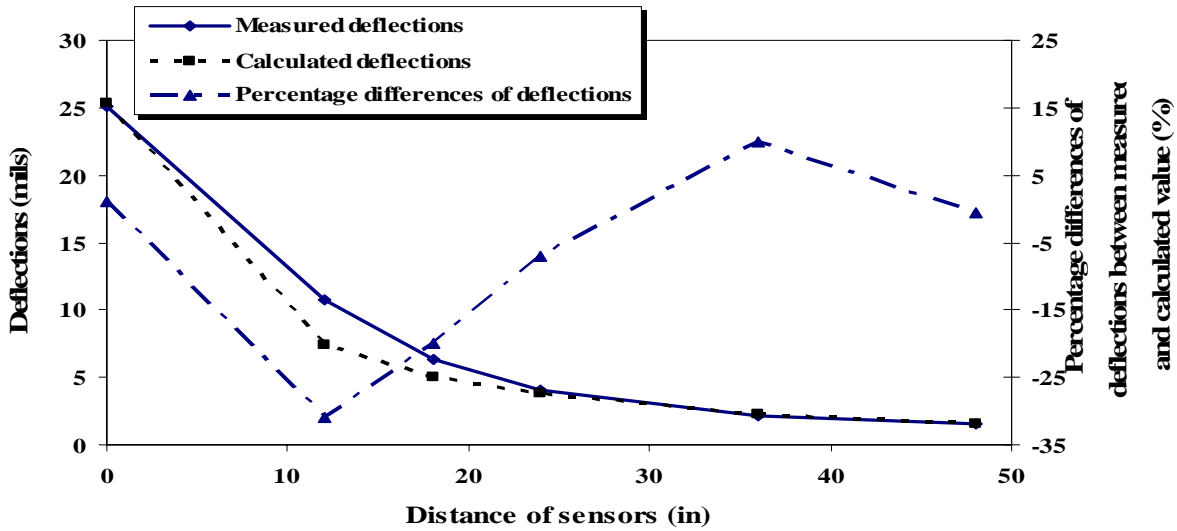


Figure 4.16. Deflections vs. the distance of sensors and the percentage differences of the deflections between the measured and the calculated values vs. the distance of sensors (RMSE= 1.36, F.S.)

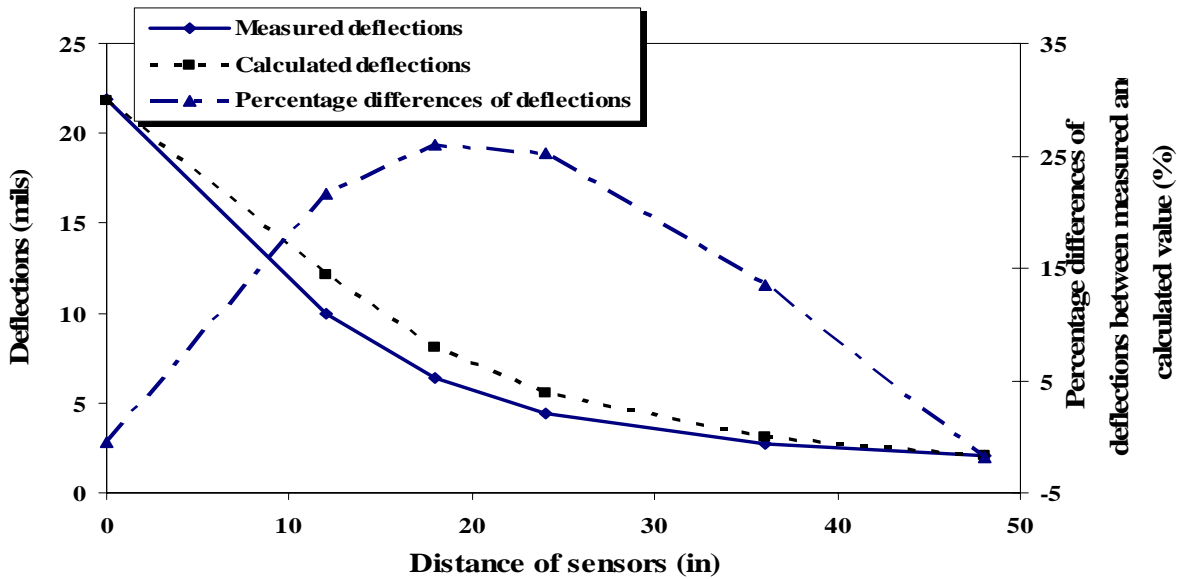


Figure 4.17. Deflections vs. the distance of sensors and the percentage differences of the deflections between the measured and the calculated values vs. the distance of sensors (RMSE= 1.12, F.S.)

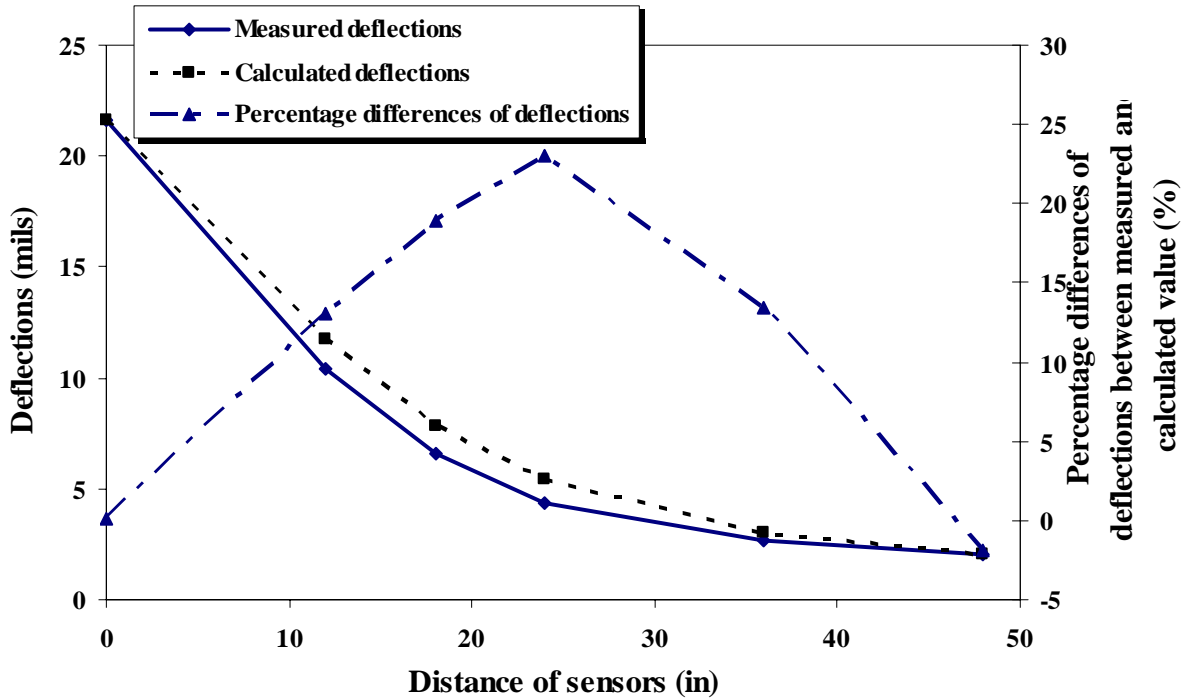


Figure 4.18. Deflections vs. the distance of sensors and the percentage differences of deflections between the measured and the calculated values vs. the distance of sensors (RMSE= 0.80, F.S.)

Figures 4.13-4.18 shows the accuracy of the fit between the measured and the calculated deflection basin. The researchers balanced the accuracy of the fit with the reasonableness of the moduli values that were provided and those obtained from structural coefficients (Table 4.3). These figures show the entire range of accuracy of the predicted and the measured values.

4.3.4. Variation of stiffness along the road for a Given Section

The variation of stiffness of each layer was analyzed along the roadway for each section. A premise was established that drastic changes in lower layers are highly unlikely. If there were any such changes the research team analyzed the data again for different loads and seed values. Once that was corrected, a similar analysis was done for surface layers.

It is well known that surface stiffness values are least accurate from the backcalculation of the FWD data. However, as observed above, the research team made extraordinary efforts to ensure that appropriate checks are in place so that the team members obtain reasonably accurate stiffness values.

The low RMSE values, the low percentage difference between the measured and the calculated deflection, a thorough evaluation of change in stiffness along the stations, and an independent evaluation of the stiffness of the lower layers gives the research team significant confidence in the accuracy of the surface layer. There was a significant discussion on the low concrete moduli values in the final presentation on August 15th, 2007. Even though these values are significantly lower, they are within the range as outlined in Table 4.3 and correlate

well with other values provided by WisDOT. In the absence of any other data, the PI has significant confidence in the values.

4.4. Summary of the Findings

The summary of the analysis for both I-94 EB and USH 18 based on the backcalculated layer stiffness are given below:

- 1) The stiffness ratios between the top HMA layer and the second layer below the HMA layer for no distress sections were between 5 to 65.
- 2) The stiffness ratios between the top HMA layer and the second layer below the HMA layer for high distress sections were between 1 to 7.

The stiffness ratio for the no distress section was higher than that for the high distress section and this was observed for all the sections where the second layer stiffness was greater than 20 ksi.

5.0. Combined Analysis of I-94 EB and USH 18

The following section describes the combined analysis of four assumptions of thicknesses of USH 18 and the actual thickness of I-94 EB.

5.1. Analysis Based on Percentage Differences of Stiffness with Stiffness Ratio

As mentioned before, the stiffness of the different layers were calculated for both no distress and high distress sections. In no distress sections, the stiffness was calculated for the full bond, which is the actual condition and assumed the full slip condition. Similarly, in high distress sections the stiffness was calculated for the full slip, which is the actual condition and the assumed full bond condition. The percentage differences of stiffness between the full bond and the full slip (P.D.) for no distress sections and high distress sections were calculated by using equations [5.1] and [5.2], respectively.

$$P.D_{F.B.} = \frac{E_{F.S.(assumption)} - E_{F.B.(actual)}}{E_{F.B.(actual)}} \times 100 \quad [5.1]$$

$$P.D_{F.S.} = \frac{E_{F.S.(actual)} - E_{F.B.(assumption)}}{E_{F.B.(assumption)}} \times 100 \quad [5.2]$$

The percentage differences of stiffness between the full bond and the full slip (P.D.) vs. the stiffness ratio (E_1/E_2) between the top two layers for the no distress section are shown in Figure 5.1. As the stiffness ratio increases, the percentage differences of stiffness between the full bond and the full slip decreases. Two zones were observed among these points. These two zones were represented by two series, which is also shown in Figure 5.1. For the same stiffness ratio the percentage differences of the stiffness between the full bond and the full slip for the points of one zone were higher than the points of the other zone.

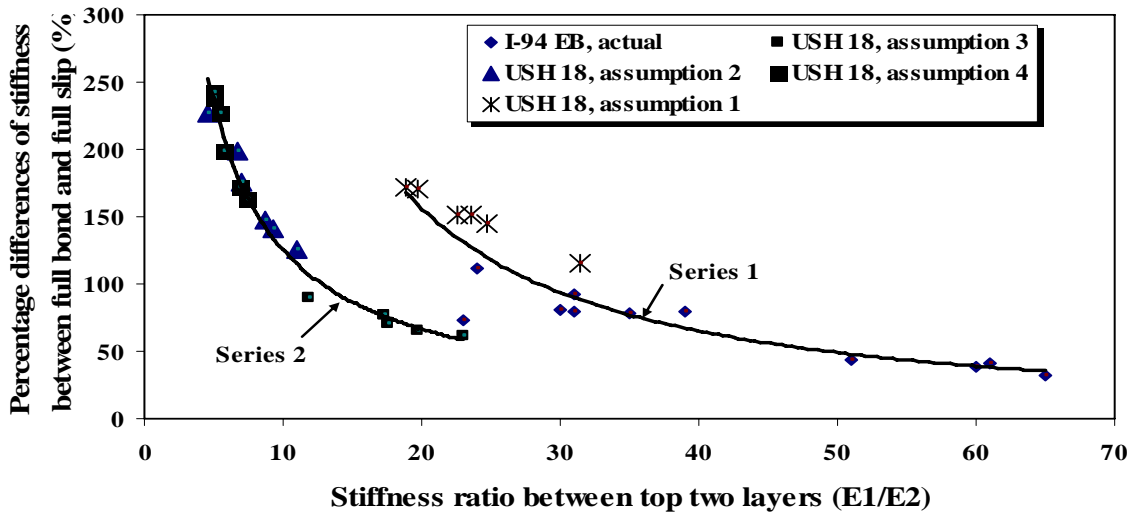


Figure 5.1. Percentage differences of stiffness between the full bond and the full slip vs. the stiffness ratio (E_1/E_2)

To identify the causes of distinction of P.D. (percentage differences of stiffness between the full bond and the full slip) of two series for the same stiffness ratio, the strain differences between the full bond and the full slip of two series were calculated for the same stiffness ratio, which is described in the following section.

5.2. Estimation of Strain Difference in KENLAYER

The strain differences between the full bond and the full slip were calculated in KENLAYER. Two stations with similar stiffness ratio were selected. These two stations were located in two series. One was station 26060' of USH 18, assumption 1, with a stiffness ratio 20 between the top HMA layer and second layer below the HMA layer. The other was station 26114' of USH 18, assumption 3, with a stiffness ratio of 20 between the top HMA layer and the second layer below the HMA layer.

For a stiffness ratio of 20, the differences of strain between the full bond and the full slip were 755 microstrains and 745 microstrains for two stations of two series, which were of similar magnitude. But for the stiffness ratio of 20, the percentage differences of the stiffness between the full bond and the full slip for two series were 171 and 66, which were not of similar magnitude.

This indicates that the effect of slippage was similar for both sections but the percentage difference alone showed that they would behave differently. The only difference between the two series was the stiffness values. The stiffness of the top layer in series 1 (stiffness range was 616 -1264 ksi) were significantly higher than that of series 2 (stiffness range was 185-511 ksi). Therefore, the percentage differences of stiffness were normalized by the stiffness of the top HMA layer. The findings of the normalized percentage differences of the stiffness with the stiffness ratio are described in the following section.

5.3. Normalized Percentage Differences of Stiffness with Stiffness Ratio

Normalized percentage differences of stiffness between the full bond and the full slip for both no distress and high distress sections were calculated by using equations [5.3] and [5.4], respectively.

$$\frac{PD}{E_1} (\text{for no distress section}) = \frac{P.D.}{E_{1(\text{actual full bond condition})}} \quad [5.3]$$

$$\frac{PD}{E_1} (\text{for high distress section}) = \frac{P.D.}{E_{1(\text{actual full slip condition})}} \quad [5.4]$$

The normalized percentage differences of stiffness between the full bond and the full slip of the no distress and high distress sections are plotted with the stiffness ratio between the top two layers, which are shown as Figure 5.2 and Figure 5.3 respectively.

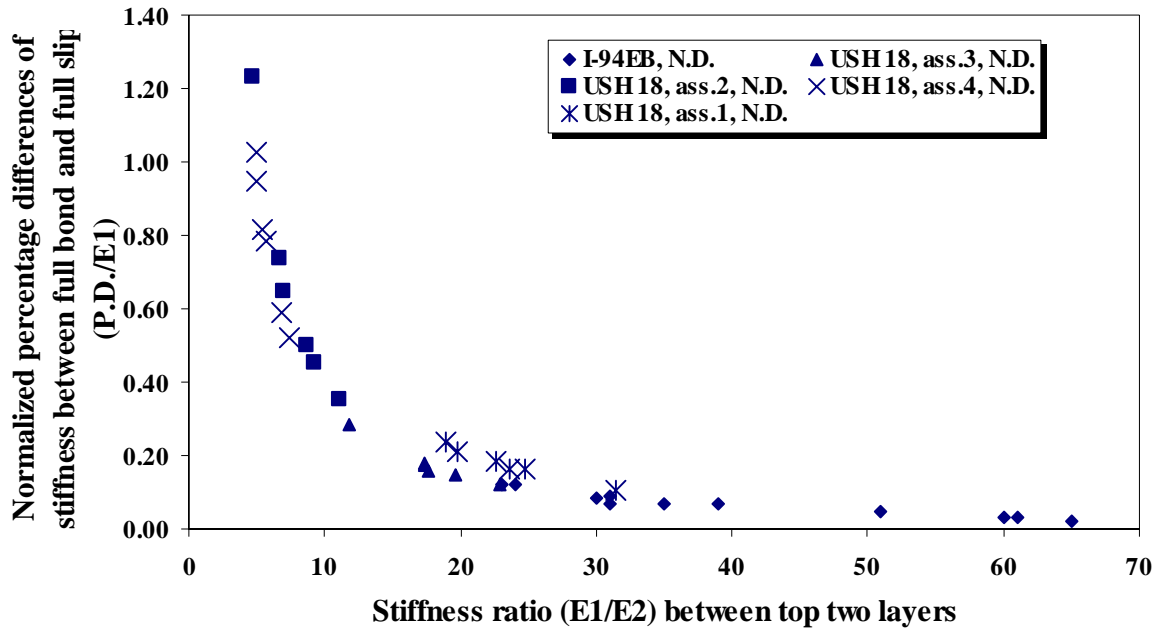


Figure 5.2. Normalized percentage differences of stiffness between the full bond and the full slip ($P.D./E_1$) vs. the stiffness ratio (E_1/E_2) for no distress sections.

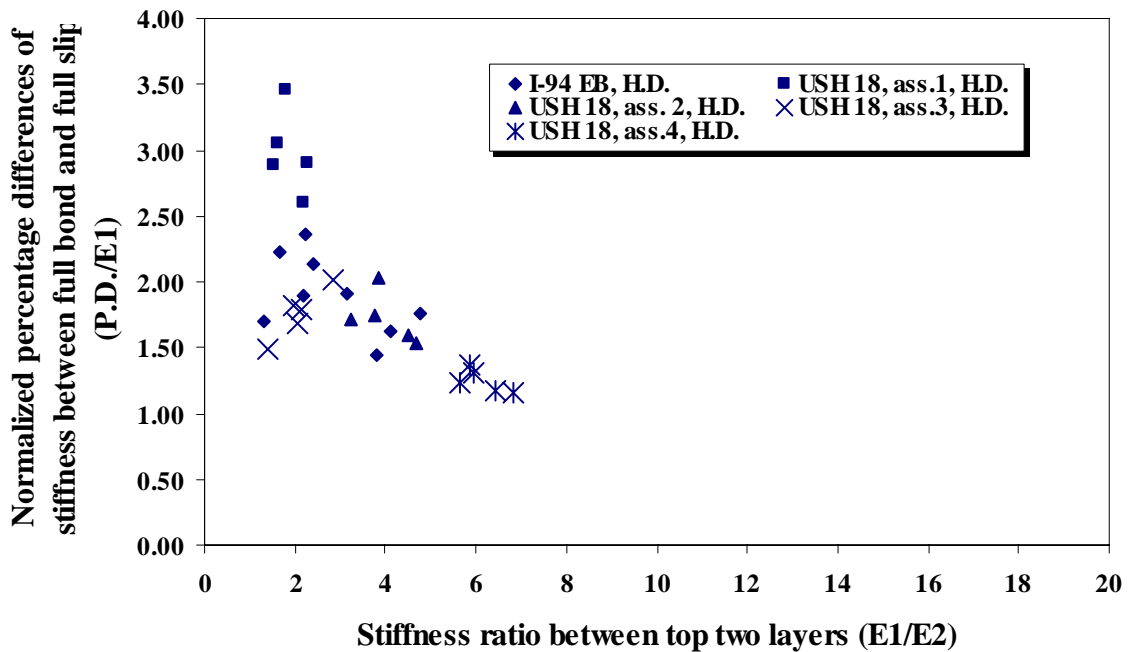


Figure 5.3. Normalized percentage differences of stiffness between full bond and full slip ($P.D./E_1$) vs. the stiffness ratio (E_1/E_2) for high distress sections.

Normalized percentage differences of stiffness between the full bond and the full slip for both the no distress and high distress sections were inversely correlated with the stiffness ratio and the root mean square value of that correlated curve was 0.94, shown as Figure 5.4.

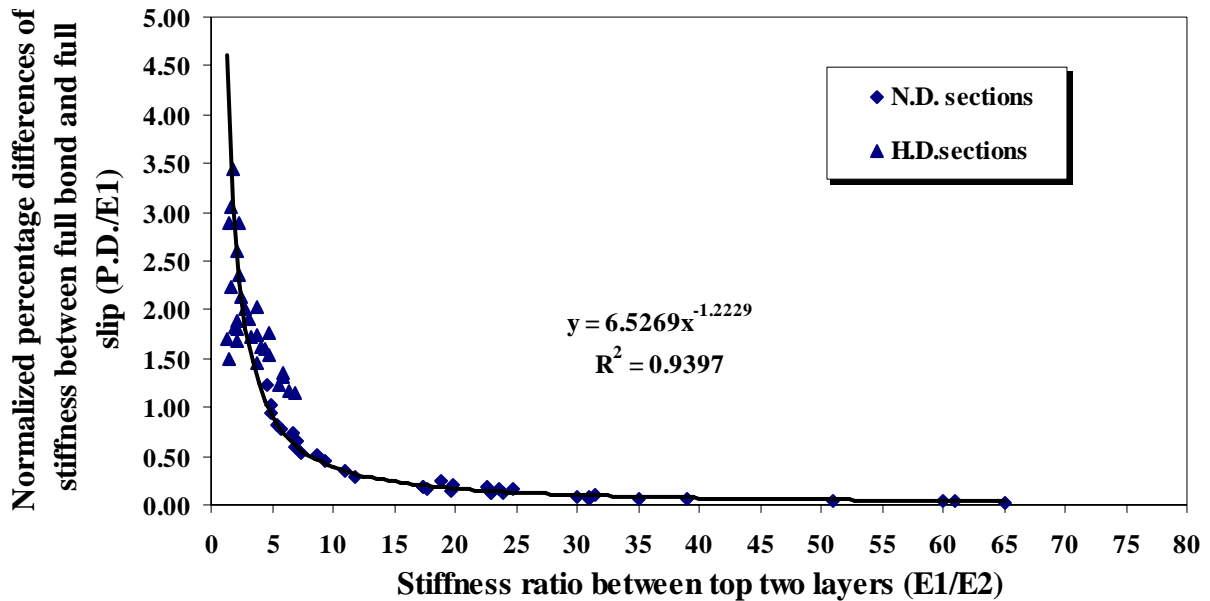


Figure 5.4. Normalized percentage differences of stiffness between the full bond and the full slip (P.D./E₁) vs. the stiffness ratio (E₁/E₂) .

The values of P.D./E₁ were changed significantly (P.D./E₁=3.5 to 1.00) at a lower stiffness ratio (E₁/E₂ = 0 to 5) and vice versa. This is because the surface layer is able to withstand much of the load itself at a higher stiffness ratio as compared to a lower stiffness ratio. This results in less of the load being transferred to the lower layers for a higher stiffness ratio and vice versa. Thus the stiffness of the surface layer for a higher stiffness ratio were not so much affected by the interlayer bonding condition as compared to the case at a lower stiffness ratio.

To quantify the stiffness ratio at which the differences of the slope of the curve are minimum, the differences in the slope of the curve (P.D./E₁ vs. E₁/E₂) vs. the stiffness ratio are plotted, which is shown in Figure 5.5. When the stiffness ratio is greater than 10 the differences in the slopes of the curve (P.D./E₁ vs. E₁/E₂) are almost zero. Since P.D./E₁ directly relates to the impact of the slip, when E₁/E₂ is greater than 10, the pavement is not as adversely impacted due to poor interlayer bonding.

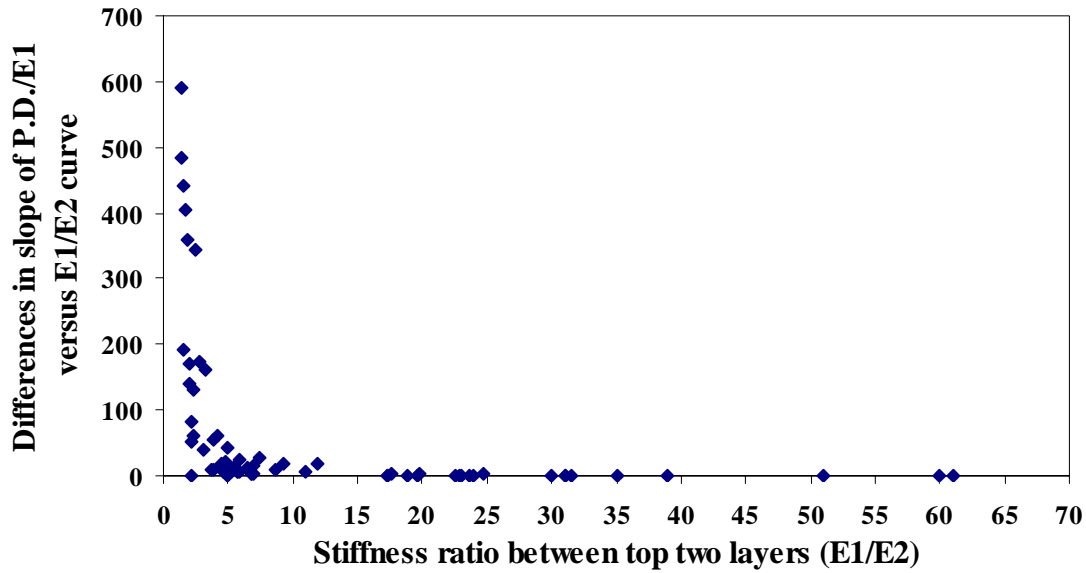


Figure 5.5. Differences in slope of curve (P.D./ E_1 vs. E_1/E_2) vs. stiffness ratio (E_1/E_2).

5.4. Summary of the Findings

The findings of the combined analysis of I-94 EB and USH 18 are summarized below:

- 1) The percentage differences of stiffness between the full bond and the full slip may not be an accurate indicator of the effect of slippage.
- 2) Normalized percentage differences of stiffness (P.D./ E_1) between the full bond and the full slip appear to correlate well with the observed distresses. For example, a higher value for high distress and a lower value for low distress.
- 3) A very strong inverse correlation was observed between P.D./ E_1 vs. E_1/E_2 with the root mean square value of the curve (P.D./ E_1 vs. E_1/E_2) of 0.94.
- 4) The stiffness ratio appeared to inversely correlate with the observed distresses. Higher E_1/E_2 ($E_1/E_2 > 10$) consistently showed a better interlayer bonding performance.
- 5) When the stiffness ratio is greater than 10 the differences in the slopes of the curve (P.D./ E_1 vs. E_1/E_2) are almost zero. Since P.D./ E_1 directly relates to the impact of the slip, when E_1/E_2 is greater than 10, the pavement is not as adversely impacted due to poor interlayer bonding.

6.0. Case Study

6.1. Data of HWY 81

As mentioned before, the data of three roads are given by WisDOT. The data of HWY 81 was analyzed as a case study to validate the recommendations in the previous chapter. The thickness data of HWY 81 given by WisDOT are shown in Table 6.1.

Table 6.1. Thickness data of HWY 81 given by WisDOT

HWY 81					
Rehabilitated section		First typical reconstruction section		Second typical reconstruction section	
HMA	3.5"	HMA	5"	HMA	3.5"
Pul. And relay asphalt pavement	4"	CABC	9"	CABC	19.5"
CABC	10"	Sal. Asphalt pavement base course	3"		

FWD data of HWY 81 for both the left wheel path (LWP) and the right edge of the pavement (REOP) were given by WisDOT. Five stations with patch sections were identified in both LWP and REOP data and two slippage stations were observed in the REOP data. But comments related to the intensity of distress were not mentioned by WisDOT in most of the other stations. As there were no specific comments, these stations were considered as the no distress section during the analysis.

6.2. No Distress Sections (LWP)

The stiffness of all layers of HWY 81 was calculated using BAKFAA software program. According to the Facilities Development Manual of Wisconsin (Procedure 14-10-5), the maximum and minimum range of stiffness for the pulverized HMA pavement are 21 to 85 ksi for base and 14 to 63 ksi for subbase, which is shown as Table 4.3. Initially the stiffness of all layers was allowed to be calculated by the program for the no distress section. However, this led to the stiffness of the base and the subbase for some stations to be outside the above-mentioned range. In some cases there was swapping between base and subbase. To avoid this problem, the stiffness of the base was kept constant at 85 ksi and analysis was conducted again in BAKFAA.

The stiffness of all layers of the no distress section (LWP) for the full bond condition and the full slip assumption are shown in Figures 6.1 and 6.2, respectively.

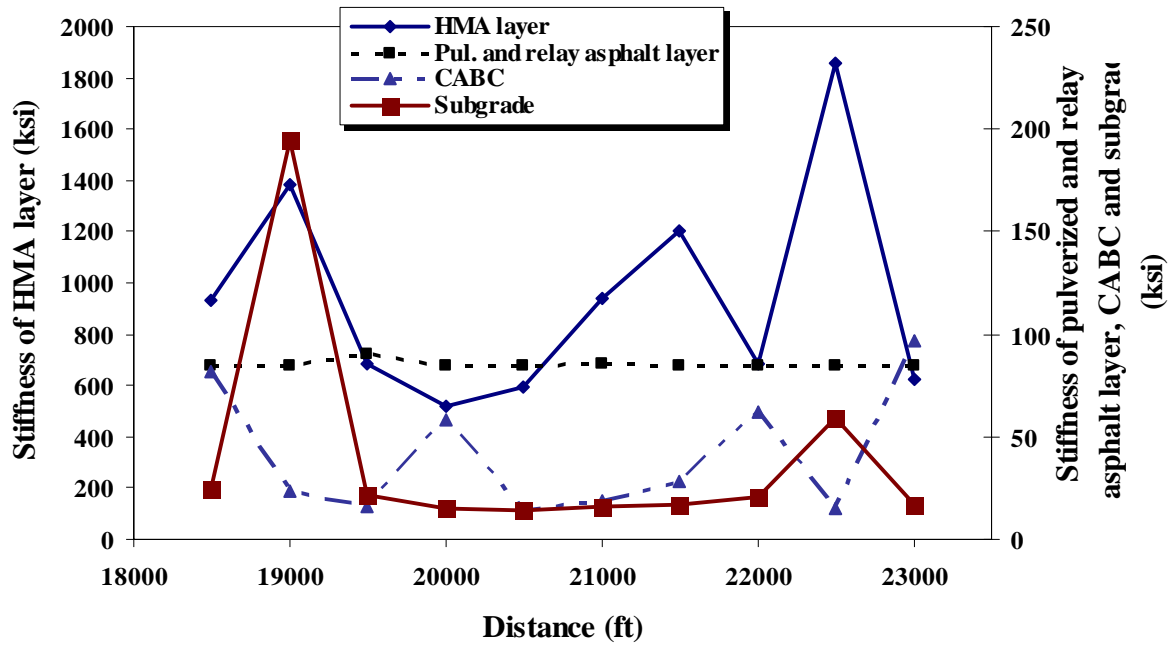


Figure 6.1. Stiffness vs. distance (N.D, HWY 81, F.B., actual)

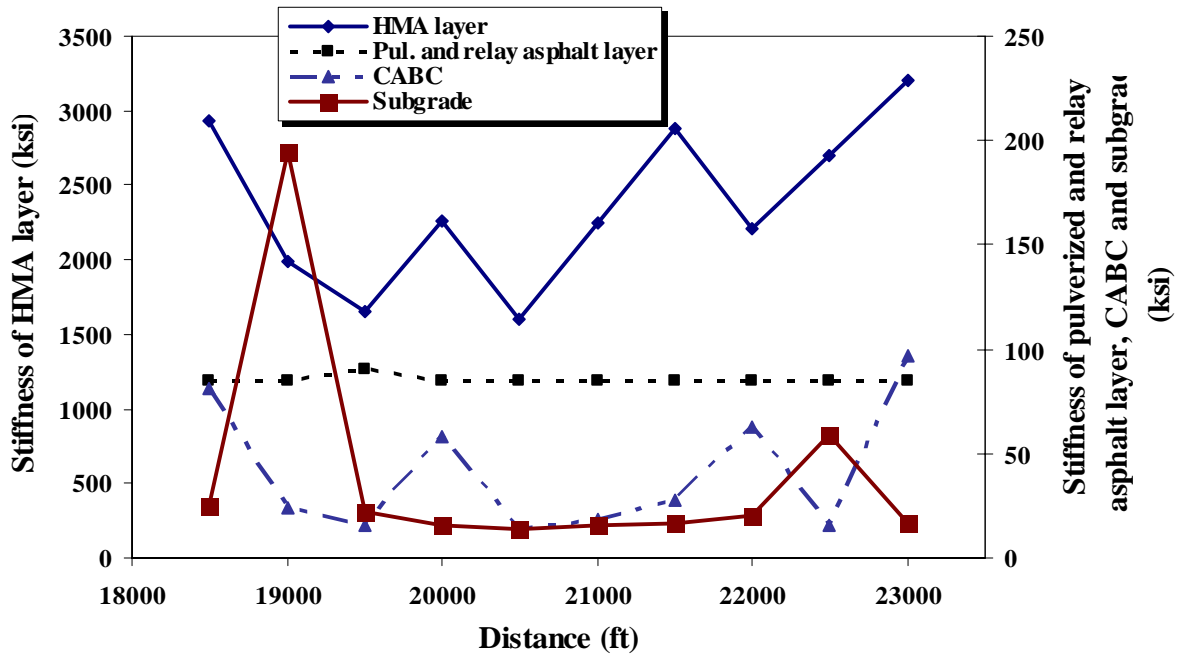


Figure 6.2. Stiffness vs. distance (N.D, HWY 81, F.S., assumption)

Stiffness ratios (E_1/E_2) between the top two layers of the no distress section were 6-22. Stiffness ratios (E_1/E_2) of the no distress section between the top two layers with the distance are shown in Figure 6.3. It was observed that for a few stations the stiffness ratios were from 6 to 10, but they were not slippage sections.

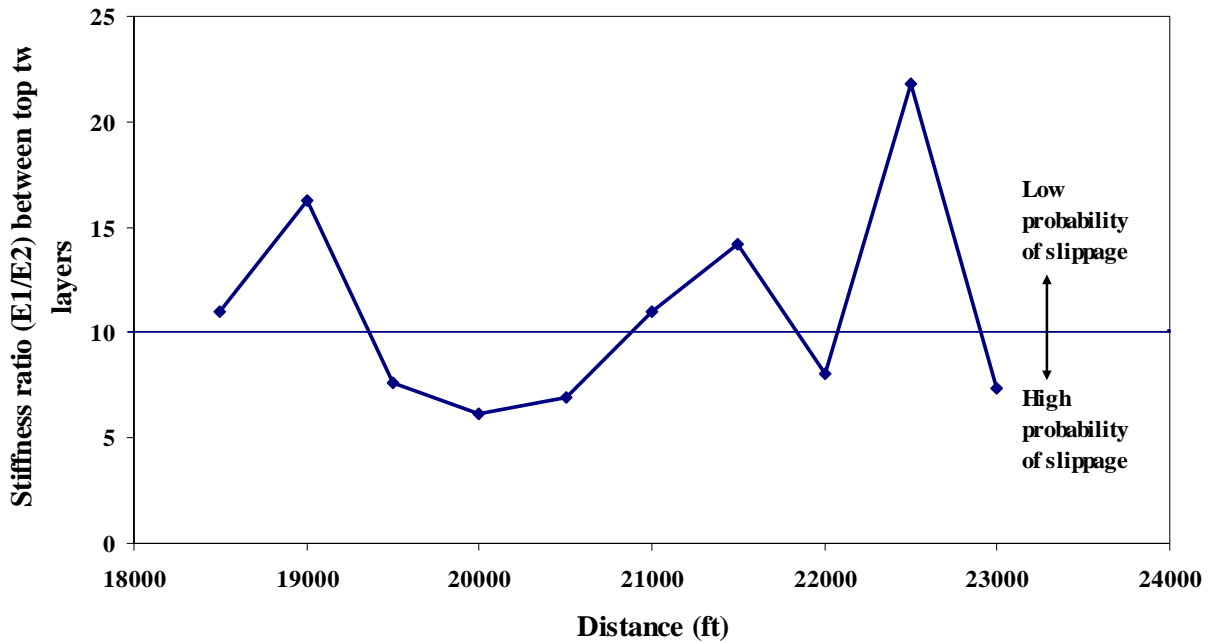


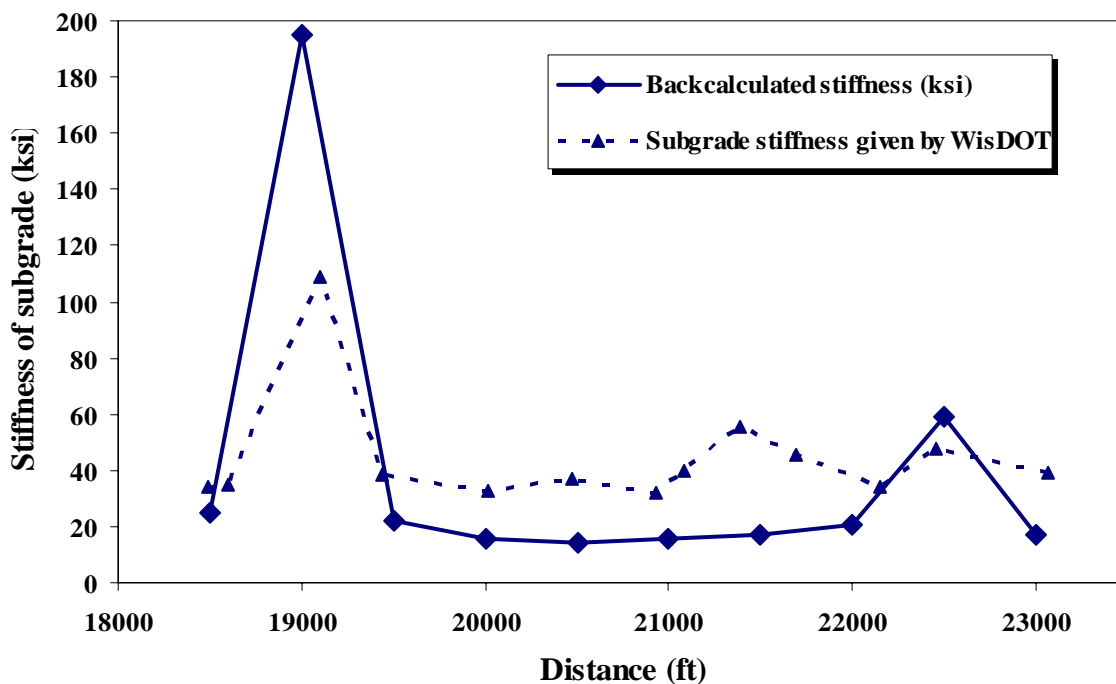
Figure 6.3. Stiffness ratio (E_1/E_2) vs. distance (N.D., HWY 81)

6.3. Slippage Section (REOP) and No Distress Section (LWP)

As mentioned before, two stations were identified by WisDOT at the right edge of the pavement as the slippage section. These stations were at 22000 ft and 22500 ft. It should be noted that the same two stations at the left wheel path (LWP) were not specifically identified as the slippage section.

No distress section at station 22000' and 22500' (LWP)

The analysis for 22000' and 22500' station for the no distress section (LWP) are summarized in Table 6.2. The RMSE values were 0.12 to 0.15 for the full bond condition and 0.19 to 0.61 for the slippage assumption. As stated earlier, the stiffness of the base was kept constant at 85 ksi. The subbase stiffness was within the specified range 14 ksi to 63 ksi. The backcalculated subgrade stiffness and the subgrade stiffness provided by WisDOT are plotted with distance, which is shown as Figure 6.4.



.Figure 6.4. Stiffness of subgrade vs. distance (N.D. LWP, HWY 81)

Slippage section at station 22000’ and 22500’ (REOP)

To get the reasonable stiffness values for the different layers which is within the specified range of the Facilities Development Manual of Wisconsin (Procedure 14-10-5), two sets of analysis were done. The results of this analysis are summarized in Table 6.3 and are discussed below:

First set of analysis

The stiffness was calculated in BAKFAA, only the subgrade stiffness was calculated manually by changing it in the program to match the measured deflection at 60” (d_{60} or D_7). The subgrade stiffness was close to the stiffness values given by WisDOT.

The RMSE values were 0.08 to 0.28 for the slippage condition and 0.26 to 0.58 for the full bond assumption. But the stiffness of the subbase of station 22500’ was 11 ksi which was lower from the specified range 14 ksi to 63 ksi. The next analysis was done by keeping the base stiffness constant which was within the specified range of the Facilities Development Manual of Wisconsin (Procedure 14-10-5).

Second set of analysis

It is reasonable to assume that the stiffness for the lower layers will be similar for the same stations at LWP and REOP. It was calculated at REOP by fixing the pulverized and the relay asphalt pavement layer (Base) as 85 ksi which was of similar magnitude at LWP. The subgrade stiffness was close to the stiffness values given by WisDOT. The RMSE values were

0.11 to 0.28 for the slippage condition and 0.25 to 0.53 for the full bond assumption. But the stiffness of the subbase at station 22500' for the second set of analysis was also 11 ksi which was lower from the specified range 14 ksi to 63 ksi.

6.4. Summary of the Findings

It was observed that the stiffness of the base, the subbase, and the subgrade were similar for both the first and the second sets of the analysis, which is shown as Table 6.3. As the stiffness of the base and the subbase for the first set of analysis were allowed to calculate by the program, the first set of analysis appeared to be more reasonable.

But the stiffness based on the FWD data appeared to have large variability between the same station at LWP and REOP. The research team established a premise that the lower layers between LWP and REOP should be similar (within 20%-25%), because a significant variation is not expected in the lower layers within 6-8 ft. Based on this premise, the two stations are discussed separately.

Station 22000'

It was observed that for the first set of analysis, the REOP stiffness values of the base and the subgrade closely matches that of LWP. But the REOP stiffness value of the subbase is lower than that of the LWP; the possible reason could be poor drainage and causing lower stiffness value, which are shown as Tables 6.2 and 6.3.

Station 22500'

It was observed that for the first set of the analysis, the stiffness of the top HMA at REOP was higher than that of LWP. But the REOP stiffness values of the base and the subbase were lower than that of LWP, the possible reason being poor drainage that causes lower stiffness values, which are shown as Tables 6.2 and 6.3. Although the REOP stiffness of the top HMA was higher than that of the LWP stiffness, drainage of lower layers at the edge may have caused distress. That distress might not be due to slippage.

Table 6.2. Analysis of HWY 81 for no distress section (LWP)

	Station	Stiffness (ksi)					RMSE, mils		P.D./ E ₁	E ₁ /E ₂
		HMA (Full bond condition)	HMA (Slippage assumption)	Pulverized and relay Asphalt pavement	CABC	Subgrade	Full bond condition	slippage assumption		
Analysis with fixing pul. base	22000	683	2205	85 (Fixed)	62	21	0.12	0.61	0.33	8
	22500	1854	2703	85 (Fixed)	16	59	0.15	.19	0.02	22

Table 6.3. Analysis of HWY 81 for slippage section (REOP)

	Station	Stiffness (ksi)					RMSE, mils		P.D./ E ₁	E ₁ /E ₂
		HMA (slippage condition)	HMA (Full bond assumption)	Pulverized and relay Asphalt pavement	CABC	Subgrade	Slippage condition	Full bond assumption		
First set of analysis	22000	684	142	95	37	17	0.08	0.58	0.56	7
	22500	2896	2147	76	11	62	0.28	0.26	0.01	38
Second set of analysis	22000	808	186	85 (Fixed)	35	17	0.11	0.53	0.41	10
	22500	3030	2151	85 (Fixed)	11	62	0.28	0.25	0.01	36

*Those stiffnesses in bold indicate that they are out of the specified range of the Facilities Development Manual of Wisconsin (Procedure 14-10-5).

Stiffness ratio at LWP and REOP

As mentioned earlier, according to given data of WisDOT, station 22000' and 22500' at REOP were slippage sections.

Station 22000'

The stiffness ratios between the top two layers at LWP and REOP (first set of analysis) for station 22000' were 8 and 7, respectively, which were of similar magnitude.

Station 22500'

The stiffness ratios between the top two layers at LWP and REOP (first set of analysis) for station 22500' were 22 and 38 respectively. But it was observed that the stiffness ratio at REOP for station 22500' was 38, which was a higher value than for the same station at LWP. This is because the top stiffness of HMA at REOP was higher than LWP, which results in a higher E_1/E_2 value. Thus, E_1/E_2 values are high for this slippage section, which reinforces our recommendations that having a higher E_1/E_2 only minimizes the effect of the slip but does not completely prevent it if the lower layers have poor drainage. Higher E_1/E_2 , preferably $E_1/E_2 > 10$, helps minimize the effect of the slippage.

7.0. Degree of Slip

7.1. Estimation of Degree of Slip

In real pavement structure the full bond and the full slip conditions between layers do not exist. It is difficult to achieve full bonded interlayer pavement structure. In practically most of the cases, some slip is present between the layers. The important factor is what percentage of the slip may be allowed for an efficient pavement. Thus, it is necessary to calculate the degree of the slip immediately after construction. Theoretically the degree of the slip can be calculated either using equation [7.1] or [7.2].

$$E_{\frac{AC}{FS}} = (1 - D_s) E_{\frac{FB}{FS}} + D_s E_{\frac{FS}{FS}} \quad [7.1]$$

$$E_{\frac{AC}{FB}} = (1 - D_s) E_{\frac{FB}{FB}} + D_s E_{\frac{FS}{FB}} \quad [7.2]$$

where,

$E_{\frac{AC}{FS}}$ = Stiffness of the partial slipped HMA layer assuming full slip between the top HMA

layer and the second layer.

$E_{\frac{FB}{FS}}$ = Stiffness of the fully bonded HMA layer assuming full slip between the top HMA

layer and the second layer.

$E_{\frac{FS}{FS}}$ = Stiffness of the fully slipped HMA layer assuming full slip between the top HMA

layer and the second layer.

$E_{\frac{AC}{FB}}$ = Stiffness of the partial slipped HMA layer, assuming a full bond between the top

HMA layer and the second layer.

$E_{\frac{FB}{FB}}$ = Stiffness of a fully bonded HMA layer, assuming full bond between the top HMA

layer and the second layer.

$E_{\frac{FS}{FB}}$ = Stiffness of a fully slipped HMA layer, assuming full bond between the top HMA

layer and the second layer.

According to these equations, the degree of slip can be calculated on the basis of the stiffness of the full bond, the full slip, and the partial slip (actual) conditions of the same sections immediately after construction to minimize the effect of structural deterioration. But practically, it is not possible to get three conditions simultaneously for the same section of the pavement immediately after construction. This is the limitation of obtaining an accurate degree of slip of the section.

The degree of slip was calculated for I-94 EB. In I-94 EB, the degrees of slip were calculated for moderate distress sections with the help of the average stiffness of the no distress and the high distress sections. But the values of the degree of slip were observed from 7% to

133% and for few stations the values were shown as negative, which is impossible. This is because an accurate quantification of distress was not available so that appropriate values can be used in the equation. The research team used the average stiffness between stations with the no distress and the high distress section.

As stated before, it is difficult to achieve a full bonded interlayer pavement structure. In practically most of the cases, some slips are present between the layers. It is very important to avoid slippage by maintaining the quality of work. Otherwise, the thickness of the top HMA layer should be increased to minimize the effect of the slip. But increasing the top thickness is expensive.

7.2. Achieving Stiffness Ratio by Increasing Thickness

As mentioned above, the stiffness ratio appeared to inversely correlate with the observed distresses. Higher E_1/E_2 ($E_1/E_2 > 10$) consistently showed a better interlayer bonding performance. Until this point, the stiffness ratio was primarily dealing with only the stiffness of the layers. However, the structural capacity of the layer depends on both the thickness and the stiffness. In several cases, it may not be cost-effective to change the material to achieve a high stiffness ratio ($E_1/E_2 > 10$). In this section, the researchers used FWD data to determine the additional thickness needed on a pavement with low E_1/E_2 ($E_1/E_2 < 10$) to provide the same structural capacity as that of a pavement with high E_1/E_2 (say, $E_1/E_2 = 10$).

To demonstrate the above concept, this analysis was done for six stations with a stiffness ratio between the top two layers of two ($E_1/E_2 = 2$). All six stations were taken from the high distress sections of I-94 EB and USH 18. It was observed that the additional thickness needed to achieve the stiffness ratio of $E_1/E_2 = 10$ depended on the existing top layer thickness. By increasing the thickness of an existing 2 in the pavement layer, the structural capacity of the pavement increased from a lower stiffness ratio of 2 to as high as the stiffness ratio of 10 for an existing 2 in top layer thickness, which are shown as Figures 7.1 and 7.2. On the other hand, the structural capacity of a pavement with an existing 3 inch top layer was increased by a 4 inch thick surface layer for an increase in stiffness ratio from 2 to 10, which are shown as Figures 7.3 and 7.4. The influence of the thicker surface layer on the deflection basin is greater than that of the thinner layer. Therefore, the thicker surface layer with the lower stiffness needs to be modified significantly more than that for a thinner layer to change the shape of the deflection basin. For that reason, the existing 3 inch layer needed more thickness as compared to the 2 inch layer to achieve the structural capacity of a higher stiffness ratio from the initial value of 2.

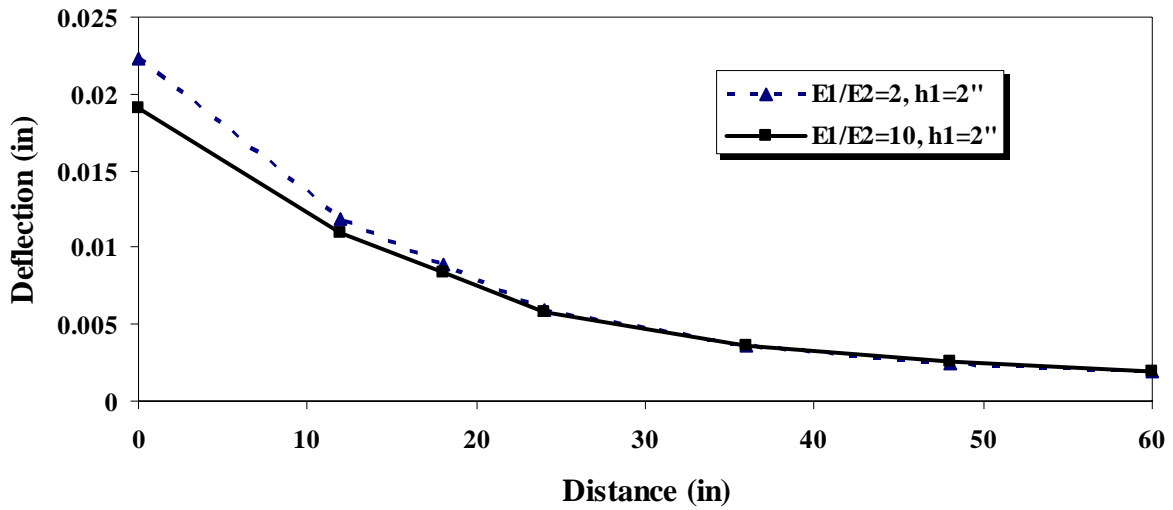


Figure 7.1. Deflections of the surface layer (2") vs. distance from the FWD load.

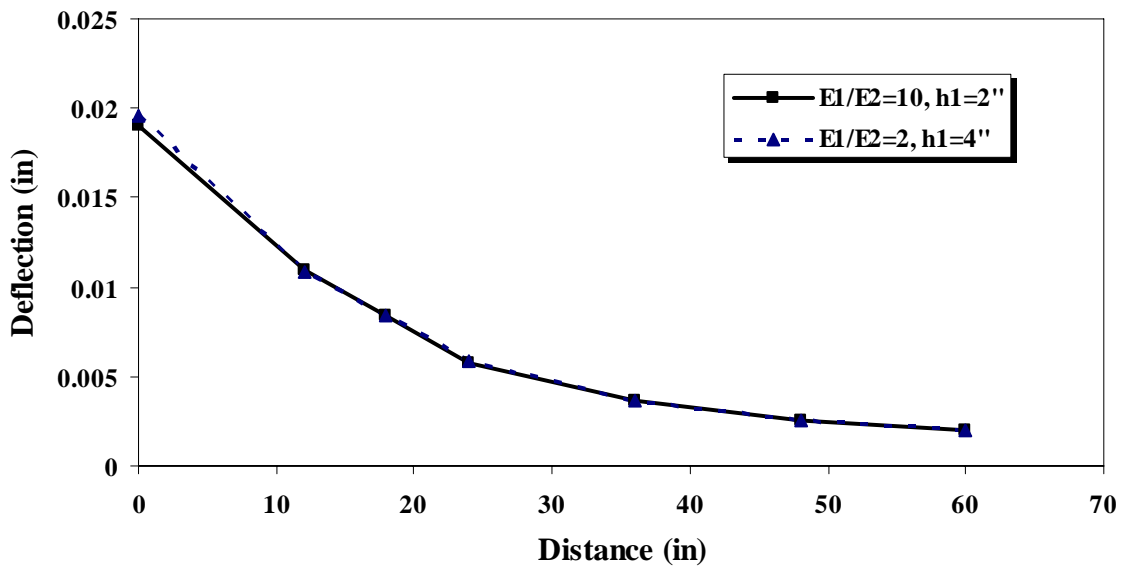


Figure 7.2. Deflections of the surface layer vs. distance from the FWD load

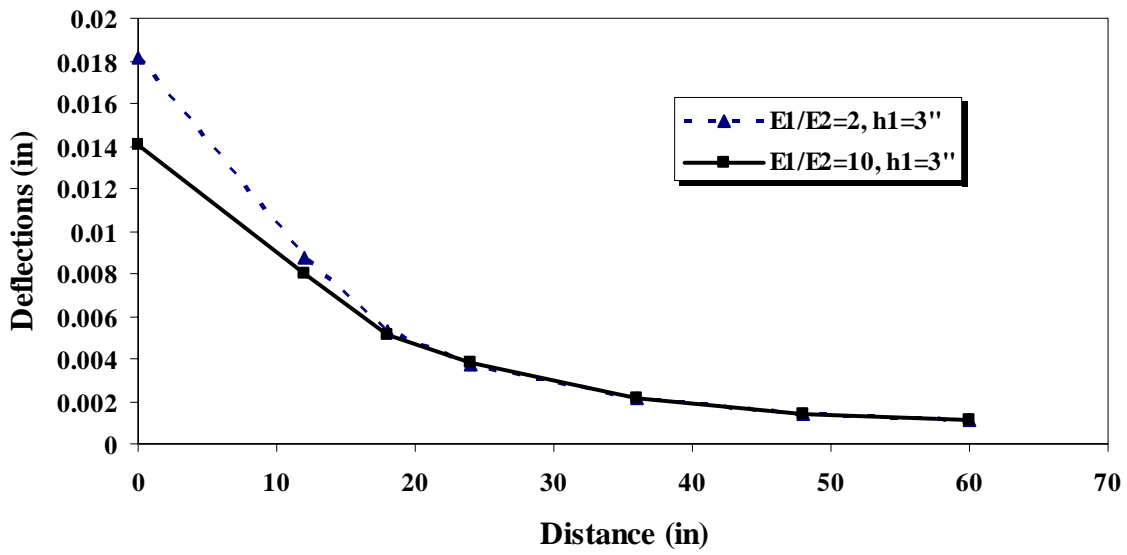


Figure 7.3. Deflections of the surface layer (3") vs. the distance from the FWD load.

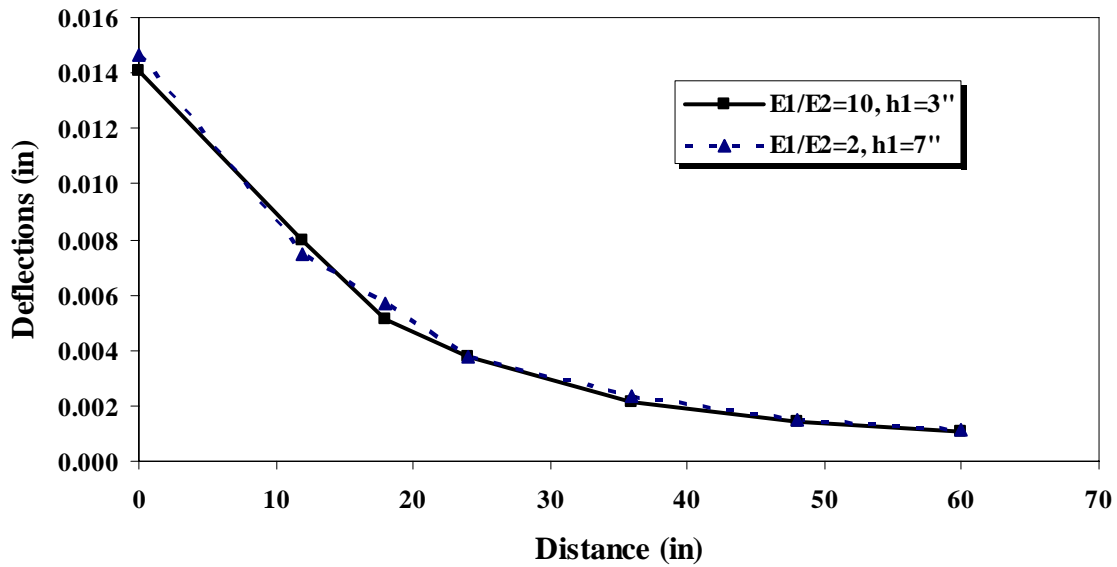


Figure 7.4. Deflections of the surface layer vs. the distance from the FWD load.

8.0. Summary of the Findings and Recommendations

8.1. Summary of the Findings

The following was found after analyzing the I-94 EB and USH 18 of WisDOT.

- 1) Distresses observed by WisDOT correlated with the tensile strain at the bottom of the asphalt concrete for I-94 EB, which were indicative of slippage failure. But distresses observed by WisDOT did not correlate with the tensile strain at the bottom of the asphalt concrete for USH 18. This may be because the distress was observed in shoulders but the FWD might be taken along the main lane.
- 2) Distresses observed by WisDOT for both I-94 EB and USH 18 did not correlate with parameters such as AREA and surface flexural rigidity because these parameters are influenced by the stiffness and the thickness of the entire pavement system.
- 3) The stiffness ratio between the top two layers for no distress sections were between 5 and 65 which were higher than that of the high distress sections between 1 and 7; this was observed for all sections where the second layer stiffness was greater than 20 ksi.
- 4) The percentage differences of the stiffness between the full bond and the full slip may not be an accurate indicator of the effect of slippage.
- 5) Normalized percentage differences of the stiffness ($P.D./E_1$) between the full bond and the full slip appeared to correlate very well with the observed distresses.
- 6) A very strong inverse correlation was observed between $P.D./E_1$ vs. E_1/E_2 with the root mean square value of the curve ($P.D./E_1$ vs. E_1/E_2) of 0.94.
- 7) The stiffness ratio appeared to inversely correlate with the observed distresses. Higher E_1/E_2 ($E_1/E_2 > 10$) consistently showed a better interlayer bonding performance.
- 8) When the stiffness ratio was greater than 10 the differences in the slopes of the curve ($P.D./E_1$ vs. E_1/E_2) were almost zero. Since $P.D./E_1$ is directly related to the effect of the slip, when E_1/E_2 was greater than 10, the pavement was not as adversely impacted due to poor interlayer bonding.
- 9) By providing an additional thickness of 2 in (on existing 2 in top layer) and 4 in (on existing 3 in top layer) on the pavement with low E_1/E_2 ($E_1/E_2 < 10$) can be changed to the same structural capacity as that of a pavement with high E_1/E_2 (say $E_1/E_2 = 10$).

8.2. Recommendation

If the stiffness ratio between the top HMA layer and the second layer is greater than 10 during the design and if the second layer stiffness is greater than 20 ksi, the pavement will be less affected by slippage than that when the stiffness ratio is less than 10.

Based on limited cases, this study demonstrated that the structural capacity of the slipped pavement with $E_1/E_2 = 2$ can be increased to the stiffness ratio of $E_1/E_2 = 10$ by increasing the thickness of the surface layer. The additional top layer thickness is 2 in for an existing 2 in top layer thickness and 4 in for an existing 3 in top layer thickness.

9.0. References

Federal Aviation Administration (2000). *BAKFAA Pavement Backcalculation Program*.

Gomba, S., Liddle, J., and Mehta, Y. A. (2005). "Evaluation of Interlayer Bonding in Hot Mix Asphalt Pavements." *The International Journal of Pavements*, Vol. 4 No. 1 and 2, pp. 13-24.

Garg, N., and Thomson, M.R., (1998). "Triaxial Characterization of MnROAD Granular Materials." *Transportation Research Record 1577, TRB*, Washington D.C., pp. 22-36.

Huang, Y. H. (1993). *Pavement Analysis and Design*, Prentice-Hall, Inc., Upper Saddle River, New Jersey. page 413.

Mehta, Y.A., and Roque, R. (2003). "Evaluation of FWD Data for Determination of Layer Moduli of Pavements." *Journal of Materials in Civil Engineering Volume 15, Issue 1*, pp. 25-31.

Ping, W.V., and Xiao, Y. (2007). "Evaluation of the Dynamic Complex Modulus Test and Indirect Diametral Test for Implementing the AASHTO 2002 Design Guide for Pavement Structures in Florida." *FDOT Research Contract No. BC-352-12, FSU Project No. OMNI 008664*, Florida Department of Transportation.

Shahin, M. Y., Blackmon, E. W., Van Dam, T., Kirchner, K. (1987). "Consequence of Layer Separation on Pavement Performance." *Report No. DOT/FAA/PM-86/48*. Federal Aviation Administration, Washington, D.C.

Uzan, J., Livneh, M., Eshed, Y. (1978). "Investigation of Adhesion Properties between Asphalt-Concrete Layers." *Journal of the Association of Asphalt Paving Technologists*, Vol.47, pp. 495-521.

WisDOT (2005). *Facilities Development Manual of Wisconsin*, Procedure 14-10-5.

WisDOT (2006). *Standard Specifications of Wisconsin Department of Transportation*.

Appendix A

**Wisconsin Highway Research Program
0092- 03-13**

**PHASE 1: EVALUATION OF INTERLAYER
BONDING IN HMA PAVEMENTS**

Final Report

by

Yusuf A. Mehta, Ph.D., P.E.

Stephen M. Gomba

of the

Department of Civil and Environmental Engineering
Rowan University, Glassboro NJ 08028

Submitted to the

**Wisconsin Department of
Transportation**

February 2004

DISCLAIMER

This research was funded through the Wisconsin Highway Research Program by the Wisconsin Department of Transportation and the Federal Highway Administration under Project # (0092- 03-13). The contents of this report reflect the views of the authors who are responsible for the facts and the accuracy of the data presented herein. The contents do not necessarily reflect the official views of the Wisconsin Department of Transportation or the Federal Highway Administration at the time of publication.

This document is disseminated under the sponsorship of the Department of Transportation in the interest of information exchange. The United States Government assumes no liability for its contents or use thereof. This report does not constitute a standard, specification or regulation.

The United State Government does not endorse products or manufacturers. Trade and manufacturers' names appear in this report only because they are considered essential to the object of the document.

Technical Report Documentation Page

1. Report No. WHRP 07-07	2. Government Accession No	3. Recipient's Catalog No	
4. Title and Subtitle Evaluation of Interlayer Bonding in HMA Pavements		5. Report Date September 2007	6. Performing Organization Code Univ. of Wisconsin - Madison
7. Authors Yusuf Mehta		8. Performing Organization Report No.	
9. Performing Organization Name and Address Department of Civil and Environmental Engineering Rowan University		10. Work Unit No. (TRAIS)	11. Contract or Grant No. WisDOT SPR# 0092-02-13
12. Sponsoring Agency Name and Address Wisconsin Department of Transportation Division of Business Services Research Coordination Section 4802 Sheboygan Ave. Rm 104 Madison, WI 53707		13. Type of Report and Period Covered Final Report, 2002-2004	14. Sponsoring Agency Code
15. Supplementary Notes			
<p>16. Abstract</p> <p>This study investigates the potential of falling weight deflectometer (FWD) data for use in quantifying the level of interlayer bonding achieved in pavements. Data was obtained and used from the Federal Aviation Administration's (FAA) National Airport Pavement Test Facility located in Atlantic City, New Jersey. In this test facility, a section of the pavement had encountered a loss of bond between lifts of the surface hot mix asphalt (HMA) layer. FWD tests had been performed at locations throughout the pavement, on a monthly basis for the duration of the loading period. The FWD data, along with detailed material property data, was available through the FAA Airport Technology Research and Development Branch's web page. The material properties and FWD data were used to calculate the stiffness moduli for each layer in the pavement using forward calculations. It was determined that calculated stiffness moduli for surface layers can be used as a parameter to determine the quality of interlayer bonding. To further investigate the level of bonding, a tack failure ratio was determined for each section, by modifying an equation for the equivalent modulus of two combined asphalt layers, and that was correlated to the slip between layers. This study developed a framework for the application of FWD data in identifying and quantifying interlayer slippage in HMA pavements.</p>			
17. Key Words Asphalt, backcalculation, falling weight deflectometer, interlayer bonding, pavement, tack coat.		18. Distribution Statement No restriction. This document is available to the public through the National Technical Information Service 5285 Port Royal Road Springfield VA 22161	
19. Security Classif.(of this report) Unclassified	19. Security Classif. (of this page) Unclassified	20. No. of Pages	21. Price

Executive Summary

Project Summary

The Federal Aviation Administration's (FAA) National Airport Pavement Test Facility (NAPTF), located in Atlantic City, New Jersey, is a fully enclosed pavement test track. In this facility, nine sections of different pavement structures are evaluated under accelerated aircraft loading. One of the sections experienced extensive slipping between layers. Similar failures have been observed on highways in various states, such as Florida, Louisiana, Minnesota, New Jersey, and Wisconsin. This slippage can cause secondary failures like cracks and potholes, resulting in extensive failure of the pavement structure.

The purpose of this study is to form a framework to use nondestructive Falling Weight Deflectometer (FWD) data to identify the lack of bonding in hot mix asphalt pavements. In particular, this study will address the lack of bonding between lifts in asphalt layers with the same material properties. The intent is that eventually interlayer bonding will be evaluated during the construction of pavements. The ability to identify bonding failures directly after construction will save money by minimizing future rehabilitation caused by the interlayer bonding failures.

Background

This study is based on interlayer bonding issue. This is a first phase of research. Many studies, as will be discussed below, have been and are continuing to be done on tack coats, proper use of tack coats, and their effects on interlayer strength. Through review of these studies, many things have been noted regarding tack coats, interlayer, and the various effects on pavement.

The first item of note from the literature review is what type of problems interlayer bonding failures cause. The typical signal that a pavement is experiencing interlayer bonding failure is slippage cracking, an example of which may be viewed in Figure 2.1. This slippage cracking consists of crescent shaped cracks that develop at the pavement surface and are the direct result of a slippage of the upper asphalt layer over the lower layer (Shahin, et al., 1987b; Uzan, et al., 1978). The slippage between the layers is the result of a weak interlayer bond. The crescent cracks, while certainly a problem themselves, are not the only problem resulting from slippage. As the interlayer bond is weakened and broken as the upper layer slips, the pavement system as a whole is weakened. This is because the broken bond reduces the stiffness of the system as a whole and loads may no longer be supported and distributed by the system as designed (Shahin, et al., 1987b).



Figure 1. Slippage Cracking

The Department of Civil and Environmental Engineering at Rowan University conducted this research project through the Wisconsin Highway Research Program. The research team includes, Dr. Yusuf Mehta (Associate Professor), Stephen M. Gomba (Graduate student) and Joseph Cugino (Undergraduate student).

Process

The hypotheses of this study are:

1. Surface layer moduli calculated from FWD data can be used to identify a lack of interlayer bonding in pavements.
2. The effect of slip between two asphalt layers of similar properties can be determined by the ratio of moduli of the top layer and the moduli of the bottom layer.

The time period of this study was 24 months.

This study utilized data obtained from the databases on the FAA's NAPTF website. All analyses were performed with data from the Medium subgrade strength Flexible pavement Conventional base (MFC) section within the "Medium Strength Subgrade" section of the test pavement (as described in a later chapter). The MFC pavement section was composed of two sections, both of which were used for this study:

1. Unfailed section: a pavement section in which the interlayer bond was intact.
2. Failed section: a pavement section in which delamination occurred at the interlayer.

The data used in the study was of two types:

1. Material data: various material properties for the materials used in all layers of the pavement in the MFC section.
2. FWD data: 116 individual FWD tests within the MFC section, 60 of which were in the unfailed section, and 56 of which were in the failed section. Loads used in the tests included the following nominal loads: 9,000lb, 14,000lb, 25,000lb, 12,000lb, 24,000lb, and 35,000lb. Tests were conducted over a time span of 12 months.

Findings

In analyzing the Federal Aviation Administration National Airport Pavement Testing Facility's MFC section, the following was found:

1. The surface layer moduli obtained from Falling Weight Deflectometer (FWD) data was significantly different between failed and unfailed sections at early loading times, for all loads and temperatures.
2. A difference in calculated layer moduli between different sections may indicate the presence of interlayer bonding failure.
3. In pavements where slip occurs between two asphalt layers of similar properties, a Tack Coat Failure Ratio (TFR) can be defined as the ratio of the modulus of the top layer to the modulus of the lower layer:

$$\text{TFR} = \frac{E_{\text{top-asphalt-layer}}}{E_{\text{bottom-asphalt-layer}}}$$

4. The effect of slip at the interface can be measured by the difference in radial stresses at points just above and just below the interface.
5. Given enough material data, a TFR and Effect of Slip correlation may be established for a pavement structure.

Conclusions

It can be concluded that:

1. Surface layer moduli calculated from FWD data can be used to identify a lack of interlayer bonding in pavements.
2. The effect of slip between two asphalt layers of similar properties will be reflected by the moduli of the top layer being lower than the moduli of the bottom layer ($E_{\text{top-asphalt-layer}} < E_{\text{bottom-asphalt-layer}}$).

This study will provide a tool for state agencies to detect interlayer bonding failure from widely used FWD data. State agencies could use this methodology to detect failures immediately after construction of a given section and rectify, if necessary, any construction procedure to prevent them in the future. This methodology could also be used as a pavement management and rehabilitation tool, provided that the agencies have material data independently available. This methodology could reduce expenses for all, due to less pavement maintenance costs on the part of the roadway owners and less vehicle maintenance costs for the roadway users.

Recommendations

Based on the findings and conclusions, the following recommendations are made:

1. The procedure outlined in this study should be evaluated for a pool of pavement sections to determine the extent of its validity.
2. The outlined procedure should be tested on a different pavement section that also has detailed material data available, for two reasons:
 - a. To ensure that the methods used are accurate for various pavement systems.
 - b. To verify whether or not the TFR / Effect of Slip correlation obtained in this study is unique for different pavements.
3. Effect of slip should be correlated to physical results of slippage. That is, the results of slippage should be measured in some way and related to the effect of slippage, so that when one calculates the effect of slippage, one knows what failures may be expected, if any.
4. Modifications should be made to the procedure so that slip can be evaluated between layers other than layers of similar materials, such as slip between asphalt concrete and a base course.

SURVEY DATA

The research team has contacted various state agencies to collect the following data:

- a. Issues/Concerns related to interlayer pavement bonding.
- b. If yes, are they related to pavement structure, type of tack coat, or construction practice.
- c. Pavement structural data/FWD data and quality control data on good and poor performing sections with tack coat, if any.
- d. Current specifications on tack coat and its application or on other techniques used to ensure bonding.
- e. HMA pavement design manuals.
- f. Obtain data on various projects exhibiting both poor and good interlayer bonding performance from Wisconsin DOT.

Out of the 48 state agencies were contacted, and nineteen of them provided all the necessary information.

The Survey Questionnaire sheet

Date:

State:

Contact Information:

Name:

Phone/email:

Other:

Questions concerning construction issues:

1. Number of construction projects using tack coat per year:
2. Are any other techniques used for interlayer bonding?
3. Are there any specific conditions under which tack coat is applied?
(example: traffic, pavement surface, weather conditions)
4. Are there any issues with strength of tack? Premature stiffening of tack?

5. Any specific problems observed during application?
6. Are there any issues with following specifications?
7. Are there any penalties for following specifications? (re-do's?)
8. Any difference in pavement performance due to tack coat?
Any aging concerns? (example: sliding, shoving, rutting, failure cracking)
9. What are the pavement structures like? (layers, thicknesses)
(both with and without tack)
10. Any overall concerns?
11. Any monitoring of pavement performance related to tack coat? (FWD's?)
12. Availability of the data of pavement sections / performance where tack coat or any other techniques were used?
13. Open ended question:
Based on experience, should the state of the art of practice change?
14. Who supplies the tack coat? Is application out-sourced?

Questions concerning Specifications: (a copy of relevant specifications is requested)

1. Type of tack?
2. Application rate?
3. Curing period?
4. Temperature of tack?
5. Required uniform application?
6. Uniformity at junction of applications?
7. Air temperature range?
8. Weather conditions? (mist, rain, snow conditions?)
9. Milled / non-milled?
10. Surface condition? (Clean of debris? Dry?)

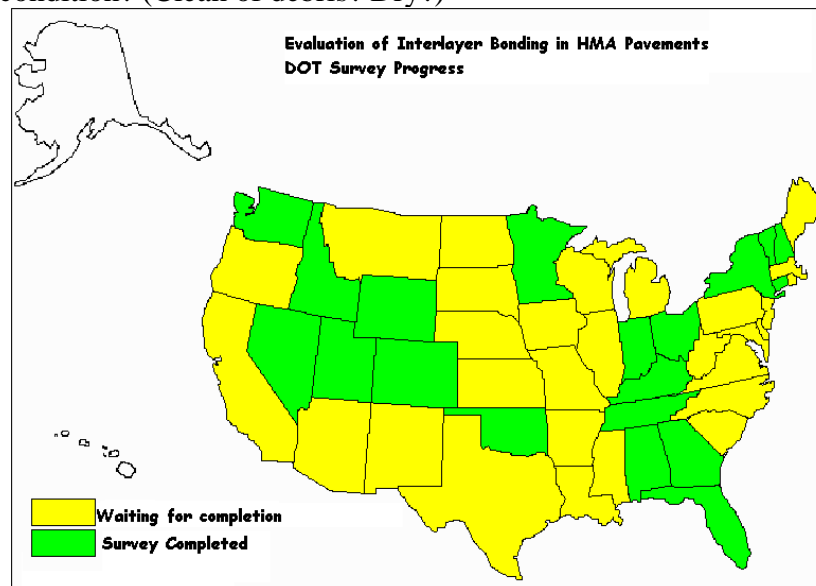


Figure 2. Status of Survey to Date

Survey Results to Date

A weak bonding between bituminous pavement layers may develop during construction due to the following reasons: 1) insufficient compaction of the surface course; 2) poor quality control, 3) lack of tack coat, 4) contamination of the lower layer or laying in cold weather, 5) absorption

of the binder coat by porous aggregates, and 6) inadequate structural design of surface course resulting in excessively large shear stresses at interlayer. Some of these problems could be directly related to type of tack coat, application rate and temperature of tack coat and environmental conditions. This section presents the results of the survey based on these parameters.

TACK TYPE

Tables 1 a and b shows the types of tack coat used in various states. Figure 2 shows the number of states using various types of tack coat.

Table 1a. Tack Types Allowed Based on Survey and Specification Data (Part 1/2)

	SS-1	SS-1h	CSS-1	CSS-1h	MS-1	MS-2	RS-1	RS-2	CRS-1	CRS-2	CRS-2h
Alabama	-	-	X	X	-	-	-	-	-	X	X
Colorado	-	-	-	X	-	-	-	-	-	-	-
Connecticut	X	X	X	X	-	-	X	-	X	-	-
Florida	-	-	-	-	-	-	X	X	-	-	-
Georgia	-	-	-	-	-	-	-	-	-	-	X
Idaho	-	-	X	-	-	-	-	-	-	-	-
Indiana	-	-	-	-	-	-	-	-	-	-	-
Minnesota	X	X	X	X	X	-	X	X	X	X	-
Nevada	X	X	X	X	-	-	-	-	-	-	-
New Hampshire	-	-	-	-	-	-	-	-	-	-	-
New York	-	X	-	X	-	-	-	-	-	-	-
Ohio	X	X	X	X	-	-	X	-	X	-	-
Oklahoma	X	-	-	-	-	-	-	-	-	-	-
Vermont	-	-	-	-	-	X	X	-	-	-	-
Washington	-	-	X	X	-	-	-	-	-	-	-
Wisconsin*	X	X	X	X	-	X	-	-	-	-	-
TOTAL	6	6	8	9	1	2	5	2	3	2	2

* Obtained only from Specification

Table 1b. Tack Types Allowed Based on Survey and Specification Data (Part 2/2)

	CRS-3	CQS-1h	CQS-1hp	STE-1	HFMS-2h	AC-5	M140	M208	AE-T
Alabama	-	X	X	-	-	-	-	-	-
Colorado	-	-	-	-	-	-	-	-	-
Connecticut	-	-	-	-	-	-	X	-	-
Florida	-	-	-	-	-	X	-	-	-
Georgia	X	-	-	-	-	-	-	-	-
Idaho	-	-	-	-	-	-	-	-	-
Indiana	-	-	-	-	-	-	-	-	X
Minnesota	-	-	-	-	-	-	-	-	-
Nevada	-	X	-	-	-	-	-	-	-
New Hampshire	-	-	-	-	-	-	X	X	-
New York	-	-	-	-	X	-	-	-	-
Ohio	-	-	-	-	-	-	-	-	-
Oklahoma	-	-	-	-	-	-	-	-	-
Vermont	-	-	-	-	-	-	-	-	-
Washington	-	-	-	X	-	-	-	-	-
Wisconsin*	-	-	-	-	-	-	-	-	-
TOTAL	1	2	1	1	1	1	2	1	1

* Obtained only from Specification

Tack Coat Types

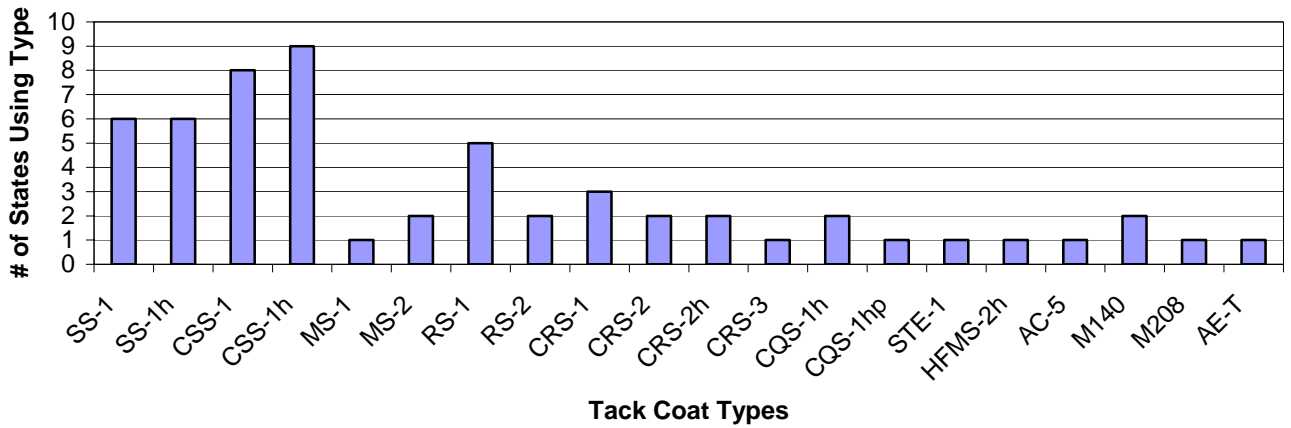


Figure 2. Number of States Using Different Types of Tack Coat

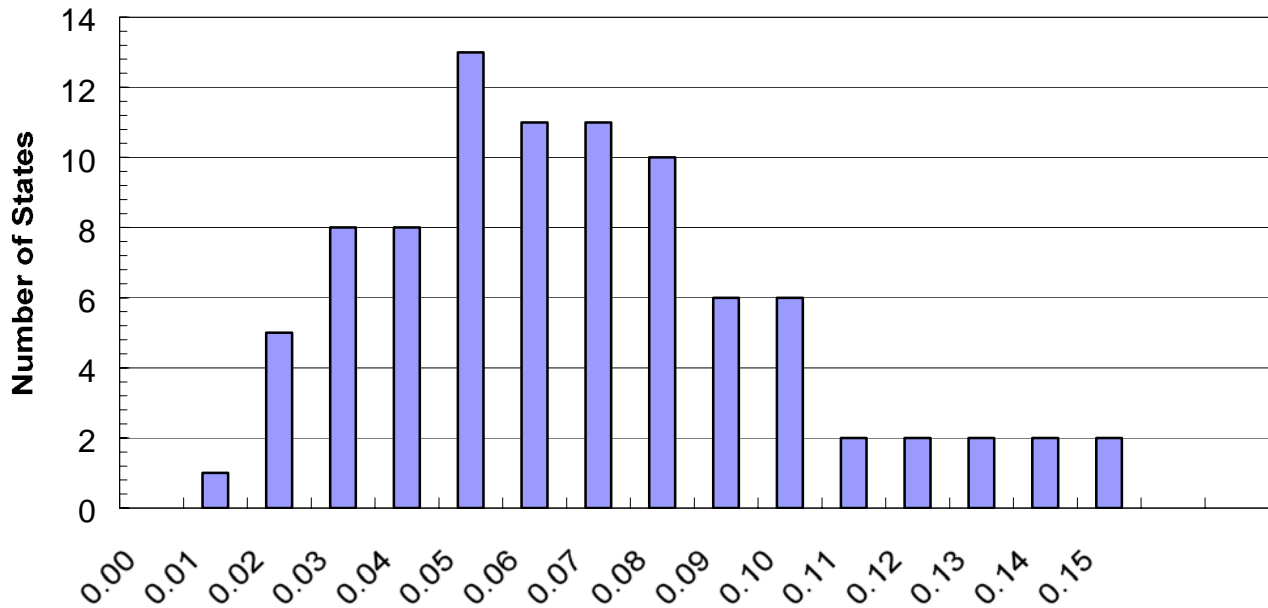
APPLICATION RATES

Table 2 shows the application rate based on the survey and specification data.. Figure 3 shows the number of states using various application rates.

Table 2. Application Rates Required.

	Application Rate (Gallons per Square Yard)															
	0.00	0.01	0.02	0.03	0.04	0.05	0.06	0.07	0.08	0.09	0.10	0.11	0.12	0.13	0.14	0.15
Alabama	-	-	-	-	-	X	X	X	X	X	X	-	-	-	-	-
Colorado	-	-	-	-	-	X	X	X	X	X	X	X	X	X	X	X
Connecticut	-	-	-	X	X	X	X	X	X	X	X	-	-	-	-	-
Florida	-	-	X	X	X	X	X	X	X	-	-	-	-	-	-	-
Georgia	-	-	X	X	X	X	X	X	X	-	-	-	-	-	-	-
Idaho	-	-	-	-	-	X	-	-	-	-	-	-	-	-	-	-
Indiana	-	-	-	X	X	X	X	X	X	-	-	-	-	-	-	-
Minnesota	-	-	-	-	-	X	X	X	X	X	X	X	X	X	X	X
Nevada	-	-	-	-	X	X	X	X	X	X	-	-	-	-	-	-
New Hampshire	-	-	X	X	X	X	-	-	-	-	-	-	-	-	-	-
New York	-	-	-	X	X	X	X	X	-	-	-	-	-	-	-	-
Oklahoma	-	-	-	-	-	-	-	-	-	-	X	-	-	-	-	-
Utah	-	-	-	-	-	X	X	X	X	X	X	-	-	-	-	-
Vermont	-	X	X	X	-	-	-	-	-	-	-	-	-	-	-	-
Washington	-	-	X	X	X	X	X	X	X	-	-	-	-	-	-	-
TOTAL	0	1	5	8	8	13	11	11	10	6	6	2	2	2	2	2

Tack Coat Application Rates



Tack Coat Application Rate

Figure 3. Number of States Using Different Types of Tack Coat

TACK COAT TEMPERATURE

Table 3 shows the tack coat temperatures required based on survey and specification data and Figure 4 shows the number of states requiring various tack coat temperatures.

Table 3. Tack Coat Temperatures Required.

	Tack Coat Temperature (°F)															
	40	50	60	70	80	90	100	110	120	130	140	150	160	170	180	190
Alabama	-	-	-	-	-	-	-	-	X	X	X	X	X	X	-	-
Colorado	-	-	-	-	-	-	-	-	-	X	-	-	-	-	-	-
Connecticut	X	X	X	X	X	X	X	X	X	X	X	X	X	-	-	-
Florida	-	-	-	-	-	-	-	-	-	-	X	X	X	X	X	-
Georgia	-	-	-	-	-	-	-	-	-	-	X	X	X	X	X	-
Minnesota	-	-	-	X	X	X	X	X	X	X	X	X	X	X	X	-
Nevada	-	-	-	-	X	X	X	X	X	X	-	-	-	-	-	-
Ohio	-	X	X	X	X	X	X	X	X	X	X	X	X	-	-	-
Oklahoma	-	X	X	X	X	X	X	X	X	X	X	X	X	X	X	-
Utah	-	-	-	-	-	-	X	-	-	-	-	-	-	-	-	-
Washington	-	-	-	X	X	X	X	X	X	X	X	-	-	-	-	-
Wisconsin*	-	-	-	X	X	X	X	X	X	X	X	X	X	-	-	-
TOTAL	1	3	3	6	7	7	8	7	8	9	9	8	8	5	4	0

* Obtained only from Specification

Tack Coat Temperatures

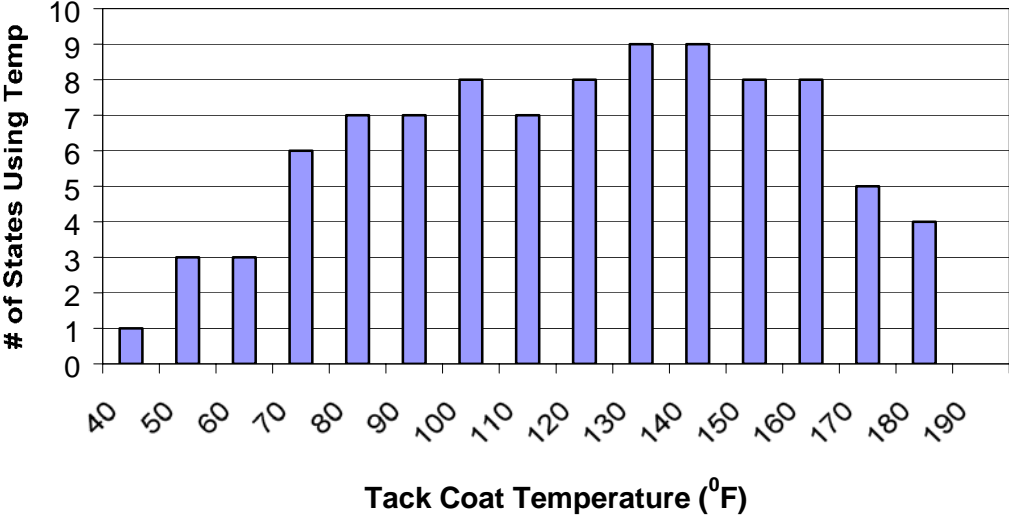


Figure 4. Number of States Using Different Tack Coat Temperatures

AIR TEMPERATURES

Table 4 shows minimum allowable air temperatures during tack coat application based on survey and Specification data. Figure 5 shows the number of states requiring various tack coat temperatures.

Table 4. Minimum Air Temperatures Required.

	Minimum Air Temperature (°F)															
	0	5	10	15	20	25	30	32	35	40	45	50	55	60	65	70
Alabama	-	-	-	-	-	-	-	-	-	X	-	-	-	-	-	-
Colorado	-	-	-	-	-	-	-	-	-	X	-	-	-	-	-	-
Connecticut	-	-	-	-	-	-	-	X	-	-	-	-	-	-	-	-
Florida	-	-	-	-	-	-	-	-	-	X	-	-	-	-	-	-
Georgia	-	-	-	-	-	-	X	-	-	-	-	-	-	-	-	-
Nevada	-	-	-	-	-	-	-	-	-	X	-	-	-	-	-	-
New Hampshire	-	-	-	-	-	-	-	-	-	X	-	-	-	-	-	-
New York	-	-	-	-	-	-	-	-	-	-	-	X	-	-	-	-
Ohio	-	-	-	-	-	-	-	-	-	X	-	-	-	-	-	-
Oklahoma	-	-	-	-	-	-	-	-	-	-	-	-	-	X	-	-
Utah	-	-	-	-	-	-	-	-	-	-	-	-	X	-	-	-
Vermont	-	-	-	-	-	-	-	-	-	-	X	-	-	-	-	-
Washington	-	-	-	-	-	-	-	-	-	-	-	X	-	-	-	-
Wisconsin*	-	-	-	-	-	-	-	-	-	X	-	-	-	-	-	-
Total		0	0	0	0	0	1	1	0	7	1	2	1	1	0	0

* Obtained only from Specification

Minimum Air Temperature

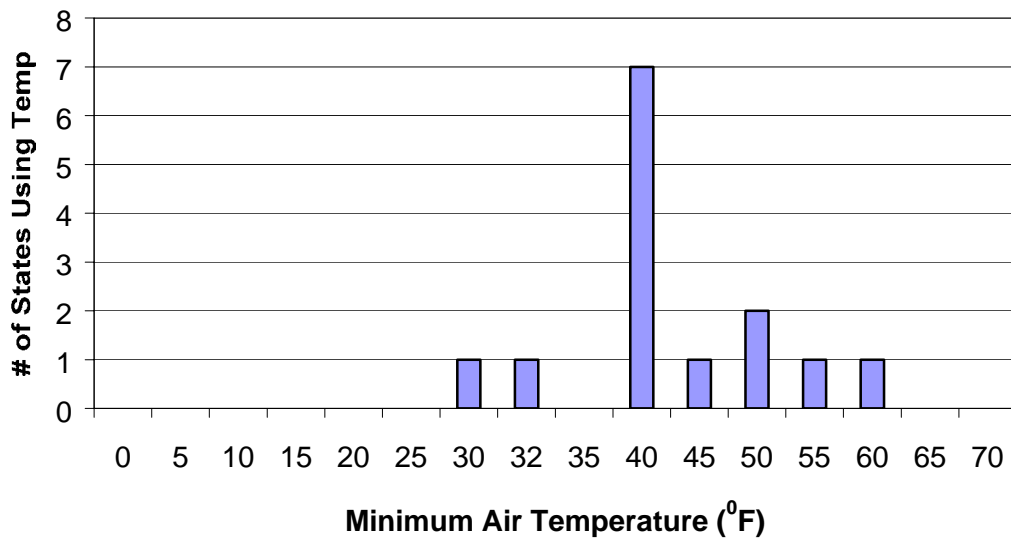


Figure 5 Number of States Requiring Minimum Air temperature During Tack Coat Application

The analysis of the survey data shows that states with varied tack coat specifications and construction methods are showing similar tack coat performance. This appears to indicate that stiffness of the pavement system (the thickness and stiffness of the top layer) may influence the performance of tack coat

TABLE OF CONTENTS

Chapter 1.	INTRODUCTION.....	A-1
1.1.	Problem.....	A-1
1.2.	Significance of Research.....	A-1
1.3.	Study Objectives.....	A-2
1.4.	Research Approach.....	A-2
Chapter 2.	LITERATURE REVIEW.....	A-4
2.1	Introduction.....	A-4
2.2	Background.....	A-4
2.3	Causes of Poor Bonding.....	A-5
2.4	Detection of Poor Bonding.....	A-7
2.5	Summary.....	A-12
Chapter 3.	DATA.....	A-13
3.1.	Introduction.....	A-13
3.2.	Federal Aviation Administration’s National Airport Pavement Test Facility.....	A-13
3.3.	Section Details.....	A-15
3.4.	Material Data.....	A-15
3.5.	Falling Weight Deflectometer Data.....	A-16
3.6.	Summary.....	A-16
Chapter 4.	FALLING WEIGHT DEFLECTOMTER ANALYSES.....	A-19
4.1.	Introduction.....	A-19
4.2.	Backcalculation of Pavement Layer Moduli.....	A-19
4.2.1.	Backcalculation Analysis of FAA NAPTF MFC Section.....	A-19
4.2.2.	Backcalculation Results.....	A-20
4.2.2.1.	Backcalculation Round 1 Results.....	A-20
4.2.2.2.	Backcalculation Round 2 Results.....	A-21
4.2.3.	Discussion of Backcalculation Results.....	A-21
4.3.	Forward Calculation Analysis of FAA NAPTF MFC Section.....	A-21
4.3.1.	Material Modeling.....	A-23
4.3.1.1.	Base and Subbase.....	A-23
4.3.1.2.	Subgrade.....	A-26
4.3.2.	Factors Affecting Forward Calculation Analysis.....	A-26
4.4.	Results of Forward Calculations.....	A-28
4.4.1.	Forward Calculation Results of All Layers.....	A-28
4.4.2.	Comparison of Forward Calculated Surface Layer Moduli.....	A-28
4.4.2.1.	Centerline Surface Layer Moduli.....	A-31
4.4.2.2.	Lane 5 Surface Layer Moduli.....	A-31
4.5.	Discussion of Forward Calculation Results.....	A-38
4.5.1.	Centerline.....	A-38
4.5.2.	Lane 5.....	A-38
4.5.3.	Results Summary.....	A-38

Chapter 5.	INTERLAYER SLIP ANALYSIS.....	A-39
5.1.	Introduction.....	A-39
5.2.	Analysis of Slip.....	A-39
5.2.1.	Background.....	A-39
5.2.2.	Asphalt Layer Moduli.....	A-39
5.2.2.1.	Splitting of Asphalt Layer.....	A-39
5.2.2.2.	Implications and Applications of Splitting Asphalt Layer.....	A-41
5.2.3.	Tack Coat Failure Ratio.....	A-41
5.3.	Effect of Slip.....	A-44
5.3.1.	Background.....	A-44
5.3.2.	Preliminary Calculations and Validations.....	A-44
5.3.3.	Determination of Effect of Slip in MFC Failed Sections.....	A-47
5.3.4.	Results.....	A-56
5.4.	Correlation of Tack Coat Failure Ratio with Effect of Slip.....	A-56
5.5.	Framework for Using FWD Data in Interlayer Slip Analysis.....	A-58
Chapter 6.	CONCLUSIONS AND RECOMMENDATIONS.....	A-61
6.1.	Summary of Findings.....	A-61
6.2.	Conclusion.....	A-61
6.3.	Recommendations.....	A-61
	REFERENCES.....	A-63

LIST OF FIGURES

2.1.	Slippage Cracking.....	A-4
2.2.	Tack Application Rates vs. Strength.....	A-6
2.3.	Excess Application.....	A-7
2.4.	Appropriate Application Amount.....	A-8
2.5.	Proper Spraying.....	A-8
2.6.	Result of Poor Spraying and Application Rate.....	A-9
2.7.	Milling Operation.....	A-9
2.8.	FWD Machine.....	A-10
2.9.	FWD Loading Plate and Sensors.....	A-11
2.10.	Typical Deflection Basin.....	A-11
3.1.	FAA NAPTF Site Layout.....	A-14
3.2.	Medium Strength Subgrade Section.....	A-14
3.3.	MFC Section Pavement Structure.....	A-15
3.4.	FAA NAPTF Lane Designations.....	A-16
4.1.	Calculation of K_1 , K_2 for Base (P-209).....	A-24
4.2.	Calculation of K_1 , K_2 for Subbase (P-154).....	A-25
4.3.	Typical Match of Measured and Calculated Deflection Basins.....	A-31
4.4.	Surface Layer Moduli of Failed and Unfailed Sections (C/L, 12 kip load).....	A-32
4.5.	Surface Layer Moduli of Failed and Unfailed Sections (C/L, 24 kip load).....	A-33
4.6.	Surface Layer Moduli of Failed and Unfailed Sections (C/L, 35 kip load).....	A-34
4.7.	Surface Layer Moduli of Failed and Unfailed Sections (Lane 5, 12 kip load).....	A-35
4.8.	Surface Layer Moduli of Failed and Unfailed Sections (Lane 5, 24 kip load).....	A-36
4.9.	Surface Layer Moduli of Failed and Unfailed Sections (Lane 5, 35 kip load).....	A-37
5.1.	Splitting of Asphalt Layer in Failed Section.....	A-40
5.2.	Structure and Evaluation Points Used for Preliminary Investigation.....	A-45
5.3.	Radial Stresses at Points Above and Below Interface, for Varied Slip.....	A-46
5.4.	Radial Stress Differences vs. BISAR Slip Number in BISAR Investigation.....	A-47
5.5.	MFC Failed Section Analysis, Pavement Structure Cases.....	A-48
5.6.	Layers and Evaluation Points Used in BISAR.....	A-50
5.7.	Typical Vertical Displacement Plot.....	A-52
5.8.	Typical Vertical Stress Plot.....	A-53
5.9.	Typical Radial Stress Plot.....	A-53
5.10.	Typical Plot of Radial Stresses Just Above and Below the Interface.....	A-55
5.11.	Typical Plot of Radial Stress Difference at Interface.....	A-55
5.12.	Effect of Slip / TFR Correlation.....	A-57
5.13.	Framework of FWD Data Use in Interlayer Slip Analysis.....	A-59
5.14.	Agency Use of Effect of Slip / TFR Correlation.....	A-60

LIST OF TABLES

3.1.	Available Material Property Data.....	A-17
3.2.	Locations and Dates of FWD Tests Used in Analysis.....	A-18
4.1.	Expected Layer Moduli.....	A-20
4.2.	Pavement Structure.....	A-21
4.3.	Structure used in Forward-Calculations.....	A-22
4.4.	Dates and Loading Information for FWD Tests.....	A-27
4.5(a)	Forward Calculation Results (Lane 5).....	A-29
4.5(b)	Forward Calculation Results (C/L).....	A-30
5.1.	Asphalt Moduli and TFR for Lane C/L, 1 Day.....	A-42
5.2.	Asphalt Moduli and TFR for Lane 5, 1 Day.....	A-43
5.3.	BISAR / KENLAYER Interface Values.....	A-46
5.4.	Properties of Sections Analyzed.....	A-49
5.5.	Effect of Slip Results.....	A-56
5.6.	TFR and Effect of Slip.....	A-57

CHAPTER ONE

INTRODUCTION

1.1. Problem

The Federal Aviation Administration's (FAA) National Airport Pavement Test Facility (NAPTF), located in Atlantic City, New Jersey, is a fully enclosed pavement test track. In this facility, nine sections of different pavement structures are evaluated under accelerated aircraft loading. One of the sections experienced extensive slipping between layers. Similar failures have been observed on highways in various states, such as Florida, Louisiana, Minnesota, New Jersey, and Wisconsin. This slippage can cause secondary failures like cracks and potholes, resulting in extensive failure of the pavement structure.

The slippage may be caused by poor bonding, which in turn may be caused by: improper amount of tack coat, improper tack coat type, poor lower layer condition, tack coat application in cold or wet weather, inadequate structural design of the surface course, and non-uniform application of tack.

In order to prevent such failures, poor bonding should be identified immediately after construction. If interlayer bonding failure can be detected in a new pavement, then steps could be taken to prevent such failures by modifying construction methodology.

The purpose of this study is to form a framework to use nondestructive Falling Weight Deflectometer (FWD) data to identify the lack of bonding in hot mix asphalt pavements. In particular, this study will address the lack of bonding between lifts in asphalt layers with the same material properties. The intent is that eventually interlayer bonding will be evaluated during the construction of pavements. The ability to identify bonding failures directly after construction will save money by minimizing future rehabilitation caused by the interlayer bonding failures.

1.2. Significance of Research

This study will provide a tool for state agencies to detect interlayer bonding failure from widely used FWD data. State agencies could use this methodology to detect failures immediately after construction of a given section and rectify, if necessary, any construction procedure to prevent them in the future. This methodology could also be used as a pavement management and rehabilitation tool, provided that the agencies have material data independently available. This methodology could reduce expenses for all, due to less pavement maintenance costs on the part of the roadway owners and less vehicle maintenance costs for the roadway users.

1.3. Study Objectives

The objectives of this study were:

1. To identify bonding failure, based on comparisons between surface layer moduli of failed and unfailed pavement sections calculated from FWD data.
2. To calculate the slip at the interlayer in the failed section.
3. To correlate the ratio of failed to unfailed pavement layer moduli with the effect of slip at the interlayer.
4. To develop a framework for using FWD data to identify interlayer bonding failures.

1.4. Research Approach

The following approaches were taken to accomplish each objective of this study:

Objective 1

1. Use pavement material data and established correlations to determine values of expected layer moduli for all layers in the pavement being analyzed.
2. Backcalculate layer moduli of the failed and unfailed pavement sections, assuming full bonding in both sections.
3. Check for reasonableness of backcalculated layer moduli.
4. If unreasonable backcalculated moduli are derived, forward calculate layer moduli of the failed and unfailed pavement sections, assuming full bonding in both sections.
5. If forward calculations are used, check for reasonableness of forward calculated layer moduli.
6. Using an established correlation, normalize the forward calculated surface layer moduli of failed and unfailed sections to a common temperature.
7. Compare the normalized calculated surface layer moduli of the failed and unfailed sections to determine if the failed sections can be identified by comparisons of failed and unfailed calculated surface layer moduli.

Objective 2

1. Calculate the stresses and vertical displacements in the failed section for each FWD test.
2. Calculate the effect of slip in the failed section for each FWD test by defining the effect of slip as being a function of the difference in radial stress at points directly above and below the failed interlayer.

Objective 3

Correlate the effect of slip with the ratio of surface moduli of failed and unfailed sections, considering the effect of slip calculated for each of the FWD tests in failed pavement sections.

Objective 4

Summarize each of the above steps so as to create a framework for using FWD data to identify interlayer bonding failures.

CHAPTER TWO LITERATURE REVIEW

2.1. Introduction

This chapter discusses the typical failures that occur due to poor interlayer bonding and the mechanism causing poor performance. This section is followed by a detailed explanation of factors that lead to poor bonding between layers and methods of detecting poor bonding.

2.2. Background

Many studies, as will be discussed below, have been and are continuing to be done on tack coats, proper use of tack coats, and their effects on interlayer strength. Through review of these studies, many things have been noted regarding tack coats, interlayers, and the various effects on pavement.

The first item of note from the literature review is what type of problems interlayer bonding failures cause. The typical signal that a pavement is experiencing interlayer bonding failure is slippage cracking, an example of which may be viewed in Figure 2.1.

This slippage cracking consists of crescent shaped cracks that develop at the pavement surface and are the direct result of a slippage of the upper asphalt layer over the lower layer (Shahin, et al., 1987b; Uzan, et al., 1978). The slippage between the layers is



Figure 2.1. Slippage Cracking

the result of a weak interlayer bond. The crescent cracks, while certainly a problem themselves, are not the only problem resulting from slippage. As the interlayer bond is weakened and broken as the upper layer slips, the pavement system as a whole is weakened. This is because the broken bond reduces the stiffness of the system as a whole and loads may no longer be supported and distributed by the system as designed (Shahin, et al., 1987b).

2.3. Causes of Poor Bonding

The factors that affect bonding are:

- Type of tack coat.
- Amount of tack coat used.
- Pavement temperatures during service life.
- Gradations of pavement mixtures.
- Condition of surface being tacked.
- Moisture being present at time of tacking.

Each of these factors are briefly discussed below.

Several studies (Hachiya, et al., 1997; Mohammad, et al., 2002; Uzan, et al., 1978) have looked at the effect of different tack coats on interlayer bonding. In these studies, it was found that at high temperatures the type of tack has little effect on the shear strength of the interlayer, but at lower temperatures the types have varying strengths, though not significantly different.

The amount of tack coat in the interlayer affects the strength of the interface as well. The strength of the bond has been found to increase as the rate of application of tack coat increases, up to an optimum amount of tack (Hachiya, et al., 1997; Mohammad, et al., 2002; Uzan, et al., 1978). This may be seen in Figure 2.2, which is a figure from Mohammad, et al., 2002. After the optimal amount the strength decreases with an increase in rate of application, since beyond the optimum amount, the excess tack introduces a slip plane to the interlayer. However, the effect of the application rate is also largely dependent on the air and pavement temperatures. At lower temperatures, an increased rate decreases the strength, however at higher temperatures the rate does not cause significant changes in the strength (Mohammad, et al., 2002). Also, the rate does not cause significant changes when placed on fresh pavement (Uzan, et al., 1978). Figure 2.3 shows an example of excess tack, while Figure 2.4 shows an appropriate application amount. Figures 2.5 and 2.6 show proper spraying and the results of poor spraying, respectively.

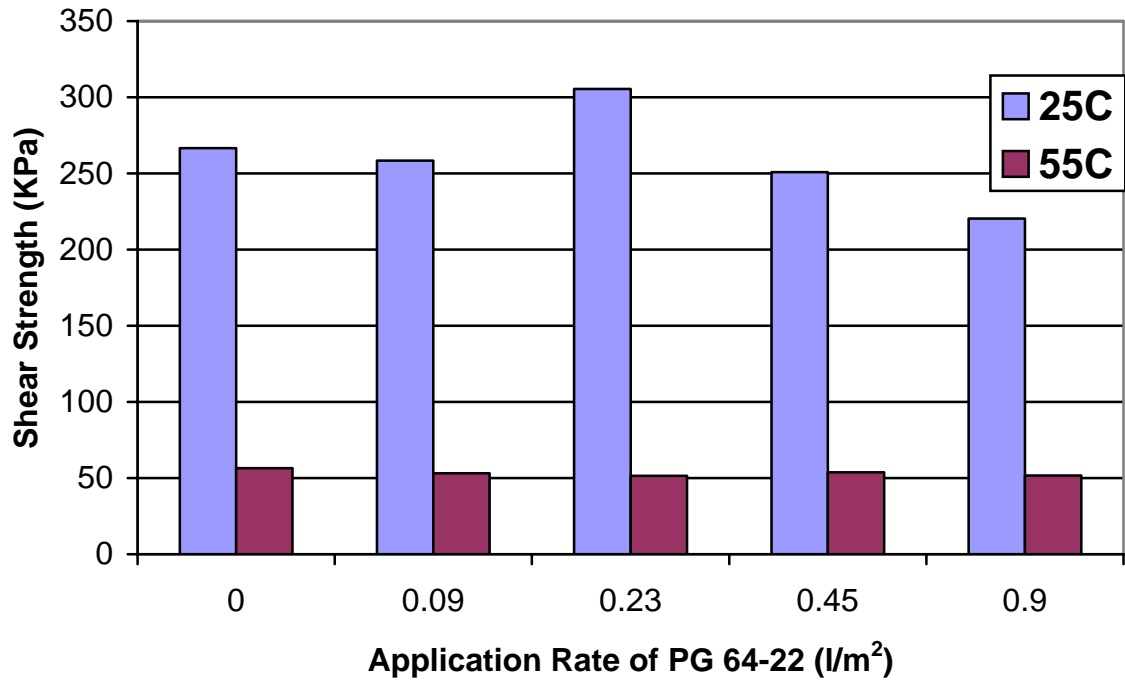


Figure 2.2. Tack Application Rates vs Strength, (Mohammad et al., 2002)

Different application rates are required for maximum effectiveness, based on the conditions of the surface being tacked and on the gradation of the asphalt mixtures used in the pavement. It has been found that milled surfaces provide a higher shear strength than do smooth and worn surfaces (Sholar et al., 2002). Similarly, it has been found that coarse asphalt mixes provide a higher strength than fine mixes, because of aggregate interlock (Sholar et al., 2002). Figure 2.7 shows a milling operation, which is recommended for effective bonding.

Finally, since weather is always a concern in construction, studies have been done on the effect of moisture on the strength of the interlayer. It was found that when moisture is on the interlayer plane at the time of paving, the strength of the interlayer decreases due to stripping (Sholar et al., 2002).

2.4. Detection of Poor Bonding

At the current time, if poor interlayer bonding was to be identified before failures occurred, this would be done through destructive testing. The destructive method used would be coring. Cores would be taken at locations along the length of pavement being tested, and the lack of bond would be identified by testing the core in shear. While this method is effective, it has the downfall of being destructive. This study looks at the potential of using a nondestructive test to identify poor interlayer bonding.



Figure 2.3. Excess Application



Figure 2.4. Appropriate Application Amount



Figure 2.5. Proper Spraying



Figure 2.6. Result of Poor Spraying and Application Rate



Figure 2.7. Milling Operation

The Falling Weight Deflectometer (FWD) is a tool used in non-destructive testing of pavements. The FWD device (Figure 2.8) is mounted on a trailer, which can be towed by a truck and easily transported between testing locations. Since it is a mobile testing device, complete road closures are not necessary when the FWD test is being performed.

In an FWD test, a weight is dropped onto the pavement, applying a dynamic load to the pavement to mimic loading by traffic. The loads used range from 3000 to 33000 pounds, but a commonly used load is 9000 pounds. As the load is applied, sensors on the FWD machine measure the deflection of the pavement as it reacts to the load. Most FWD machines have seven sensors located in positions similar to those shown in Figure 2.9.

The data obtained from the FWD test are the measured deflections of the pavement at each testing location. The deflections at each location form a deflection basin: a large deflection at the point of loading and decreasing deflections as the distance from the load increases. A typical deflection basin is shown in Figure 2.10. The FWD data is used for pavement analysis. Programs are utilized to calculate the stiffness moduli of the pavement layers based on the measured deflections. The calculated in-situ moduli are typically used to evaluate the structural condition of pavements. This study investigates the use of FWD data to analyze the bonding within pavements.



Figure 2.8. FWD Machine



Figure 2.9. FWD Loading Plate and Sensors

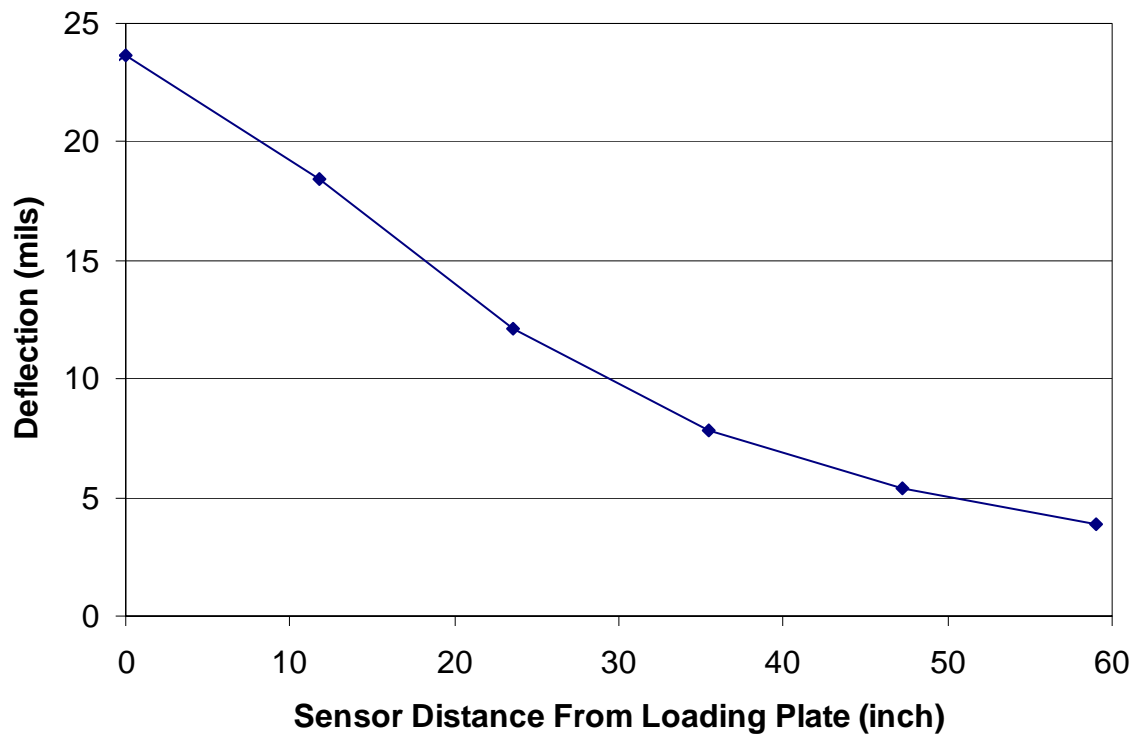


Figure 2.10. Typical Deflection Basin

2.5. Summary

This chapter discussed interlayer bonding failures, the mechanics of such failures, the causes of poor bonding, and the detection of poor bonding. These are all important topics in studies of interlayer bonding. However, for this study, the most critical topic discussed in this chapter is the detection of poor bonding. The use of FWD data to detect poor bonding is the focus of this study, and so it is discussed throughout the following chapters.

CHAPTER THREE DATA

3.1. Introduction

Chapter Two discussed the results and causes of interlayer bonding failures and the identification of poor bonding. As indicated at the end of the chapter, the use of FWD data in identifying poor bonding is the focus of this study. While FWD data was the primary set of data used, other data used included pavement section and pavement material data. This chapter discusses each set of data utilized in this study.

3.2. Federal Aviation Administration's National Airport Pavement Test Facility

The source utilized for this study was the Federal Aviation Administration's (FAA) National Airport Pavement Test Facility (NAPTF), located in Atlantic City, New Jersey. The facility is a fully enclosed test track that is 900 feet long and 60 feet wide. The test track, as shown in Figure 3.1, is composed of nine different pavement structures, with three different strength subgrades. The pavement was loaded, with a 45,000 lb load, using various airplane landing gear configurations traveling along the pavement. During the loading period, which was roughly fourteen months, FWD tests were performed monthly at various locations on the pavement. At the end of the loading period, one section of pavement was investigated in detail since it had experienced rather severe rutting. In the investigation, a trench was dug perpendicular to the centerline of the pavement to view the pavement cross-section. During these investigations, which included taking cores of the pavement, it was found that there had been delamination of the surface asphalt layer between lifts. A thin layer of dust was observed between the two lifts, which may have been the cause of the delamination (Garg, 2001). This section was within the medium strength section, which is shown in Figure 3.1, and is shown in more detail in Figure 3.2.

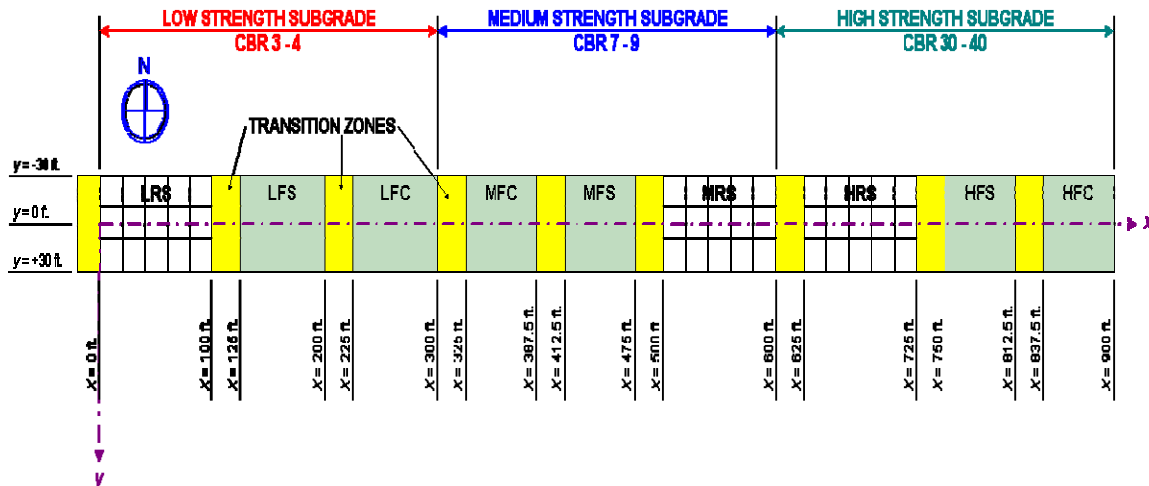


Figure 3.1. FAA NAPTF Site Layout (FAA NAPTF, 2003)

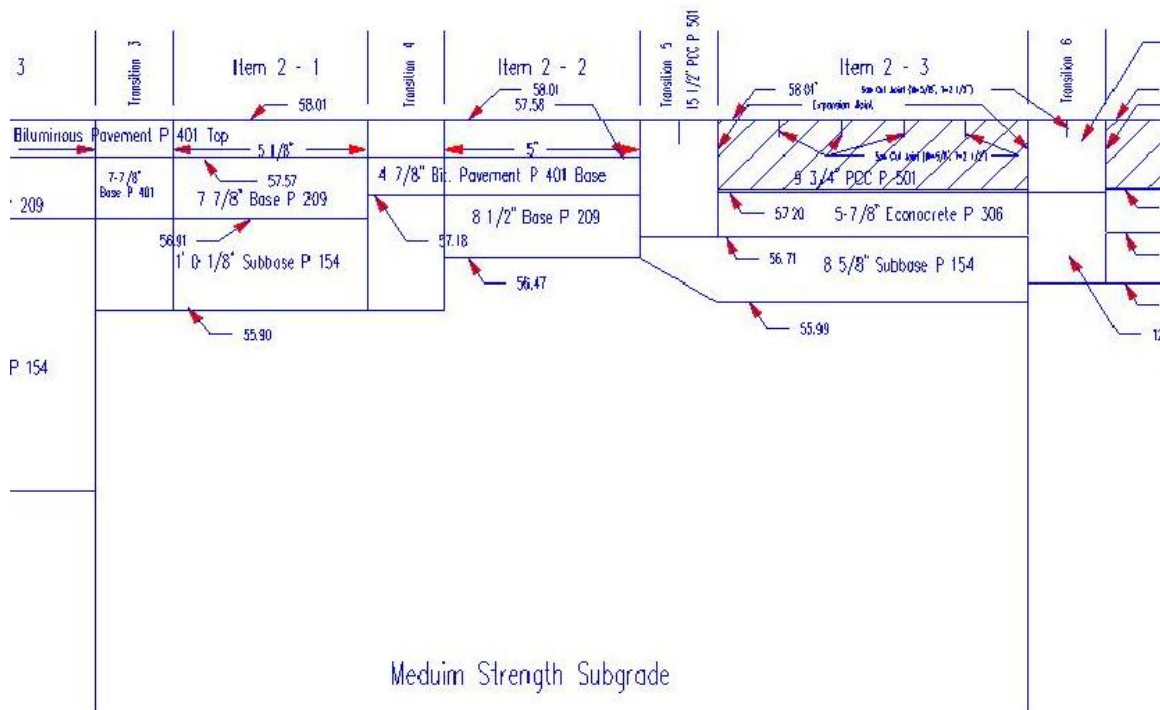


Figure 3.2. Medium Strength Subgrade Section (FAA NAPTF, 2003)

3.3. Section Details

The section in which delamination was found is the “Medium strength subgrade, Flexible pavement, Conventional base” (MFC) section (labeled as “Item 2-2” in Figure 3.2), which occupies stations 3+25 to 3+87 of the test track (stations start at the west end of the track and measure the x-distance shown in Figure 3.1). More particularly, the delamination was found in the area of 3+65 to 3+76. This MFC section was analyzed in this study. Figure 3.3 shows the pavement structure of the MFC section. The FAA NAPTF website at the address listed in the reference section of this report contains details on the loading of the test facility and the other pavement structures tested (FAA, 2003).

3.4. Material Data

Quality control during construction of the facility was strict, and material tests were performed on all materials used. Fairly extensive material property data are available in the database on the FAA NAPTF website listed in the reference section (FAA, 2003). This data was used in the FWD data analyses as discussed in a later section. Table 3.1 shows available material property data. Detailed material properties of all materials in the MFC section are shown in Appendix A (Gomba, 2004).

P-401 Asphalt Pavement (5.12 inches)
P-209 Base (7.99 inches)
P-154 Sub-Base (12.12 inches)
Medium Strength Subgrade (94.8 inches)

Figure 3.3. MFC Section Pavement Structure

3.5. Falling Weight Deflectometer Data

FWD tests were performed at regular time intervals during the life of the pavement tests. Tests were performed in Lanes 2 and 5, along with the centerline of the facility (lane designations are shown in Figure 3.4). The raw deflection data may be viewed in the Appendix B (Gomba, 2004). Information on the FWD data used in this study is given in Table 3.2.

3.6. Summary

This chapter provided an overview of all of the data utilized in this study. The pavement section being analyzed was presented, and both the material data available and the FWD tests used in the analysis were identified. The use of the material data and the analysis of the FWD data are discussed next.

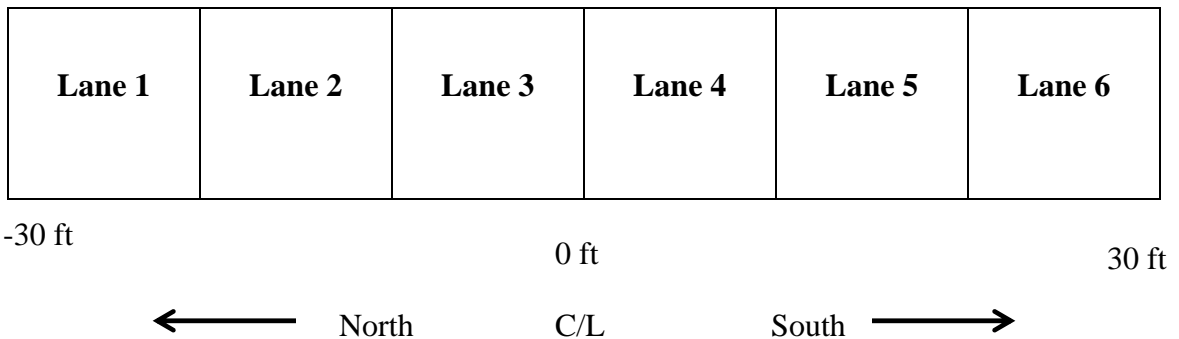


Figure 3.4. FAA NAPTF Lane Designations

Table 3.1. Available Material Property Data

Property	Layer / Material			
	P-401	P-209	P-154	Subgrade
CBR	N/A	✓	✓	✓
Moisture Content		✓	✓	✓
Dry Density		✓	✓	✓
Resilient Modulus		✓	✓	✓
Aggregate Gradations	✓	Not Applicable		
% Asphalt	✓			
% Voids	✓			
% VMA	✓			
% VFA	✓			
Stability	✓			
Flow	✓			
Maximum Specific Gravity	✓			
Bulk Specific Gravity	✓			
% Compaction	✓			

Table 3.2. Locations and Dates of FWD Tests Used in Analysis

FWD Drop Numbers *	Location of Test **	Date of Test	Condition of Interlayer
24855 - 24858	3+45: Lane 5	2/16/00	Unfailed
24859 - 24862	3+55: Lane 5	2/16/00	Unfailed
24863 - 24866	3+65: Lane 5	2/16/00	Failed
24867 - 24918	3+75: Lane 5	2/16/00	Failed
24919 - 24922	3+45: C/L	2/25/00	Unfailed
24923 - 24926	3+55: C/L	2/25/00	Unfailed
24927 - 24930	3+65: C/L	2/25/00	Failed
24931 - 24934	3+75: C/L	2/25/00	Failed
24959 - 24962	3+45: C/L	3/20/00	Unfailed
24963 - 24966	3+55: C/L	3/20/00	Unfailed
24967 - 24970	3+65: C/L	3/20/00	Failed
24971 - 24974	3+75: C/L	3/20/00	Failed
25303 - 25306	3+45: C/L	6/22/00	Unfailed
25307 - 25310	3+55: C/L	6/22/00	Unfailed
25311 - 25314	3+65: C/L	6/22/00	Failed
25315 - 25318	3+75: C/L	6/22/00	Failed

* Each FWD test performed was numbered with a 5 digit number. Refer to the Appendix for further information on each FWD drop.

** Stations indicated are distances from the west end of the facility, i.e. 0+00 = the start of the Low Strength Subgrade section.

CHAPTER FOUR

FALLING WEIGHT DEFLECTOMETER ANALYSES

4.1. Introduction

This chapter discusses in detail the analysis conducted to obtain moduli of all layers in the pavement structure from FWD deflection data. This analysis was conducted using various programs and is explained below.

4.2. Backcalculation of Pavement Layer Moduli

Once FWD data is obtained, it can be utilized to estimate the pavement layer moduli. This is done through a method called backcalculation. All backcalculation programs determine the pavement layer moduli based on the measured surface deflections. The general idea in backcalculation is to match the measured surface deflections with estimated surface deflections, accomplished by adjusting the layer moduli to change the shape of the estimated surface deflection basin.

4.2.1. Backcalculation Analysis of FAA NAPTF MFC Section

Analysis of this section was ideal, since the test facility is in a controlled environment facility. Material properties were recorded for all materials used, and FWD data is available for each month that the pavement was loaded. Material properties and FWD data may be viewed in the Appendix (Gomba, 2004). With extensive material and deflection data available, calculations involving the pavement may be made with greater confidence.

To begin the study of the MFC section, anticipated ranges of layer moduli were calculated from the available material properties for each layer shown in the Appendix. These calculations were performed using correlations found in *Pavement Analysis and Design* (Huang, 1993). For the base, subbase, and subgrade layers, expected resilient modulus values were determined from tested CBR values. For the hot mix asphalt (HMA) layer, the expected range of resilient modulus was determined from the percent binder, stiffness modulus of binder, and percent aggregate for the mix. The expected layer moduli based on the material properties are shown in Table 4.1. The expected layer moduli values were a yardstick to evaluate the reasonableness of backcalculated moduli.

Before investigating the slippage issue, the backcalculations were first validated by backcalculating the layer moduli for an unloaded or relatively unloaded section of pavement. The reason for this is that within such a pavement section, backcalculation should provide reasonable results, since loads may cause distresses in pavements which would affect backcalculated moduli. The centerline of the pavement facility is unloaded, so theoretically all FWD tests performed on the centerline would produce similar backcalculated layer moduli for different locations. This being the case, the

backcalculations were initially performed on the centerline to determine the unfailed sections for validation purposes.

Two backcalculation programs were utilized: EVERCALC 5.0 (Washington State DOT, 2001) and BAKFAA (FAA, 2000). Both programs were used to analyze FWD data from the beginning of the loading period (drop numbers 24919 to 24934 and 24959 to 24974) and the end of the loading period (drop numbers 25303 to 25318). These drop numbers were chosen because they represented times near the beginning and ending of the loading period. Dates and locations of these drops were shown in the previous chapter in Table 3.2. Two rounds of backcalculations were done for the above locations and are discussed below.

Table 4.1. Expected Layer Moduli

Layer	Minimum Expected E (psi)	Maximum expected E (psi)
P-401 HMA	145,000*	2,600,000*
P-209 Base	15,000	30,000
P-154 Subbase	10,000	20,000
Subgrade	8,000	23,000

* Assuming less aging of the asphalt than usual, since it is in an enclosed facility.

4.2.2. Backcalculation Results

The results of each round are discussed separately below.

4.2.2.1. Backcalculation Round 1 Results

For the first round of backcalculations, a stiff layer below the subgrade, with an infinite depth and a modulus of 1,000,000 psi, was added to the structure in Figure 3.3. This stiff layer represents the native soil below the constructed subgrade, since the in-situ soil is assumed to be stiff as described in a study of FWD calculations on the FAA NAPTF subgrades (McQueen et al., 2001). The structure details are shown in Table 4.2. It was assumed that all layers were fully bonded for all sections.

In Round 1, it was discovered that the programs grossly over-estimated the moduli of the subbase layer and under-estimated the moduli of the base layer. However, the calculated HMA layer and subgrade moduli were in the expected range. The pavement structure was thus slightly modified in the following round. The results of Round 1 may be viewed in Appendix C in Tables C.1-C.2 (Gomba, 2004).

Table 4.2. Pavement Structure

Layer	Round 1 (Original)			Round 2 (Modification)		
	Material	Thickness (in)	Poisson's Ratio	Material	Thickness (in)	Poisson's Ratio
1	HMA	5.12	0.35	HMA	5.12	0.35
2	Base	7.88	0.35	Merged Base/Subbase	20	0.35
3	Subbase	12.12	0.35	Subgrade	94.8	0.45
4	Subgrade	94.8	0.45	Stiff Layer	Infinite	0.45
5	Stiff Layer	Infinite	0.45	---	---	---

4.2.2.2. Backcalculation Round 2 Results

In the second round of backcalculations, the structure was similar to that of the first round, but the base and subbase layers were merged into one layer. There were two reasons for this: 1) the programs were under-estimating the base layer and over-estimating the subbase layer, and 2) there was poor reliability on the calculated moduli for both layers. Table 4.2 shows the structure details for both Round 1 and 2. Once again it was assumed that all layers were fully bonded.

The results of this round provided more reasonable moduli for the combined layer, keeping in mind that the combined moduli would be a weighted average of the individual layer moduli. The HMA layer and subgrade moduli were again in the expected range. However, there was no statistically significant difference between failed and unfailed sections. The results of Round 2 may be viewed in Appendix C in Tables C.3(a) – C.4(b) (Gomba, 2004).

4.2.3 Discussion of Backcalculation Results

The backcalculated moduli did not reflect a lack of bond because of the linear elastic analysis that was used. Linear elastic analysis may be an over-simplification that is affecting the calculated moduli, since it is well known that materials do not always behave in the linear range. This analysis did not allow for calculation of reasonably accurate layer moduli for all layers, which is critical, especially for the surface layer.

Since the linear elastic analysis did not provide reasonable results, a more extensive non-linear elastic analysis that would accurately model the material behavior was necessary. This non-linear elastic analysis is discussed in the next section.

4.3. Forward Calculation Analysis of FAA NAPTF MFC Section

Since reliable non-linear analysis backcalculation tools were not available, a forward calculation program that allowed non-linear analysis was used. The forward calculation program used was KENLAYER.

In forward calculations, like backcalculations, the FWD data is used to calculate layer moduli. The difference is that in forward calculations the programs calculate deflections based on the inputs of layer moduli and FWD loads. The layer moduli are changed manually by the user so that the calculated deflection basins match the measured deflection basins.

Forward calculations have been performed on both Lane 5 and the centerline (C/L), with FWD data from times 1 day (FWD drop numbers 24855 to 24918 and 24919 to 24934) and 8 weeks of loading (FWD drop numbers 25303 to 25318). The dates and locations of these drops are shown in Chapter 3 in Table 3.2.

The structure analyzed in KENLAYER was slightly different from the structures used in the backcalculations. The main reason for this is that the program allows the use of nonlinear elastic materials. The base, subbase, and subgrade were all considered as nonlinear layers.

Since moduli values change with stress and hence depth, the principle of finite element analysis was used to accurately model the pavement behavior, and the base and subbase layers were subdivided into smaller layers. As non-linear material layers, the moduli values depend on the stress invariant, which varies with depth (as discussed in the next section). Since the subgrade was considered to be sufficiently far from the surface, it was considered as one layer with nonlinear material properties. Again, a stiff layer was included below the subgrade. The structure used in the forward calculations is shown in Table 4.3.

Table 4.3. Structure used in Forward Calculations

Layer #	Material	Thickness (in)	Poisson's Ratio	Unit Weight (lb/in³)
1	HMA	5.12	0.35	0.088
2	Base	1.315	0.35	0.088
3	Base	1.315	0.35	0.088
4	Base	1.315	0.35	0.088
5	Base	1.315	0.35	0.088
6	Base	1.315	0.35	0.088
7	Base	1.325	0.35	0.088
8	Subbase	2.02	0.35	0.074
9	Subbase	2.02	0.35	0.074
10	Subbase	2.02	0.35	0.074
11	Subbase	2.02	0.35	0.074
12	Subbase	2.02	0.35	0.074
13	Subbase	2.02	0.35	0.074
14	Subgrade	94.8	0.45	0.0537
15	Stiff Layer	Infinite	0.45	0.0537

4.3.1. Material Modeling

4.3.1.1. Base and Subbase

The program calculated the nonlinear layer moduli for the base and subbase by using equations that include constants derived from material property tests: the unconfined or triaxial compression tests. For granular materials, i.e. the base and subbase, the equation used was:

$$E = K_1 * \theta^{K_2} \quad (4.1)$$

where:

E = Stiffness modulus of material

K₁ = Material constant, derived through material testing

θ = Stress invariant, which is the sum of the three principle stresses derived through material testing

K₂ = Material constant, derived through material testing

The program also used K₀, which was the coefficient of earth pressure and was assumed to be 0.6, as recommended by Huang, 1993. The values of K₁ and K₂ for each material were determined by fitting the above equation using the material data of the respective layer. Each respective layer had data from 2 samples that were tested, and so for each layer there were two data plots and two equations, as shown in Figures 4.1 and 4.2. The average K₁ and K₂ of the two samples for each layer's material was used. For the base, K₁ and K₂ were 4088 and 0.6, respectively. For the subbase, K₁ and K₂ were 3729 and 0.56, respectively.

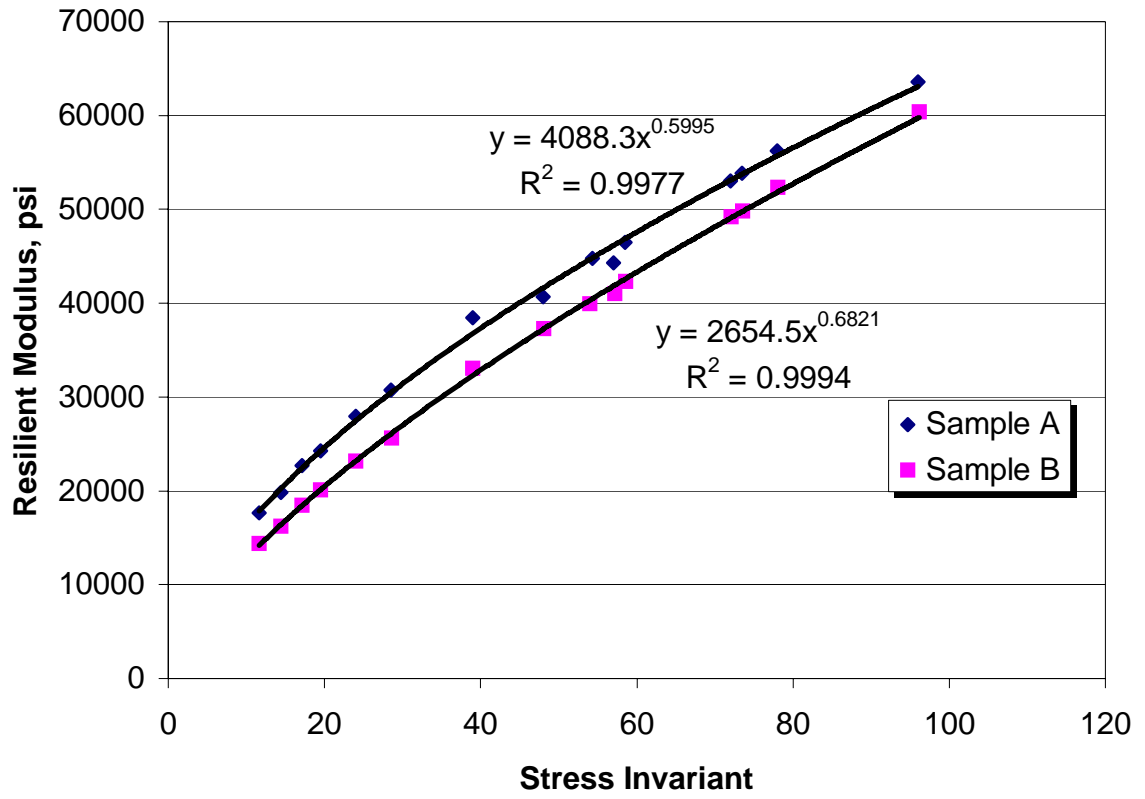


Figure 4.1. Calculation of K_1 , K_2 for Base (P-209)

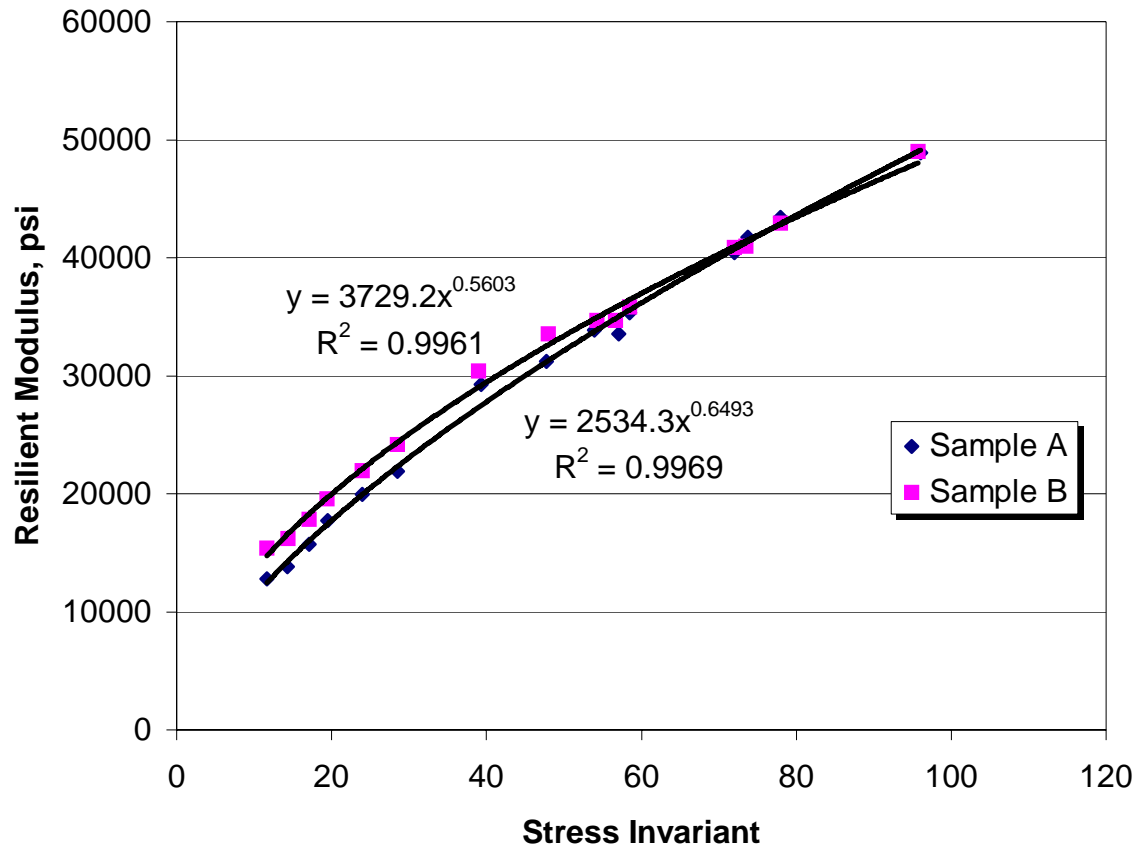


Figure 4.2. Calculation of K_1 , K_2 for Subbase (P-154)

4.3.1.2. Subgrade

For the nonlinear clay materials, i.e. the subgrade, the equations used were:

$$E = K_1 + K_3(K_2 - \sigma_d), \text{ when } \sigma_d < K_2 \quad (4.2)$$

$$E = K_1 + K_4(\sigma_d - K_2), \text{ when } \sigma_d > K_2 \quad (4.3)$$

where:

E = Stiffness modulus

K_1 , K_2 , and K_3 = Material constants, determined through laboratory testing

σ_d = Deviator stress, derived from triaxial test

For this study, the values used were as recommended by Huang: $K_2 = 6.2$, $K_3 = 1110$, and $K_4 = 178$ (Huang, 1993), while K_1 was changed so that the calculated deflection basin matched the measured deflection basin.

4.3.2. Factors Affecting Forward Calculation Analysis

Many factors influenced the deflections of the pavement under applied loads. This is especially true since FWD data is being analyzed from tests performed at different times over a span of a year, during which the pavement was heavily trafficked. Some of the main factors that were found to influence the calculated E values were: time, load, and temperature. Additionally, since two lanes were involved in the analysis, the lanes were also a factor to be considered, along with the sections of each lane. Each of these factors is briefly discussed below.

Time

The time of the tests, that is the date on which the tests were taken, is an important factor. This is because as the pavement is loaded, its condition deteriorates. There were fifteen different dates in which FWD testing was performed. However, the pavement was not loaded between all of these dates, so in this paper the FWD tests are identified by both the FWD number and by the number of days or weeks of loading to date. The dates of FWD tests and the “time loaded to date” information for FWD tests of the MFC section are shown in Table 4.4. Those that were used in the forward calculation analysis are shown in bold. More detailed information on trafficking between FWD test dates may be viewed in Appendix D (Gomba, 2004).

Load

The load applied by the FWD machine is an important factor because the base, subbase, and subgrade were all modeled as non-linear materials. The calculated moduli of these non-linear layers were thus different for each load.

Lane

In this study, two lanes have been analyzed. These are Lane 5, which is loaded, and the C/L, which is not loaded. The difference in loading between lanes makes a

difference in the calculated moduli for each lane. For this reason, the results of each lane may not be compared with those of other lanes.

Table 4.4. Dates and Loading Information for FWD Tests ^{*1}

Date of FWD Test	Days Loaded to Date ^{*2}	Weeks Loaded to Date ^{*3}	Traffic Repetitions to Date
6/14/1999	0	0	0
11/17/1999	0	0	0
1/11/2000	0	0	0
2/11/2000	0	0	0
2/16/2000	1	0.14	28
2/25/2000	1	0.14	28
3/20/2000	1	0.14	28
4/7/2000	8	1.14	931
4/14/2000	12	1.71	1892
4/20/2000	15	2.14	2746
4/26/2000	19	2.71	3556
5/6/2000	26	3.71	5015
5/23/2000	37	5.29	8040
6/22/2000	54	7.71	11948
8/31/2000	58	8.29	12952

*1 Those tests in bold indicate data used in forward calculation analysis.

*2 1 Day = 1 day of traffic repetitions.

*3 1 Week = 7 days of traffic repetitions (not 7 consecutive calendar days).

Section

Each lane consisted of two sections. An unfailed section, at stations 3+45 and 3+55, where there was no delamination, and a failed section at stations 3+65 and 3+75, where delamination was found.

Temperature

The pavement temperature at the time of the FWD tests is very important, since asphalt stiffness is significantly affected by temperature. In order to make any comparison between FWD tests performed at different temperatures, it was necessary to make adjustments to all calculated asphalt moduli to adjust them to a common temperature. The average temperature, 13°C (55°F), was used as the common temperature to minimize error through having large adjustments. This adjustment was made with the temperature adjustment factor, recommended by Briggs et al., 2000. This adjustment factor, for adjusting backcalculated asphalt moduli, is given by:

$$ATAF = 10^{slope(T_r - T_m)} \quad (4.4)$$

where:

ATAF = Asphalt temperature adjustment factor

slope = slope of the log modulus versus temperature equation

(-0.0195 used for Lane 5 and -0.021 used for the C/L)

T_r = Reference mid-depth of HMA layer (13°C used)

T_m = Mid-depth temperature of HMA layer at time of FWD test

The temperatures and adjusted calculated surface layer moduli may be viewed in Appendix G in Table G.1(a) – G.1(b) (Gomba, 2004).

4.4. Results of Forward Calculations

4.4.1. Forward Calculation Results of All Layers

The P-401 and P-154 layer moduli were mostly in the expected ranges. Several P-209 moduli, for FWD loads of 35,000 pounds, were over the expected values by up to 16,000 psi. This is likely attributed to the fact that a larger load was applied. However, most were in the expected range. Only 29% were greater than 5% over the maximum expected, and only 17% were greater than 10% over the maximum expected. The calculated subgrade moduli were mostly in the expected range, though towards the high end. A few were slightly higher than expected, but minimally so (+1000 psi). The calculated layer moduli of all layers for Lane 5 and the C/L are shown in Table 4.5(a) and Table 4.5(b), respectively. The author had confidence in these values because the deflection basins matched very well (typical deflection basin match shown in Figure 4.3) and the calculated layer moduli were all in or reasonably close to the expected range. Deflection basins for Lane 5 and the C/L are shown in Appendix E and Appendix F, respectively (Gomba, 2004).

4.4.2. Comparison of Forward Calculated Surface Layer Moduli

With the calculated P-401 moduli adjusted to a single reference temperature, the forward calculated moduli were compared between failed and unfailed sections. The comparison was made by first sorting the results by lane, contact pressure, and time. The average modulus and 95% confidence interval were calculated for each data set. The average surface layer moduli of the failed sections were compared with those of the unfailed sections, for both Lane 5 and the C/L, as discussed below. Additionally, a statistical analysis of the calculated P-401 moduli was conducted using SPSS to identify what factors (time, load, temperature, lane, section) significantly affected the calculated P-401 moduli. These results may be seen in Appendix H in Table H.1 (Gomba, 2004).

Table 4.5(a). Forward Calculation Results (Lane 5)*

FWD #	FWD Load (lb)	E_{P-401} (psi)	E_{P-209} (psi)	E_{P-154} (psi)	E_{subgrade} (psi)
24856	11,000	1,700,000	16,600	12,902	22,800
24857	23,000	1,510,000	23,655	16,142	20,580
24858	35,000	1,200,000	30,130	18,512	19,220
24860	11,000	1,625,000	16,717	12,917	22,080
24861	23,000	1,470,000	23,767	16,147	20,230
24862	35,000	1,150,000	30,380	18,517	19,010
24864	11,000	1,500,000	16,978	13,025	22,210
24865	23,000	1,050,000	25,090	16,635	20,830
24866	35,000	700,000	33,448	19,200	19,600
24916	11,000	1,525,000	16,972	13,050	22,710
24917	23,000	1,150,000	24,813	16,567	20,910
24918	35,000	775,000	32,875	19,200	20,010

* Values in bold designate values that were outside the expected range.

Table 4.5(b). Forward Calculation Results (C/L) *

FWD #	FWD Load (lb)	E_{P-401} (psi)	E_{P-209} (psi)	E_{P-154} (psi)	E_{subgrade} (psi)
24920	11,000	1,700,000	16,528	12,922	24,320
24921	23,000	1,600,000	23,705	16,337	22,260
24922	35,000	1,310,000	30,008	18,808	20,710
24924	11,000	1,800,000	16,617	13,003	24,790
24925	23,000	1,612,000	23,748	16,358	22,240
24926	35,000	1,230,000	30,378	18,892	20,700
24928	11,000	1,571,000	16,875	13,053	23,730
24929	23,000	1,300,000	24,497	16,592	22,110
24930	35,000	820,000	32,520	19,177	20,220
24932	11,000	1,550,000	16,888	13,073	24,330
24933	23,000	1,000,000	25,577	17,007	22,680
24934	35,000	515,000	35,385	19,845	21,030
25304	11,000	450,000	19,667	13,870	22,160
25305	23,000	141,400	33,175	18,193	20,880
25306	35,000	72,000	46,082	21,595	19,870
25308	11,000	500,000	19,670	13,963	23,130
25309	23,000	155,000	32,865	18,225	21,380
25310	35,000	65,000	46,645	21,745	20,160
25312	11,000	525,000	19,518	13,915	23,160
25313	23,000	275,000	30,355	17,668	20,930
25314	35,000	73,000	45,875	21,482	19,580
25316	11,000	460,000	19,902	14,092	24,080
25317	23,000	148,000	32,935	18,255	21,580
25318	35,000	64,000	46,770	21,707	19,860

* Values in bold designate values that were outside the expected range.

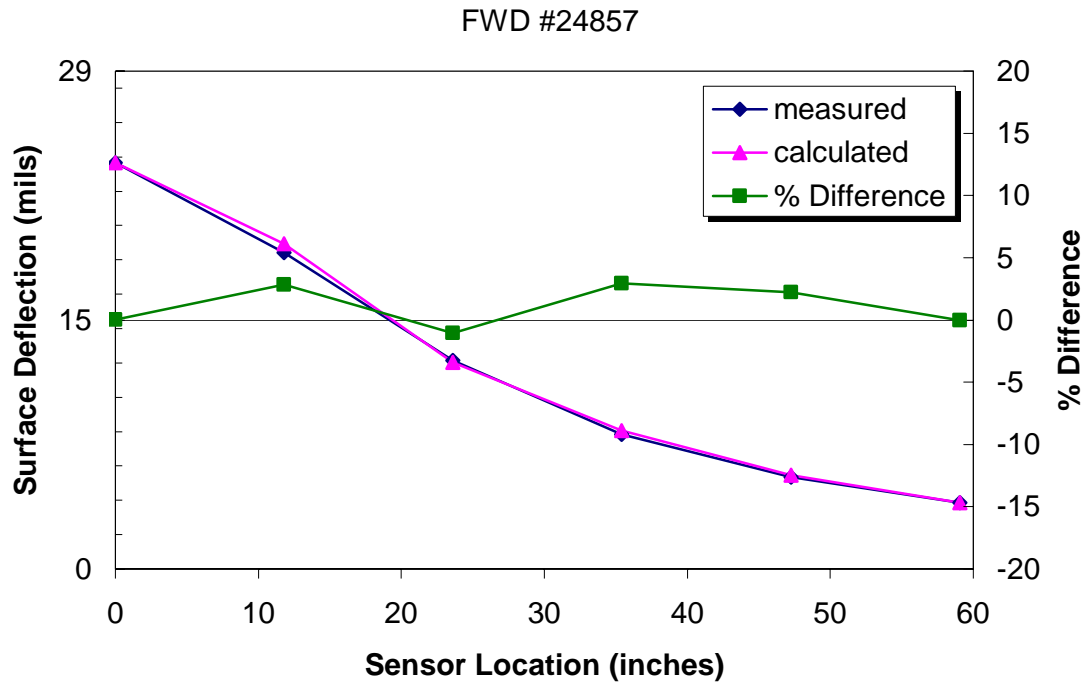


Figure 4.3. Typical Match of Measured and Calculated Deflection Basins

4.4.2.1. Center Line Surface Layer Moduli

Figures 4.4 – 4.6 compare the average surface layer moduli between failed and unfailed section in the C/L. It is seen that at 1 Day, the difference between the failed and unfailed sections is clear. Irrespective of the load, the unfailed section has higher moduli than the failed section and the 95% confidence intervals for each do not overlap, indicating a statistically significant difference. At 8 Weeks, the moduli of both sections were much lower than the moduli at 1 Day. The moduli for both sections at 8 Weeks were essentially equal, with no statistically significant difference between sections.

4.4.2.2. Lane 5 Surface Layer Moduli

The loading period of 8 Weeks was not analyzed for Lane 5, due to the results found for the C/L. The C/L was not directly loaded, yet the moduli decreased dramatically and there was no statistically significant difference between sections. Since this occurred on the unloaded C/L, similar results were expected for the loaded Lane 5, but with even more dramatic decreases in moduli. Therefore, Figures 4.7 – 4.9 compare the average surface layer moduli between failed and unfailed section in Lane 5, at the loading period of 1 Day. For each load, the moduli of the unfailed section are

consistently higher than the moduli of the failed section. The 95% confidence intervals for each section do not overlap, indicating a statistically significant difference.

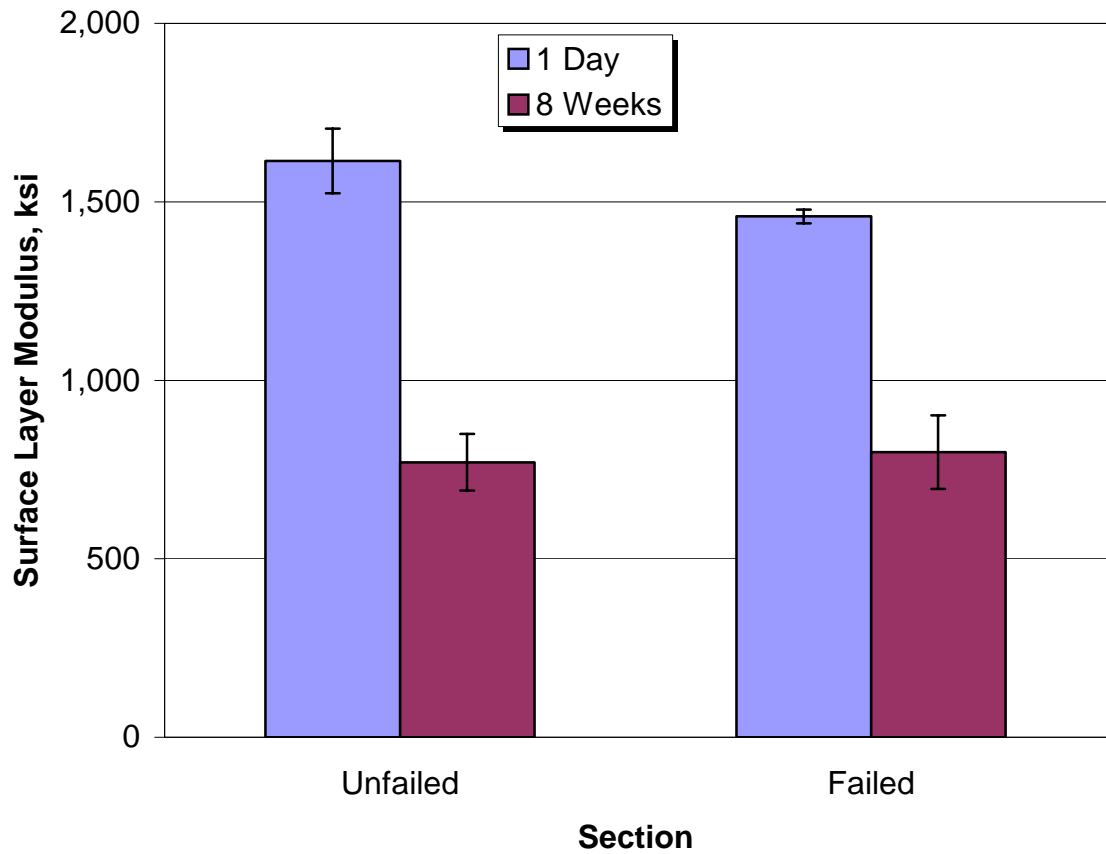


Figure 4.4. Surface Layer Moduli of Failed and Unfailed Sections (C/L, 12 kip load)

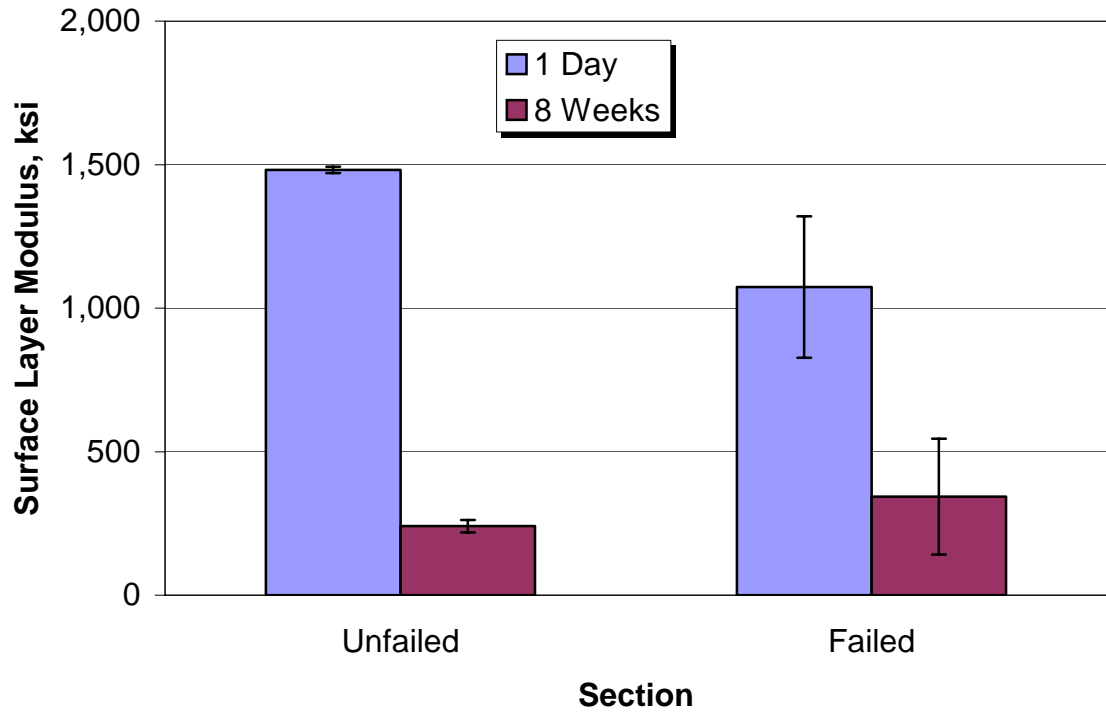


Figure 4.5. Surface Layer Moduli of Failed and Unfailed Sections (C/L, 24 kip load)

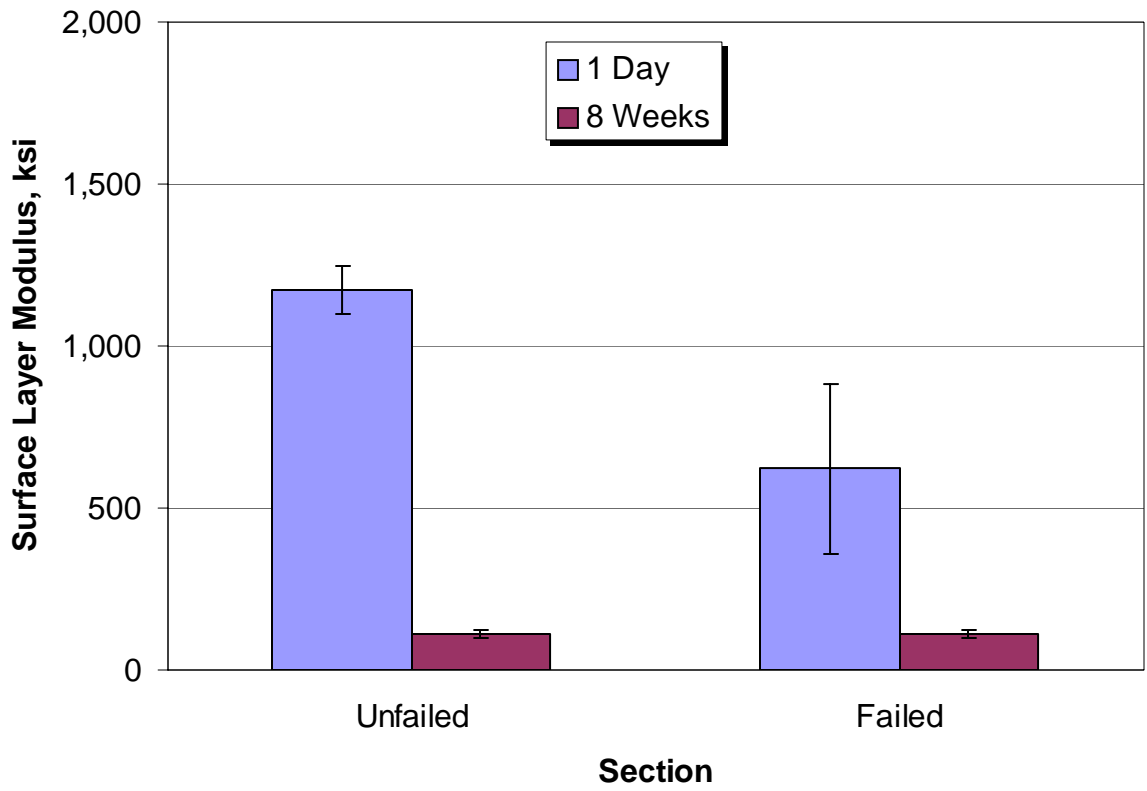


Figure 4.6. Surface Layer Moduli of Failed and Unfailed Sections (C/L, 35 kip load)

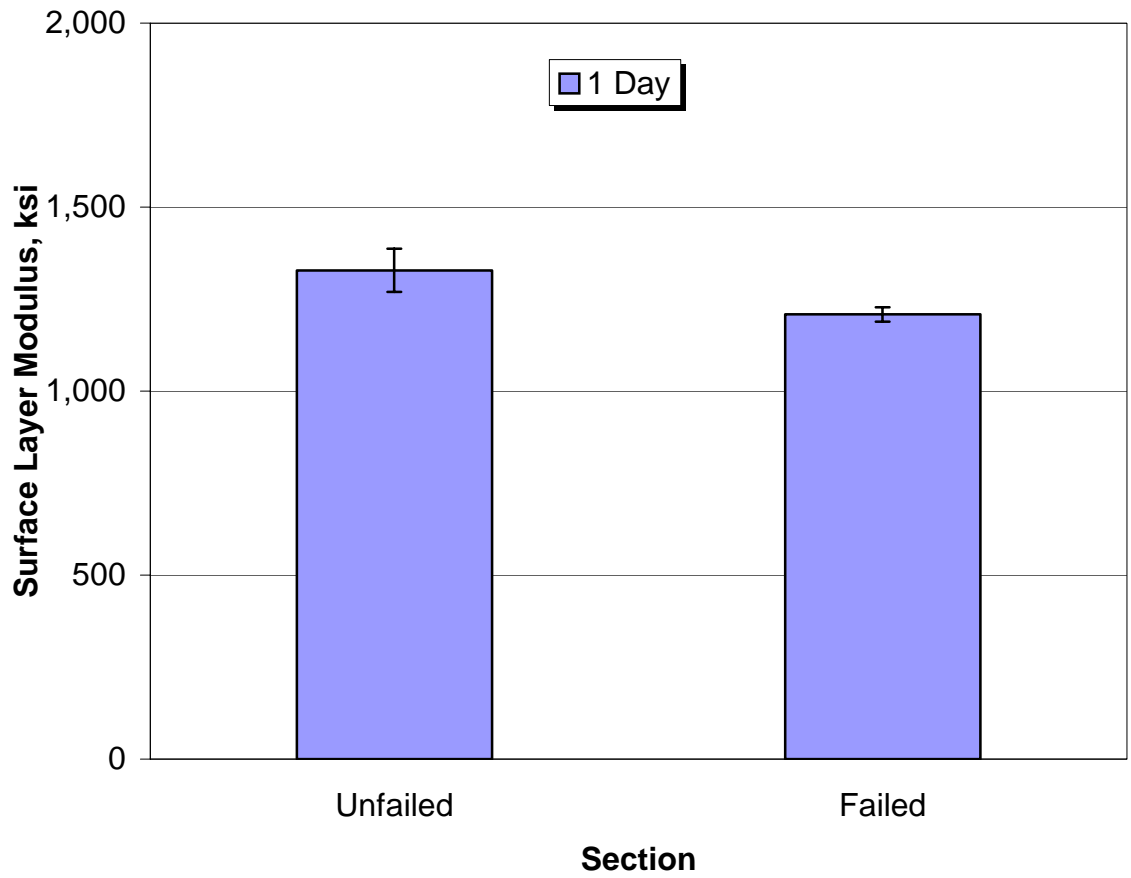


Figure 4.7. Surface Layer Moduli of Failed and Unfailed Sections (Lane 5, 12 kip load)

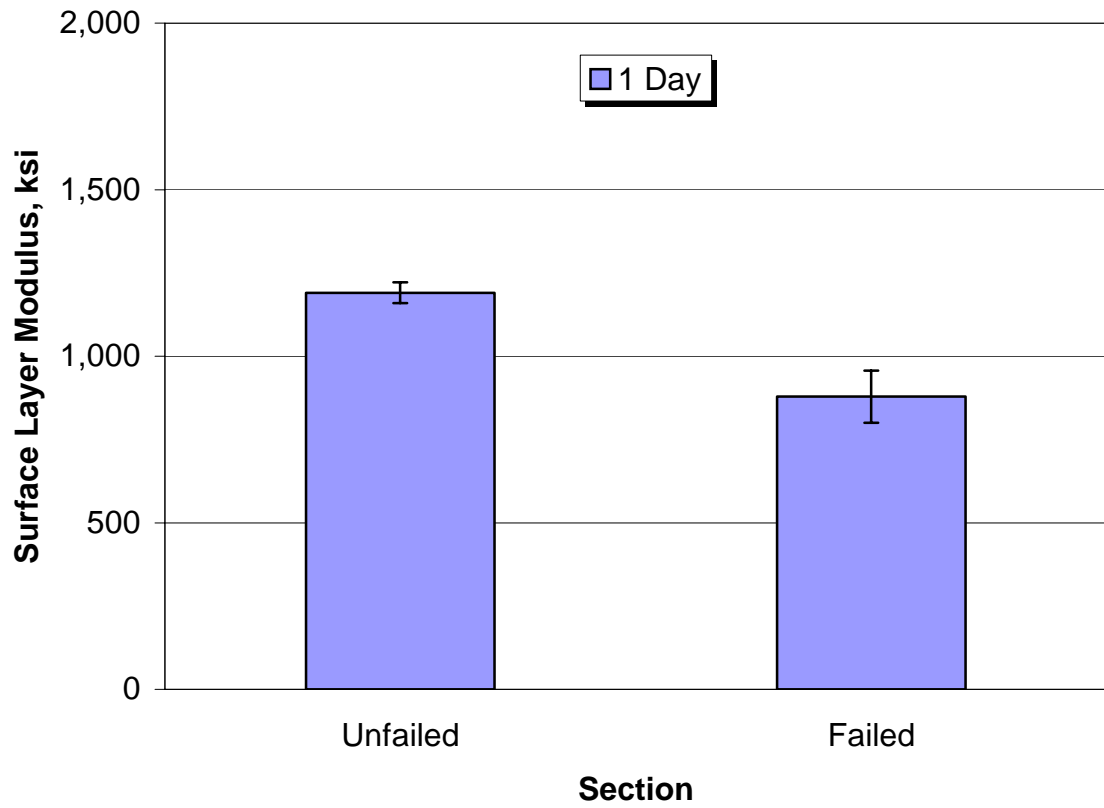


Figure 4.8. Surface Layer Moduli of Failed and Unfailed Sections (Lane 5, 24 kip load)

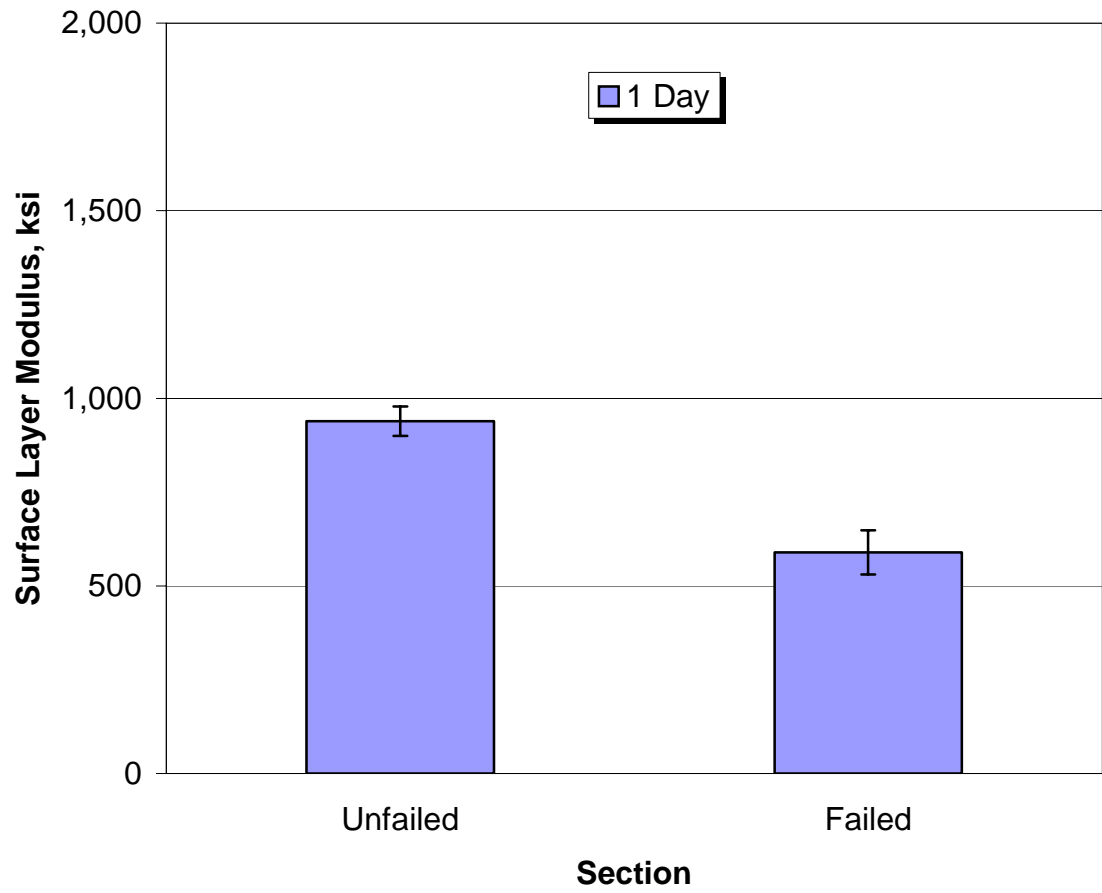


Figure 4.9. Surface Layer Moduli of Failed and Unfailed Sections (Lane 5, 35 kip load)

4.5. Discussion of Forward Calculation Results

4.5.1. Centerline

Figures 4.4 – 4.6 clearly indicate a statistically significant difference between failed and unfailed sections at 1 Day. Irrespective of the load, the failed section has lower moduli than the unfailed section. This seems to indicate that where interlayer bonds are poor, surface layer moduli are lower. Similarly, this seems to indicate that where interlayer bonds are intact, the surface layer moduli are higher. This is also an indication that any load may be able to identify sections with poor interlayer bonds.

At 8 Weeks, there is no statistically significant difference between sections. This may be because of structural deterioration. At that time, the pavement loading had been nearly completed and the pavement may have experienced a structural failure, which would mask the interlayer bonding as seen from FWD data. The results for 8 Weeks indicate the importance of testing pavements early in the pavement's life, so that other pavement distresses do not mask potential interlayer bond problems.

4.5.2. Lane 5

Figures 4.7 – 4.9 clearly show a statistically significant difference between failed and unfailed sections at 1 Day, for each load. Irrespective of the load, the failed section has lower moduli than the unfailed section. As in the C/L results, this seems to indicate that sections with poor interlayer bonds will exhibit lower surface layer moduli than sections with good interlayer bonds. This also indicates that there is no certain load magnitude required for identifying poor interlayer bonds.

The loading period of 8 Weeks was not analyzed for Lane 5, because as indicated in the results for the C/L, the pavement may have experienced structural deterioration. Since this was found for the C/L, which was not directly loaded, the structural condition of Lane 5, which was directly loaded, was expected to be worse. With the structural deterioration, as shown in the C/L results, there would be no statistically significant difference between failed and unfailed sections, since the structural failure masks the interlayer bonding failure.

4.5.3. Results Summary

The failed and unfailed sections were assumed to be fully bonded during the FWD analysis. The surface deflections, however, are influenced by the lack of bonding in the failed section. This phenomenon was observed by the difference in forward calculated moduli of failed and unfailed sections. It is emphasized that both the sections were constructed at the same time and exposed to similar environmental and loading conditions. Therefore, the moduli are similar for both sections, and so the difference in forward calculated moduli can be attributed to the lack of bonding.

CHAPTER FIVE INTERLAYER SLIP ANALYSIS

5.1. Introduction

This chapter discusses the effect of slip within the MFC pavement section. Section 5.2 provides background information on the analysis of the effect of slip. Section 5.3 discusses the calculation of pavement mechanical responses in the failed sections of the MFC pavement. Section 5.4 discusses the determination of the effect of slip occurring in the failed pavements.

5.2. Analysis of Slip

5.2.1. Background

As explained in the previous chapter, the surface moduli were significantly different between failed and unfailed sections. This indicated that the FWD data was able to identify the lack of interlayer bonding. However, simply knowing that a lack of bonding exists is not enough. In some pavements, a lack of bond may be present, but if the surface layer is sufficiently thick, the effect of slip due to that lack of bond may be negligible. Therefore, the effect of slip that occurs as a result of the lack of bonding needs to be found, since the effect of slip will vary with pavement structure and loading.

To determine the effect of slip that was occurring, radial stresses at the interlayer were used as the basis of comparison. The effect of slip was defined by the algebraic difference between radial stresses directly above and directly below the interlayer.

However, in earlier calculations, the asphalt was considered as one layer. Since the slippage occurred between lifts of the asphalt layer, the layer was split into two layers for stress/slip calculations. After splitting the asphalt layer, stresses were calculated in the pavement for each FWD drop on failed sections, to eventually find the effect of slip in each FWD drop. This process is explained in detail below.

5.2.2. Asphalt Layer Moduli

5.2.2.1. Splitting of Asphalt Layer

In the forward calculation process, the asphalt layer was considered as one single layer. Technically, since the interlayer failure at the FAA NAPTF occurred in between lifts of the asphalt layer, the asphalt was divided into two layers. This was not a concern as far as the forward calculations were concerned, since FWD calculations are unable to accurately distinguish between thin layers. However, in order to analyze the slip, the asphalt layer needed to be split into two (shown in Figure 5.1).

5.2.2.2. Implications and Applications of Splitting Asphalt Layer

The implication of the above equation is this: in sections that are fully bonded (no slippage), E_F will be equal to E_{UF} . In sections in which slippage occurred, E_F will be lower than E_{UF} . The reason for this is that the equation assumes full bonding. If there is actually slippage, then E_F is reduced to account for the worsened performance of the pavement system caused by the slippage.

The purpose of the equation was to determine the modulus of each asphalt layer, so that slip at the interlayer could be evaluated. The unfailed sections were assumed fully bonded, so the equation was only applied to the failed sections. Furthermore, since the forward calculation analysis results indicated that statistically significant differences between failed and unfailed sections were only found at the loading period of 1 Day, the equation was only applied to the failed sections at 1 Day. The results of the asphalt layer moduli computations are shown in Tables 5.1 – 5.3 at the end of the next section.

5.2.3. Tack Coat Failure Ratio

A goal of this study is to determine a way to easily identify and quantify the effect of slip in a pavement under the design loads. In order to make this a simple procedure, a term called the Tack Coat Failure Ratio (TFR) was created. This term is simply the ratio of the calculated modulus of the top asphalt layer to the calculated modulus of the lower asphalt layer (E_F to E_{UF}), as they are defined above and shown in Figure 5.1. In equation form, the TFR is:

$$TFR = \frac{E_{topHMA\text{layer}}}{E_{lowerHMA\text{layer}}} = \frac{E_F}{E_{UF}} \quad (5.3)$$

where: E_F and E_{UF} are as explained previously.

TFR = 1 for fully bonded interlayer

TFR = 0 for complete lack of interlayer bonding

The TFR was calculated for each of the FWD drops in the failed sections at 1 Day, as shown in Tables 5.1 – 5.2. These TFR's were later correlated with the effect of slip in the pavement section. The intent is that in the future, a TFR can be calculated from FWD calculations, and from the TFR/slip correlation the effect of slip in the pavement may easily be determined.

Table 5.1. Asphalt Moduli and TFR for the C/L, 1 Day

FWD ID	Station	Load (kip)	Section	FWD-Calculated E_T (ksi)	Average E_T (ksi)	E_T (ksi)	E_F (ksi) (Calculated from Equation)	E_{UF} (ksi) (Avg. E_T, UF Section)	TFR
24920	3+45	11	UF	1,700	1,750	-	-	-	-
24924	3+55	11	UF	1,800		-	-	-	-
24928	3+65	11	F	1,571	-	1,571	1,405	1,750	0.803
24932	3+75	11	F	1,550		1,550	1,366	1,750	0.780
24921	3+45	23	UF	1,600	1,606	-	-	-	-
24925	3+55	23	UF	1,612		-	-	-	-
24929	3+65	23	F	1,300	-	1,300	1,036	1,606	0.645
24933	3+75	23	F	1,000		1,000	570	1,606	0.355
24922	3+45	35	UF	1,310	1,270	-	-	-	-
24926	3+55	35	UF	1,230		-	-	-	-
24930	3+65	35	F	820	-	820	491	1,270	0.387
24934	3+75	35	F	515		515	141	1,270	0.111

Table 5.2. Asphalt Moduli and TFR for Lane 5, 1 Day

FWD ID	Station	Load (kip)	Section	FWD-Calculated E_T (ksi)	Average E_T (ksi)	E_T (ksi)	E_F (ksi) (Calculated from Equation)	E_{UF} (ksi) (Avg. E_T, UF Section)	TFR
24856	3+45	11	UF	1,700	1,662	-	-	-	-
24860	3+55	11	UF	1,625		-	-	-	-
24864	3+65	11	F	1,500	-	1,500	1,380	1,662	0.811
24916	3+75	11	F	1,525		1,525	1,395	1,662	0.839
24857	3+45	23	UF	1,510	1,490	-	-	-	-
24861	3+55	23	UF	1,470		-	-	-	-
24865	3+65	23	F	1,050	-	1,050	706	1,490	0.474
24917	3+75	23	F	1,150		1,150	866	1,490	0.581
24858	3+45	35	UF	1,200	1,175	-	-	-	-
24862	3+55	35	UF	1,150		-	-	-	-
24866	3+65	35	F	700	-	700	374	1,175	0.318
24918	3+75	35	F	775		775	477	1,175	0.407

5.3. Effect of Slip

5.3.1. Background

Pavements with poor interlayer bonding experience an effect of slip. The effect of slip experienced by the pavement varies with several different conditions. Different loads on the pavement will produce varied effects of slip: a small car driving on a road may not cause any effect of slip, but a heavily loaded tractor-trailer on the same road may cause a high effect of slip for the same interlayer. The pavement structure itself affects the effect of slip in the pavement. Structures with very stiff and/or very thick surface layers may experience low effects of slip. Alternatively, structures with soft and/or thin surface layers may experience high effects of slip. The reason for this is that stiff and/or thick surface layers are able to withstand much of the load itself, causing less of the load to be transferred to the lower pavement structure, and thus lower stresses and strains in the lower pavement structure, including the interlayer.

The effect of pavement structure on the effect of slip can be explained by the TFR, which was described and calculated in the previous section. The TFR, being a ratio of E_F to E_{UF} , is a direct indication of the stiffness of the surface layer, relative to the layer below the interlayer. This being the case, a high TFR (1.0) would indicate a relatively stiff surface layer and thus a lower effect of slip. A low TFR (0.0) would indicate a large difference in stiffness between the two top layers and thus a higher effect of slip.

The TFR's were previously determined for each of the failed locations, and so effect of slip needed to be determined for each location. As mentioned previously, the effect of slip was determined by comparing radial stresses directly above and below the interlayer under the FWD loads. This process is described in detail below.

5.3.2. Preliminary Calculations and Validations

The initial intent was to use the program KENLAYER to calculate the stresses for each location and FWD drop, since it was used to calculate the layer moduli. However, KENLAYER only computes slips of 0 and 1; that is, only full slip and full bond, and no intermediate degrees of slip. Since the pavement had some intermediate degree of slip, the program BISAR was used instead.

Some preliminary investigation was necessary before the program was used for the actual analysis though. BISAR uses two different numbers to account for the bonding in the modeled pavements: there is an unnamed input number (named in this paper as "BISAR slip number"), and a "spring compliance" number that appears in the output and is used to represent the degree of bonding within the program. In order to effectively use the program to determine the effect of slip, a correlation between the BISAR slip number and the output spring compliance number was necessary. Additionally, a correlation was made between BISAR's input/output and KENLAYER's output for both fully bonded and fully slipped pavements, in order to verify that BISAR was being used properly.

To calibrate the BISAR slip number, and to validate the BISAR calculations, a simple three-layer pavement structure was analyzed using both KENLAYER and BISAR. The system used was a simplified MFC system: two 2.56 inch asphalt layers over a 7.88 inch gravel layer (shown in Figure 5.2). The gravel layer was used since the only layers that were critical for this investigation were the two asphalt layers. If different sub-layers had been used, the results would have been the same. The values for the moduli and loading were those for FWD drop # 24864. The following mechanical responses were computed in KENLAYER and BISAR for the fully bonded and fully slipped interface cases: vertical displacement, vertical stress, vertical strain, radial stress, and radial strain. These were computed directly under the load, at depths of 0, 1.28, 2.55, 2.57, 3.84, and 9.08 inches (as shown in Figure 5.2).

Through this analysis, it was determined that the range of BISAR slip number values was 0 to 1,000,000, with the 0 corresponding to the BISAR spring compliance number of 0.0 and the 1,000,000 corresponding to a spring compliance of 1.0. It was also found that the spring compliance of 0.0 matched the KENLAYER slip of 1(full bond), and the spring compliance of 1.0 matched the KENLAYER slip of 0 (full slip). These findings are shown in Table 5.3.

Slip was measured by the difference in radial stresses between points just above and just below the interface. Figure 5.3 shows the radial stresses for varied degrees of slip at the points directly above and below the interface, directly under the load. This demonstrates the increase of radial stress due to slip, and it also demonstrates the increase in radial stress difference between the two points with the increase in slip. Figure 5.4 shows the difference in radial stress versus the BISAR slip number.

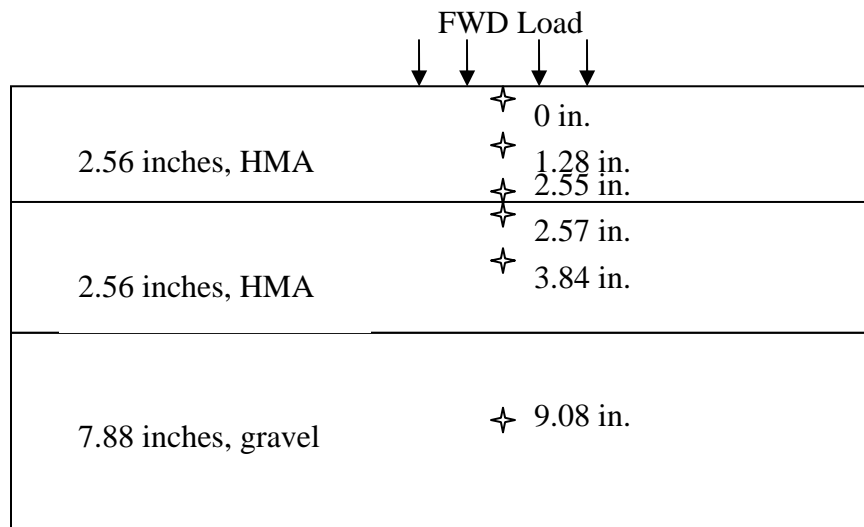


Figure 5.2. Structure and Evaluation Points Used for Preliminary Investigation

Table 5.3. BISAR / KENLAYER Interface Values

KENLAYER Interface Number	BISAR Slip Number	BISAR Interface Spring Compliance	Physical Meaning
1	0	0.0	Fully Bonded
0	1,000,000	1.0	Fully Slipped

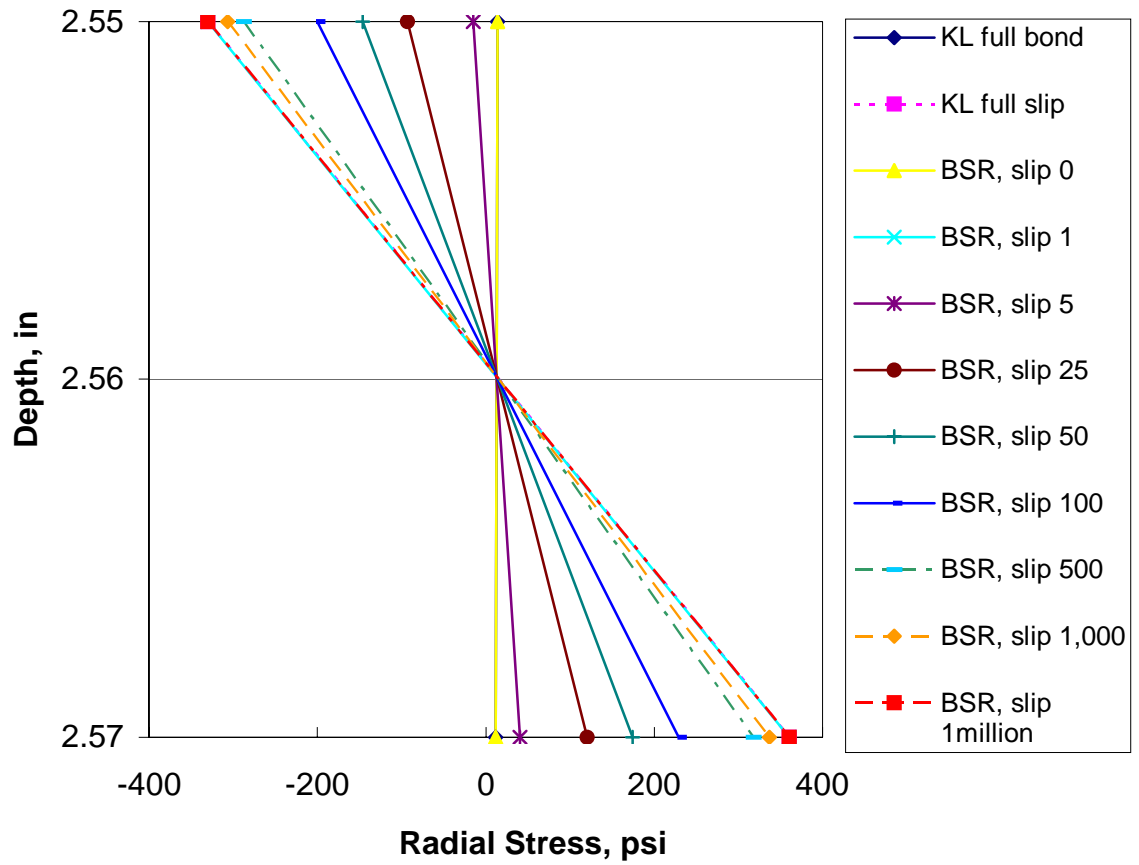


Figure 5.3. Radial Stresses at Points Above and Below Interface, for Varied Slip

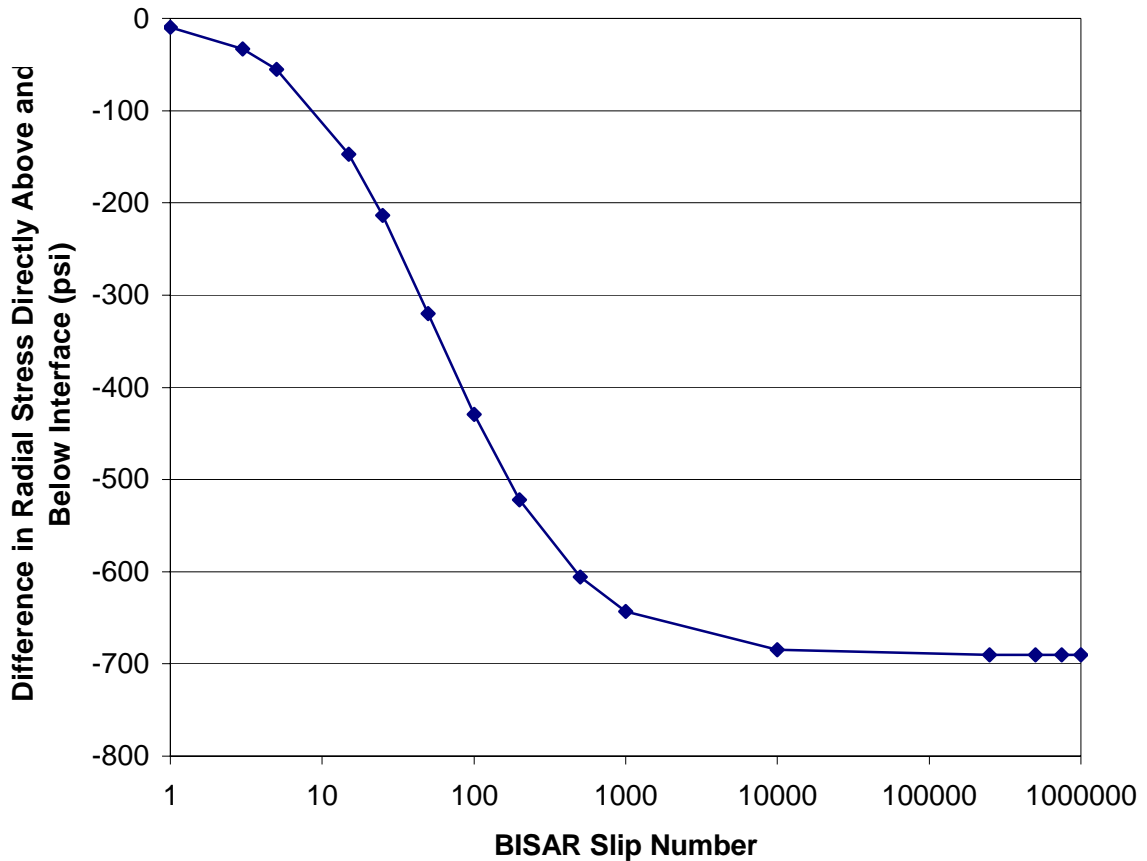


Figure 5.4. Radial Stress Differences vs. BISAR Slip Number in BISSAR Investigation

5.3.3. Determination of Effect of Slip in MFC Failed Sections

The next step in the study was to determine the effect of slip in the failed sections. As explained before, backcalculation programs do not evaluate various degrees of slip. Thus this analysis was done indirectly, with the use of BISSAR. This analysis was performed in four steps, as described below.

Step 1: Calculation of Mechanical Responses in “Surrogate Pavement”

Analysis of a “surrogate pavement” was conducted. The “surrogate pavement” is a representation of a failed section in which there is full bonding but the calculated moduli of the top asphalt layer (E_F) is lower than the moduli of the lower asphalt layer (E_{UF}), as described previously in Section 5.2.2. That is, the $TFR < 1$. Figure 5.5(a) shows the “surrogate pavement” analyzed. The asphalt moduli E_F and E_{UF} used are shown below in Table 5.4.

Mechanical responses, calculated at locations directly under the load, were: vertical displacement, vertical stress, and radial stress. Figure 5.6 shows the layer thicknesses and evaluation points that were used.

Step 2: Calculation of Mechanical Responses in “Actual Pavement”

Analysis was conducted on the “actual pavement”. The “actual pavement”, as described previously in Section 5.2.2, has both asphalt layer moduli of E_{UF} , as shown in Figure 5.5(b). The values of E_{UF} used are shown below in Table 5.4.

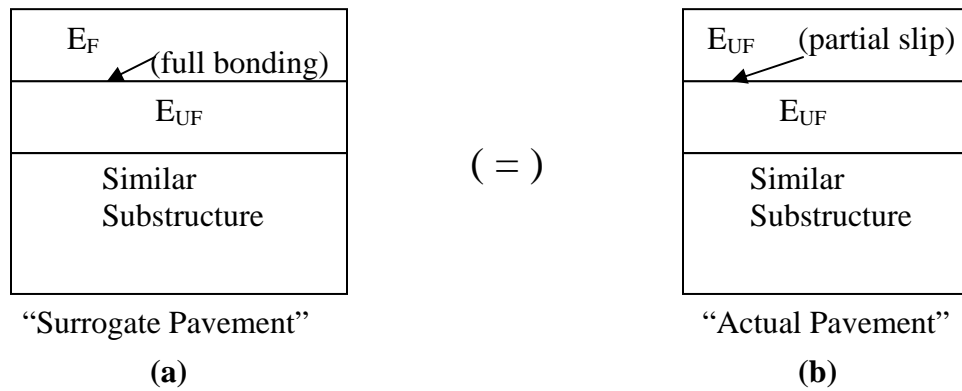


Figure 5.5. MFC Failed Section Analysis, Pavement Structure Cases

Table 5.4. Properties of Sections Analyzed

FWD ID	Load (lb)	Lane	Case *	E_F (ksi)	E_{UF} (ksi)	E_{P-209} (ksi)	E_{P-154} (ksi)	E_{subgrade} (ksi)
24928	11592	C/L	Surrogate	1,405	1,750	16.875	13.053	23.730
			Actual	1,750				
24932	11492	C/L	Surrogate	1,366	1,750	16.888	13.073	24.330
			Actual	1,750				
24929	23244	C/L	Surrogate	1,036	1,606	24.497	16.592	22.110
			Actual	1,606				
24933	23315	C/L	Surrogate	570	1,606	25.577	17.007	22.680
			Actual	1,606				
24930	35055	C/L	Surrogate	491	1,270	32.520	19.177	20.220
			Actual	1,270				
24934	34869	C/L	Surrogate	141	1,270	35.385	19.845	21.030
			Actual	1,270				
24864	11726	5	Surrogate	1,380	1,662	16.978	13.025	22.210
			Actual	1,662				
24916	11726	5	Surrogate	1,395	1,662	16.972	13.050	22.710
			Actual	1,662				
24865	23367	5	Surrogate	706	1,490	25.090	16.635	20.830
			Actual	1,490				
24917	23424	5	Surrogate	866	1,490	24.813	16.567	20.910
			Actual	1,490				
24866	35190	5	Surrogate	374	1,175	33.448	19.200	19.600
			Actual	1,175				
24918	35153	5	Surrogate	477	1,175	32.875	19.200	20.010
			Actual	1,175				

*In the Surrogate Case, interlayer is fully bonded. In the Actual Case, the interlayer has varied degrees of slip.

	✦ 0 in.
2.56 inches, P-401	✦ 1.28 in.
	✦ 2.555 in.
2.56 inches, P-401	✦ 2.565 in.
	✦ 3.84 in.
	✦ 5.12 in.
2.63 inches, P-209	✦ 6.43 in.
2.63 inches, P-209	✦ 9.05 in.
2.63 inches, P-209	✦ 11.68 in.
6.06 inches, P-154	✦ 16.03 in.
6.06 inches, P-154	✦ 22.09 in.
94.8 inches, Subgrade	✦ 72.52 in.
Infinite depth, 1 million psi Stiff-layer	

Figure 5.6. Layers and Evaluation Points Used in BISAR

As explained in the previous section, BISAR is able to calculate mechanical responses in pavements with various degrees of slip, which are designated by the BISAR slip number. In this analysis, therefore, the slip between asphalt layers was varied. Six

different degrees of slip were analyzed, ranging from full bond (BISAR slip number = 0) to full slip (BISAR slip number = 1 million). The same mechanical responses were calculated as for the “surrogate pavement”.

The results of both Step 1 and 2 were plotted together for each FWD number analyzed. Typical plots of vertical displacement, vertical stress, and radial stress may be viewed in Figures 5.7 – 5.9, respectively. These plots show the increase of vertical displacement, vertical stress, and radial stress, as the BISAR slip number increases (the mechanical responses all increase as slip at the interlayer increases). The results for each analyzed FWD drop number may be viewed in Appendix I (Gomba, 2004). The mechanical responses calculated in Steps 1 and 2 were utilized in two stages: Step 3 used the vertical displacement and vertical stress results, and Step 4 used the radial stress results.

Step 3: Comparison of “Surrogate Pavement” and “Actual Pavement”

The vertical displacement and vertical stress results were used to determine the BISAR slip number that most accurately described the interlayer condition that existed for each of the sections mentioned previously in Table 5.4. The plots of vertical displacement and vertical stress (typical plots in Figures 5.7 and 5.8) were used in determining the slip in the pavement for each of the previously mentioned sections and cases. Comparisons were made between the “surrogate pavement”, which reflects the existing pavement, and the “actual pavements” with varied slip. In the figures, the “surrogate pavement” curve matched up with an “actual pavement” curve. The “actual pavement” curve that matched indicated the BISAR slip number that best described the interlayer at that particular section. For example, for FWD #24864, (the results for which are used in the typical plots shown in Figures 5.7 and 5.8), the curve corresponding to BISAR Slip Number 5 matches closely with the curve corresponding to the “surrogate pavement”. Thus, for FWD #24864, the slip in the pavement was that which corresponds to the BISAR Slip Number 5. Now that a BISAR slip number was known for each section, the effect of slip was determined in Step 4.

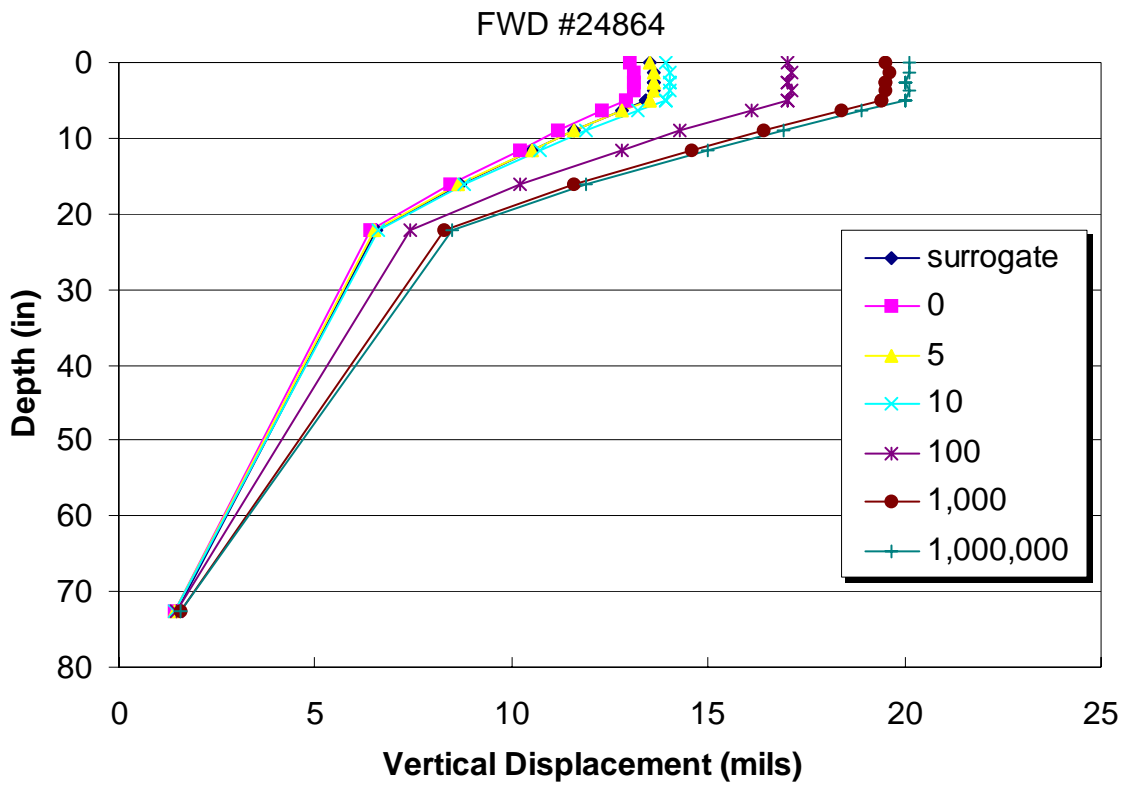


Figure 5.7. Typical Vertical Displacement Plot

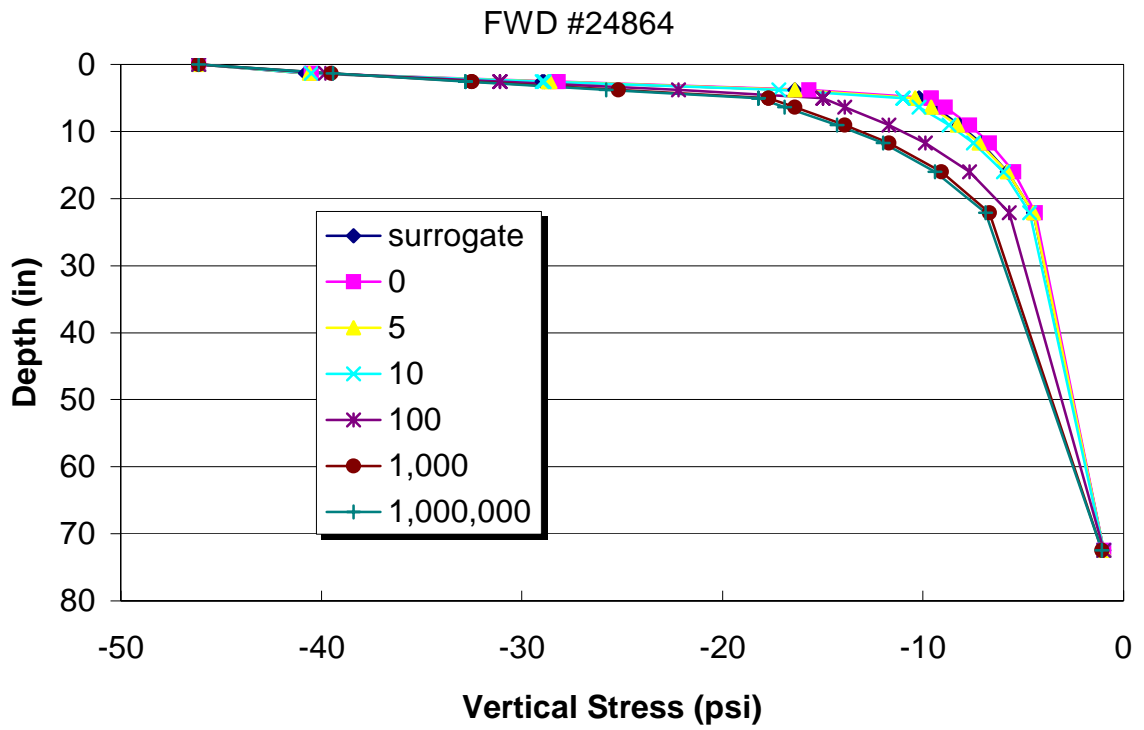


Figure 5.8. Typical Vertical Stress Plot

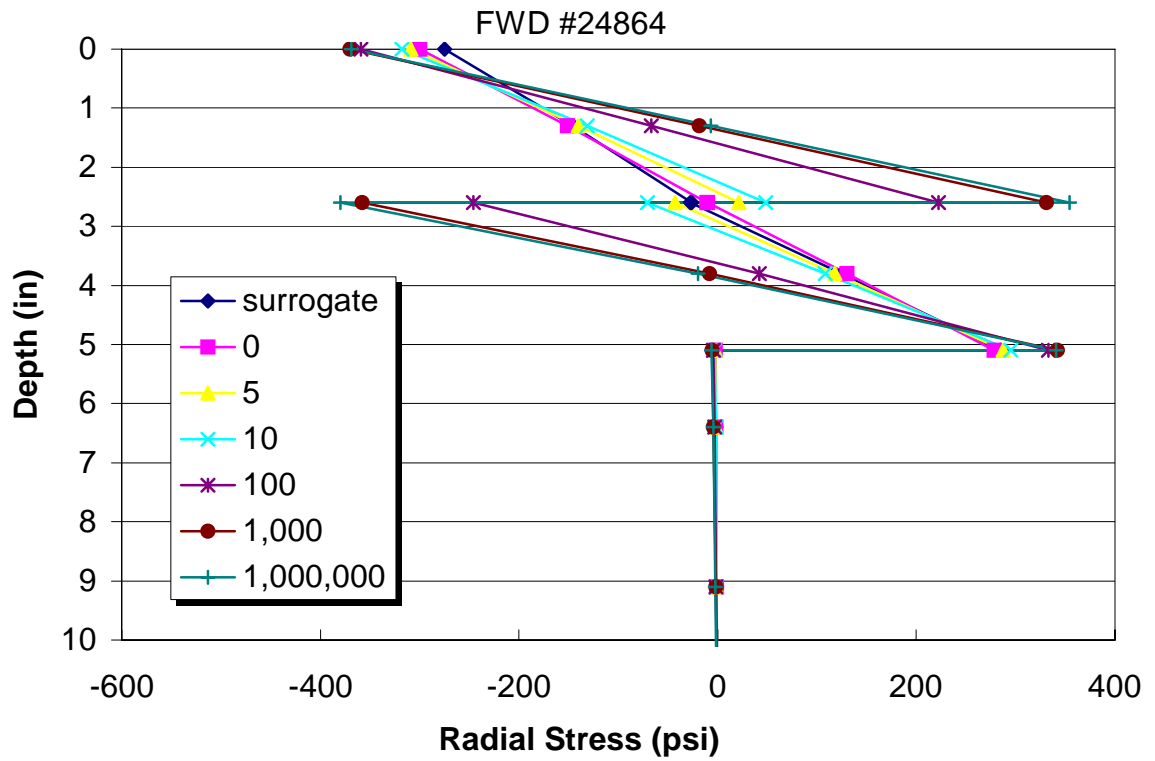


Figure 5.9. Typical Radial Stress Plot

Step 4: Determination of Effect of Slip

The effect of slip was now determined by using the radial stress results from Steps 1 and 2. Based on the preliminary investigations with BISAR (discussed previously), the radial stresses just above and below the interface were used to determine the effect of slip. Figure 5.10 shows a typical plot of radial stresses just above and below the interface. The difference in radial stress between depths 2.555 and 2.565 inches was calculated for each case (interlayer located at 2.56 inches). The differences were then plotted against the BISAR slip number. The resulting plots (shown in Appendix J, (Gomba, 2004)) were similar to the typical plot shown in Figure 5.11.

Using the plot of “radial stress difference at interface”, the radial stress difference at the interface in the actual pavement section was identified by identifying the radial stress difference that matched the BISAR slip number found in Step 3.

Finally, the effect of slip in the pavement was calculated as being the ratio of the difference in radial stress at interface (just identified) to the maximum difference in radial

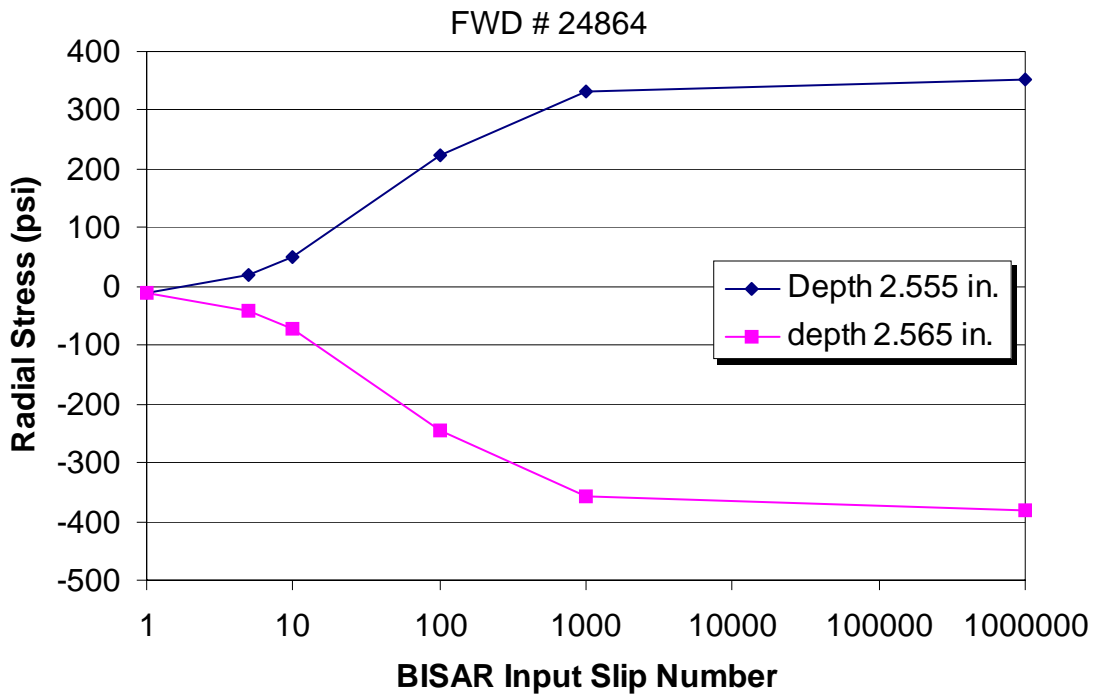


Figure 5.10. Typical Plot of Radial Stresses Just Above and Below the Interface

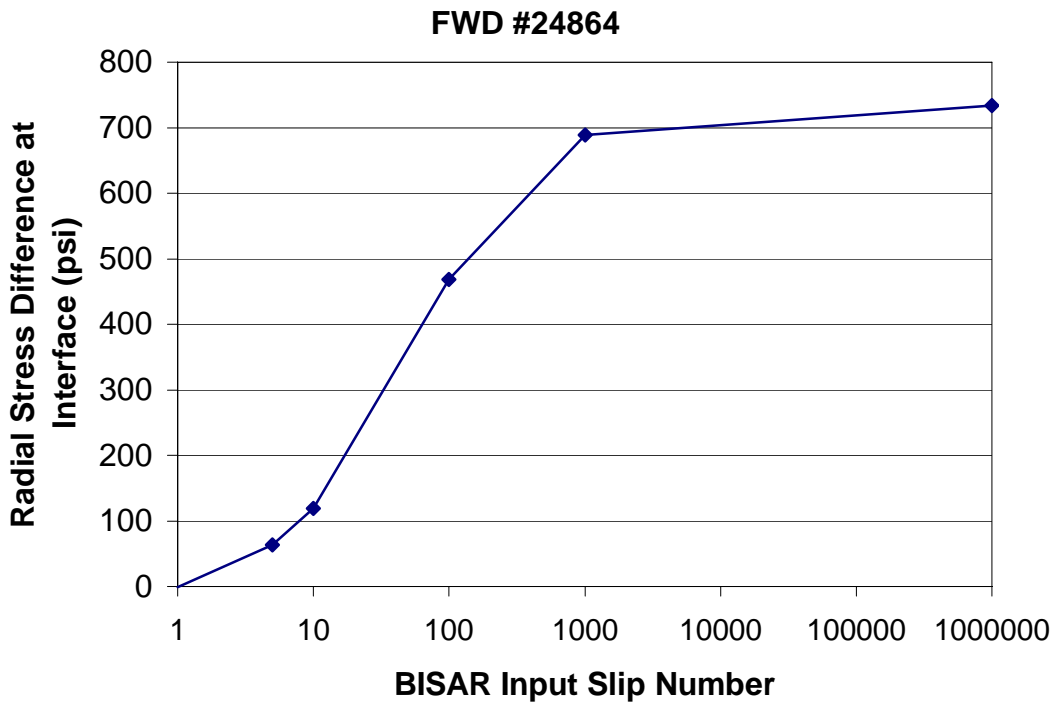


Figure 5.11. Typical Plot of Radial Stress Difference at Interface

stress at interface. The maximum difference in radial stress at the interface is that which occurs at full slip (BISAR slip number = 1 million), and was obtained from the same plot of “radial stress difference at interface” (typical plot, Figure 5.11). The resulting effect of slip values found are shown in the next section.

5.3.4. Results

The effect of slip, as calculated using the method described above, is shown for each FWD number in Table 5.5. These results were correlated to the previously determined TFR’s. This correlation is discussed in the next section.

5.4. Correlation of Tack Coat Failure Ratio with Effect of Slip

The calculated TFR’s were plotted against the calculated effect of slip values. For convenience, both the TFR and Effect of Slip values are repeated in Table 5.6. The plot of these is shown in Figure 5.12. A correlation was developed. The line is described by a trinomial equation, as shown in the figure. It is hypothesized that this equation is unique for this particular pavement, and that every pavement structure will have its own curve and equation. Therefore, if this is the case, then in order to determine the effect of slip in another pavement, one must follow the procedures outlined in this study to find the TFR/Effect of Slip correlation for that pavement, instead of using the correlation that resulted from this study. Also, it must be recognized that this result is valid only for situations similar to what existed at the FAA NAPTF: slippage between layers of a common material. In a situation where slippage occurs between layers of different materials, such as between a surface course and base course, the outlined procedure may need to be modified to account for this difference.

Table 5.5. Effect of Slip Results

FWD ID	Load (lb)	Lane	BISAR # Corresponding to Theoretical Pavement	Radial Stress Difference for Corresponding BISAR # (psi)	Maximum Radial Stress Difference at Interface (psi)	Corresponding Effect of Slip (%)
24928	11592	C/L	5	66.7	739	9
24932	11492	C/L	5	66.1	731	9
24929	23244	C/L	10	215.5	1281	17
24933	23315	C/L	60	552	1264	44
24930	35055	C/L	50	560	1543	36
24934	34869	C/L	800	1320	1524	87
24864	11726	5	5	63.8	734	9
24916	11726	5	5	63.8	733	9
24865	23367	5	30	331	1242	27
24917	23424	5	20	267	1248	21
24866	35190	5	70	693	1517	46
24918	35153	5	50	536	1521	35

Table 5.6. TFR and Effect of Slip

FWD ID	Load (lb)	Lane	TFR	Effect of Slip (%)
24928	11592	C/L	0.803	9
24932	11492	C/L	0.780	9
24929	23244	C/L	0.645	17
24933	23315	C/L	0.355	44
24930	35055	C/L	0.387	36
24934	34869	C/L	0.111	87
24864	11726	5	0.811	9
24916	11726	5	0.839	9
24865	23367	5	0.474	27
24917	23424	5	0.581	21
24866	35190	5	0.318	46
24918	35153	5	0.407	35

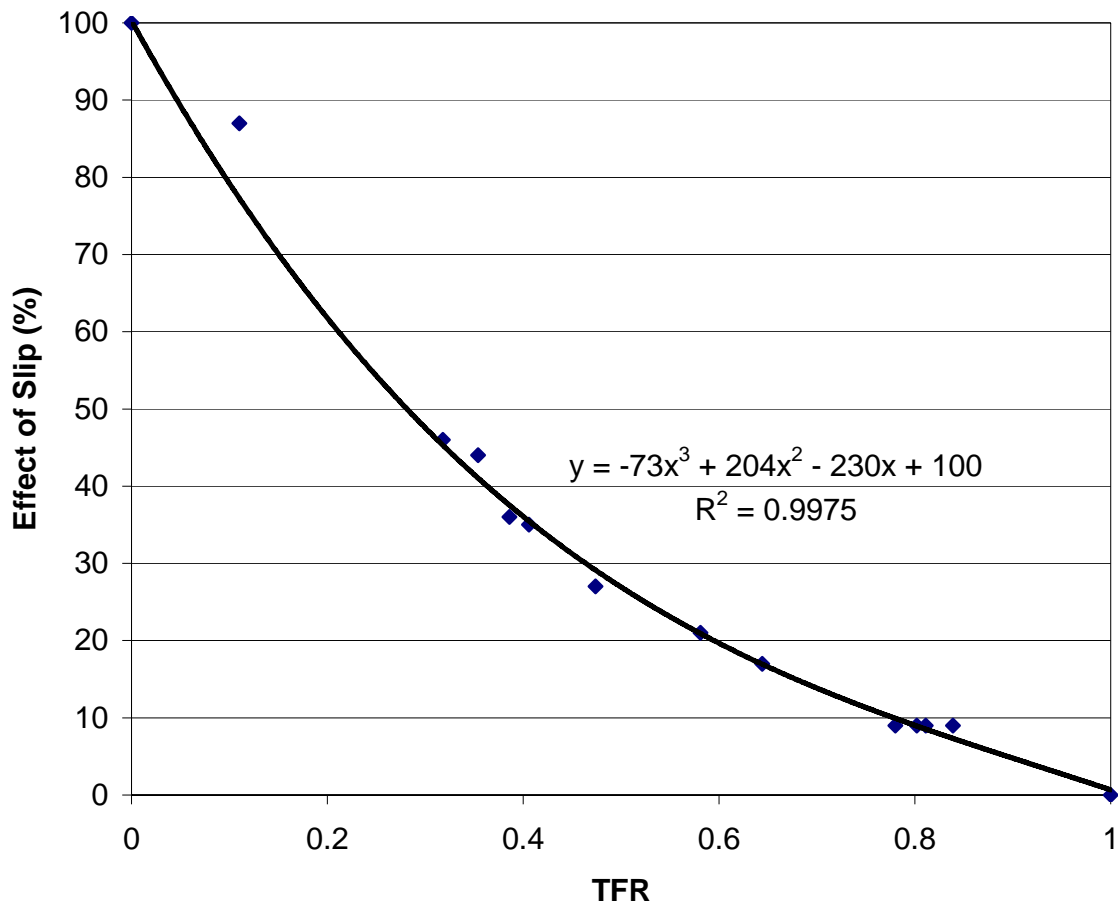


Figure 5.12. Effect of Slip / TFR Correlation

5.5. Framework for Using FWD Data in Interlayer Slip Analysis

The above analysis, along with the preceding analyses in this study, may be summarized into a framework that outlines the application of FWD data in identifying poor interlayer bonding in a pavement and quantifying the effect of slip resulting from poor bonding. This outline is shown below in Figure 5.13. This outline would be followed to analyze the effect of slip at one or more locations along a given roadway. If more than one location were analyzed, an effect of slip / TFR correlation could be developed, similar to that which was developed in this study.

A state agency would be able to use this correlation to evaluate interlayer bonding in the same roadway or even different roadways of similar pavement structure. In this event, the agency would only have to compute the TFR's on a roadway and use the correlation to determine the effect of slip, instead of calculating the mechanical responses and determining the effect of slip manually for each location. For example, Figure 5.14 shows a typical correlation that a state agency may have developed for a pavement. The agency would calculate the TFR's of other locations using the above framework, and then use the correlation to determine the effect of slip. If a significant effect of slip is observed in a new pavement, then appropriate modifications to construction practices could be made to avoid future problems. Additionally, the effect of slip data may be used for pavement management, to help prioritize and schedule rehabilitation projects.

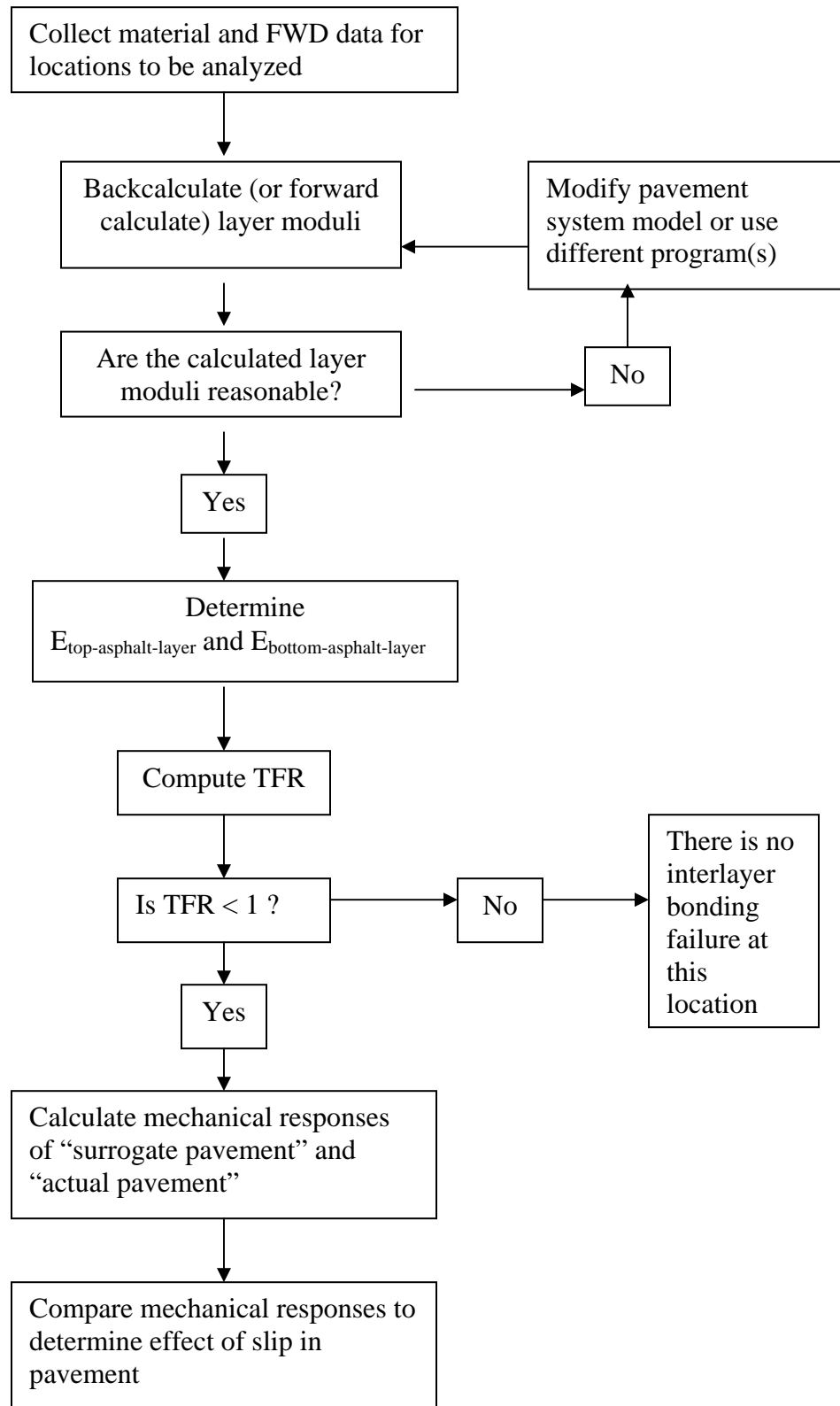


Figure 5.13. Framework of FWD Data Use in Interlayer Slip Analysis

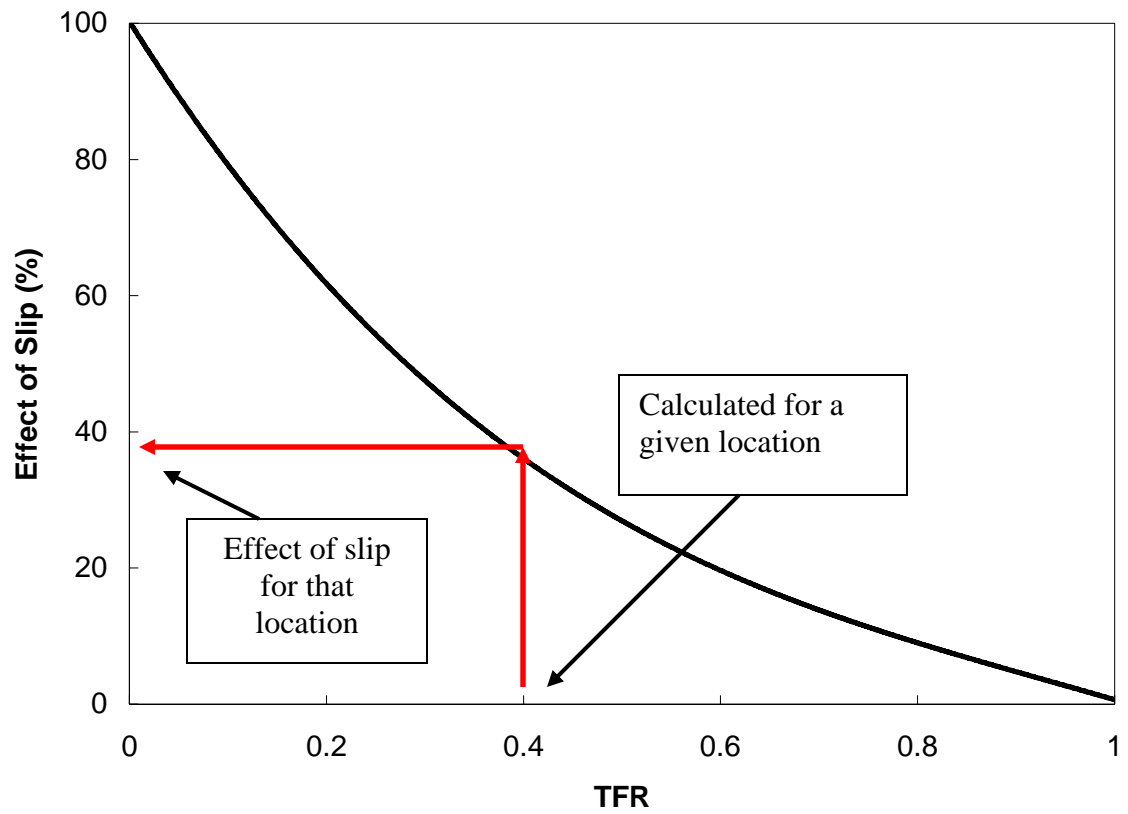


Figure 5.14. Agency Use of Effect of Slip / TFR Correlation

CHAPTER SIX

CONCLUSIONS AND RECOMMENDATIONS

6.1. Summary of Findings

In analyzing the Federal Aviation Administration National Airport Pavement Testing Facility's MFC section, the following was found:

1. The surface layer moduli obtained from Falling Weight Deflectometer (FWD) data was significantly different between failed and unfailed sections at early loading times, for all loads and temperatures.
2. A difference in calculated layer moduli between different sections may indicate the presence of interlayer bonding failure.
3. In pavements where slip occurs between two asphalt layers of similar properties, a Tack Coat Failure Ratio (TFR) can be defined as the ratio of the modulus of the top layer to the modulus of the lower layer:

$$\text{TFR} = \frac{E_{\text{top-asphalt-layer}}}{E_{\text{bottom-asphalt-layer}}}$$

4. The effect of slip at the interface can be measured by the difference in radial stresses at points just above and just below the interface.
5. Given enough material data, a TFR and Effect of Slip correlation may be established for a pavement structure.

6.2. Conclusion

It can be concluded that:

1. Surface layer moduli calculated from FWD data can be used to identify a lack of interlayer bonding in pavements.
2. The effect of slip between two asphalt layers of similar properties will be reflected by the moduli of the top layer being lower than the moduli of the bottom layer ($E_{\text{top-asphalt-layer}} < E_{\text{bottom-asphalt-layer}}$).

6.3. Recommendations

Based on the findings and conclusions, the following recommendations are made:

1. The procedure outlined in this study should be evaluated for a pool of pavement sections to determine the extent of its validity.
2. The outlined procedure should be tested on a different pavement section that also has detailed material data available, for two reasons:
 - a. To ensure that the methods used are accurate for various pavement systems.
 - b. To verify whether or not the TFR / Effect of Slip correlation obtained in this study is unique for different pavements.
3. Effect of slip should be correlated to physical results of slippage. That is, the results of slippage should be measured in some way and related to the effect of

slippage, so that when one calculates the effect of slippage, one knows what failures may be expected, if any.

4. Modifications should be made to the procedure so that slip can be evaluated between layers other than layers of similar materials, such as slip between asphalt concrete and a base course.

REFERENCES

- Briggs, R., Lukanen, E., and Stubstad, R., *Temperature Predictions and Adjustment Factors for Asphalt Pavement*. Report No. FHWA-RD-98-085. Federal Highway Administration, 2000.
- Federal Aviation Administration, BAKFAA Pavment Backcalculation Program. July 2000.
- Federal Aviation Administration, National Airport Pavement Testing Facility, FAA NAPTF website: <http://www.airporttech.tc.faa.gov/NAPTF/database%20intro.asp>
- Garg, N., *Posttraffic Testing at the National Airport Pavement Test Facility: Test Item MFC*. Report DOT/FAA/AR-TN01/49. U.S. Department of Transportation, Federal Aviation Administration, September 2001.
- Gomba, Stephen M., *Evaluation of Interlayer Bonding in Hot Mix Asphalt Pavements*. M.S. Thesis, Rowan University, Glassboro, NJ, 2004.
- Hachiya, Y., and Sato, K., *Effect of Tack Coat on Bonding Characteristics at Interface between Asphalt Concrete Layers*. Proceedings, Eighth International Conference on Asphalt Pavements, University of Washington, Seattle, 1997.
- Huang, Y. H., *Pavement Analysis and Design*. Prentice Hall, Inc. Englewood Cliffs, New Jersey, 1993.
- Mohammad, L.N., Raqib, M.A., and Huang, B., *Influence of Asphalt Tack Coat Materials on Interface Shear Strength*. Transportation Research Record, 2002.
- Shahin M., Kirchner, K., and Blackmon, E. W., *Analysis of Asphalt Concrete Layer Slippage and its Effect on Pavement Performance and Rehabilitation Design*. Proceedings, Sixth International Conference on the Structural Design of Asphalt Pavements. University of Michigan, Ann Arbor, Michigan, 1987.
- Shahin M, Van Dam T., Kirchner, K., and Blackmon, E. W., *Consequence of Layer Separation on Pavement Performance*. Report DOT/FAAPM-86/48, Federal Aviation Administration, Washington, D.C., 1987.
- Sholar, G.A., Page, G.C., Musselman, J.A., Upshaw, P.B., and Mosely, H.L., *Preliminary Investigation of a Test Method to Evaluate Bond Strength of Bituminous Tack Coats*. Report FL/DOT/SMO/02-459, 2002.
- Uzan, J., Liveneh, M., and Eshed, Y., *Investigation of Adhesion Properties Between Asphaltic-Concrete Layers*. Proceedings, Asphalt Paving Technology, Vol.46, Lake Buena Vista, Florida, 1978.

Wisconsin Highway Research Program
University of Wisconsin-Madison
1415 Engineering Drive
Madison, WI 53706
608/262-2013
www.whrp.org